The Strength And Behavior Of Fabricated Tubular Steel Columns.

INFORMATION TO USERS

This material was produced from a microfilm copy of the original document. While the most advanced technological means to photograph and reproduce this document have been used, the quality is heavily dependent upon the quality of the original submitted.

The following explanation of techniques is provided to help you understand markings or patterns which may appear on this reproduction.

1. The sign or "target" for pages apparently lacking from the document photographed is "Missing Page(s)". If it was possible to obtain the missing page(s) or section, they are spliced into the film along with adjacent pages. This may have necessitated cutting thru an image and duplicating adjacent pages to insure you complete continuity.

2. When an image on the film is obliterated with a large round black mark, it is an indication that the photographer suspected that the copy may have moved during exposure and thus cause a blurred image. You will find a good image of the page in the adjacent frame.

3. When a map, drawing or chart, etc., was part of the material being photographed the photographer followed a definite method in "sectioning" the material. It is customary to begin photoing at the upper left hand corner of a large sheet and to continue photoing from left to right in equal sections with a small overlap. If necessary, sectioning is continued again — beginning below the first row and continuing on until complete.

4. The majority of users indicate that the textual content is of greatest value, however, a somewhat higher quality reproduction could be made from "photographs" if essential to the understanding of the dissertation. Silver prints of "photographs" may be ordered at additional charge by writing the Order Department, giving the catalog number, title, author and specific pages you wish reproduced.

5. PLEASE NOTE: Some pages may have indistinct print. Filmed as received.

University Microfilms International
300 North Zeeb Road
Ann Arbor, Michigan 48106 USA
St. John's Road, Tyler's Green
High Wycombe, Bucks, England HP10 8HR

THE STRENGTH AND BEHAVIOR OF FABRICATED TUBULAR STEEL COLUMNS

by

David Alexander Ross

A Dissertation

Presented to the Graduate Committee

of Lehigh University

in Candidacy for the Degree of

Doctor of Philosophy

in

Civil Engineering

Lehigh University
1978

CERTIFICATE OF APPROVAL

Approved and recommended for acceptance as a dissertation in partial fulfillment of the requirements for the degree of Doctor of Philosophy.

August 16, 1978
(date)

Accepted September 11, 1978

James Tall

Lambert Tall
Professor in Charge

Special committee directing the doctoral work of Mr. David Ross

Le-Wu Lu

Professor Le-Wu Lu
Chairman

James Tall

Professor Lambert Tall
Thesis Supervisor

F. Erdogan

Professor Fazil Erdogan

David A VanHorn

Professor David A. VanHorn
Ex-Officio

ACKNOWLEDGEMENTS

The author is indebted to Professors W. F. Chen and L. Tall, who, in succession, have offered continuous guidance and encouragement as supervising professors of this dissertation. Other members of the special committee directing the author's doctoral work have been Professors F. Erdogan, L. W. Lu (Chairman) and D. A. VanHorn.

Sincere thanks are also due to Mr. Kenneth Harpel, superintendent of Fritz Laboratory, and his capable technicians, who so ably and efficiently assisted in the experimental phase of this work.

The experimental phase of this work was sponsored by a grant to Lehigh University from the American Petroleum Institute, via the Column Research Council (since 1976, known as the Structural Stability Research Council), and the theoretical investigation was commenced under a grant from the National Science Foundation (Grant No. ENG 75-10171). The direction and support of the Project Committee (of which Messrs. L. Boston and C. Miller have been chairmen) is gratefully acknowledged.

Special thanks are extended to Shirley Matlock for typing the entire manuscript with patience and care.

Last, but certainly not least, the author acknowledges his indebtedness to his wife, without whose support this dissertation would never have been completed.

TABLE OF CONTENTS

LIST OF TABLES

Table

LIST OF FIGURES

Figure

ABSTRACT

This dissertation presents a study of the axial load behavior of long fabricated tubular columns of the type commonly used in offshore oil drilling structures. Short lengths of such columns are formed by cold-rolling sheets of originally flat steel plate into cylindrical forms which are then welded longitudinally to produce closed cylindrical shapes, usually up to about 3 m (10 ft) long. A long fabricated tubular column is produced by welding short sections together, end-to-end, with circumferential, or girth welds. The completed column is thus highly discontinuous and may have material and behavior properties which vary in an essentially random manner along the column length.

An experimental program involving stub column specimens and ten long column specimens [of up to 11 m (36 ft) in length and 0.56 m (22 in) in diameter] is reported as conducted in Fritz Laboratory. The long column tests, on columns manufactured in the same manner as prototype columns, were tested in axial compression and under essentially pinned-end conditions. These tests provided a substantial addition to the available test data. Residual stresses in a fabricated tubular column were also measured in two perpendicular directions (longitudinal and circumferential).

As a prelude to a long column analysis, an analysis is presented of a tubular section using the tangent stiffness method to produce moment-axial load-curvature (M-P-Φ) curves. It is shown that in

order to accurately derive the M-P-Φ curves it is necessary to include accurate estimates of residual stresses in two perpendicular directions. A Tresca yield criterion is used to consider the interaction between stresses in two perpendicular directions.

The strength and behavior of a long fabricated tubular column is considered to be adequately modelled by use of a second-order Newton-Raphson iterative technique. The method is formulated with the capacity to consider the behavior of discrete locations at any point along a column length, and at each location the material and behavior characteristics of the section may be specified independently.

The analysis is verified by modelling of available long column test data, and a new column buckling curve for fabricated tubular columns is produced comprising an upper and a lower bound, dependent on the circumferential location of longitudinal welds. A study of the effect of initial out-of-straightness of a fabricated tubular column leads to the recommendation that current manufacturing tolerances be maintained, and a result of a study of the practice of "staggering" of longitudinal welds along a column length is that the strength of a typical column is expected to be between the upper and lower bounds predicted.

1. INTRODUCTION

During recent years there has been an increasing trend toward the use of fabricated tubular columns in the construction of offshore oil drilling structures. Since such columns may have substantial lengths in order to transfer loads from a platform above sea level to the ocean floor, it is entirely appropriate to require considerable care in the design of such members. This dissertation attempts to analyze some of the hitherto unanswered questions about the strength and behavior of such long fabricated tubular columns. It is noted at the outset, however, that this work is concerned only with the overall buckling behavior of long columns, and is not concerned with local buckling effects, which has been the subject of an entirely separate investigation.

Before commencing a discussion of the areas of investigation covered by this dissertation, it is important to adequately define a long fabricated tubular column. First, a brief summary is given of the method of manufacture of such columns as this has a substantial effect on the subsequent problems of analysis.

Fabricated tubular columns of the type considered in this dissertation are typically cold-rolled from originally flat plate. Before any rolling is undertaken, however, the plates must be cut so that one dimension of the rectangular plate is equal to the circumference of the completed column. After bevelling of the other edges, and perhaps a slight prebending to ensure subsequent matching of the

edges, the plate is cold-rolled to form a tubular section which is still open, in that two edges of the plate are facing each other but not joined. These two edges are now welded together, usually in a multi-pass operation, using a submerged arc welding process, and usually involving welding from both inside and outside of the section. The result is that a short tubular column has now been formed. The diameter of this column has been determined by the size of plate rolled, as has the height of the column. The height of the column is further limited by the capacity of the machine on which the tube was rolled, with the result that a typical short column is of the order of 3 m (10 ft) tall, and is commonly called a "can".

Clearly, a column of only three meters tall has very limited usefulness in the construction of offshore oil drilling structures, and, therefore, a number of such short columns must be joined together end-to-end to form a column of the desired length. Once again this joining of the cans is done with a welding process, after appropriate end preparation of the short columns. Specifications usually require that the longitudinal welds be staggered around the column diameter, that is, that the longitudinal welds in individual "cans" do not end up on one line along the column.

It is now possible to consider in more detail the basic problems associated with the axial load behavior of fabricated tubular steel columns, and to highlight the comparisons with columns of other cross sections. The residual stresses induced during fabrication are the first focus of this discussion. During the cold-rolling process by

which a flat steel sheet becomes an open cylinder, circumferential residual stresses are induced which vary through the thickness of the wall of the tubular column. These stresses are circumferential in direction, despite their "through-the-thickness" variation. It might well be expected that the longitudinal welding of the seams, by which process the closed section of the individual cans are formed, would induce longitudinal residual stresses in the column wall, that is, in a direction parallel to the direction of the axial stress which will resist axial loads on the completed column. Thus, even in a short column, there are stresses in two perpendicular directions, and, of course, these stresses will interact during column loading. (It is also true that the circumferential welding process by which the cans are joined together end-to-end induces residual stresses probably localized near the ends of each can, but in order to make the problem of manageable proportions, these stresses have been ignored in this investigation.)

In most previous investigations of column buckling strength, residual stresses have been assumed to be significant only parallel to the direction of loading, but here is a situation in which this assumption cannot automatically be made. One important facet of this work, therefore, is a determination of whether or not this interaction between perpendicular stresses is an important parameter of column performance.

The fabrication process described above also produces another factor of unknown importance in long column behavior. Clearly, a

completed long column is very variable in its section properties, since it is a collection of individual, identifiable sections. Because of the varying orientation of the longitudinal welded seams with respect to each other along the column length, it would be expected that sections taken through the column in one can would behave differently to sections in neighboring cans. This is particularly so when the sections are in a state of biaxial bending, as they would be when a column is considered to be initially imperfectly straight. Furthermore, there is a strong likelihood that material properties of the steel will vary between "cans" used in the assembly of a long column. For example, it is known that there can be significant variations in steel yield strength merely because it was rolled from steel of a different heat lot.

The above factors imply that it is inappropriate to assume uniform properties of all sections along a long fabricated tubular column. This fact is a result of the fabrication process, while for many other types of section which have been studied previously, the assumption of uniform section properties is entirely reasonable. An important goal of this work was, therefore, to enable conclusions to be drawn about the relative importance of a number of the complicating factors discussed above, and indeed, if necessary, suggest other factors which should be more carefully examined.

With this brief introduction to the problems and complexities which are an integral part of an investigation of long fabricated tubular columns, the approaches to possible solutions are now

outlined. This dissertation covered both experimental and theoretical investigations, both of which are introduced here.

The experimental phase of this work involved the testing in Fritz Laboratory of ten prototype long column specimens, manufactured in a manner resembling as closely as possible the fabrication process for columns used in the construction of offshore oil drilling platforms. Columns of varying diameter and length were tested with a view to considering a wide but practical range of column slenderness ratios. The columns ranged from 5.5 m (18 ft) to 11 m (36 ft) in length and were of either 0.38 m (15 in) or 0.56 m (22 in) in diameter. Steel from two different heat lots was included in each column specimen, and the columns, each made up of a number of short "cans", had the longitudinal welds staggered between cans.

The theoretical phase was itself divided into two major components. By considering essentially a column section, or a column of unit height, the section deformation relationships could be derived as the section was subjected to axial load and biaxial bending. At this stage both longitudinal and circumferential residual stresses could be considered, as well as the interaction between them. The longitudinal residual stress distribution is caused by the longitudinal welding process, which thus becomes an important factor as bending moments are applied to the section with various orientations with respect to the longitudinal weld.

This column analysis provides an opportunity for several areas of contribution of this work. First of all, the derivation of section performance under axial load and biaxial bending has not previously been attempted for a tubular cross section, with residual stresses of the type considered here included. Not only is it a recent development that an accurate assessment of longitudinal residual stresses and their distribution has been made, but the same applied also for the circumferential residual stresses. Since longitudinal residual stresses are both relatively localized and considerably varying around a tubular column circumference, the contribution made by consideration of this alone is significant. The other significant addition is the permitting of an analysis involving stresses mutually interacting in two perpendicular directions. To date, any interaction between stresses in two perpendicular directions had not been a consideration, for most sections are adequately analyzed assuming only residual stresses in a direction parallel to the direction of stresses induced by column loading, an assumption which could not be automatically made for fabricated tubular columns.

The second component of the theoretical investigation was the derivation of a method of analyzing a long fabricated tubular column with the inclusion of as many as possible of its highly variable section properties along the column length. It was considered most practicable to consider discrete sections along a particular column, at each of which the section properties could be uniquely defined. If such a discrete section could be considered to have properties

representative of other sections close to it along the column length, then the overall column behavior could be derived by considering a series of such discrete sections, each behaving independently, but linked to neighboring discrete sections by the conditions of continuity. Each section is thus considered to exhibit behavior representative of a short column (and it is desirable that the section be near the mid-height of that short column) and the linking of these short columns together ensures harmonious, connected column behavior.

Not only has such a detailed attempt to model the behavior of a fabricated tubular column not been reported hitherto, but neither has it been considered necessary previously to consider a column to have such widely differing properties - both material properties and section properties - along its length. Not only are the capabilities of two-dimensional stress analysis retained from the short column analysis, but also the theory used has been modified to allow consideration of discrete stations at any intervals along a column length. The interstation distances may or may not be constant along a column, so that any desired degree of accuracy in modelling may be achieved.

It remains now to indicate the setting-out of the subsequent chapters of this dissertation. Chapter 2 indicates the scope of work previously attempted which has direct bearing on the research reported herein. Although dealing with a number of different topics, the previous work has been treated as a harmonious unit because of the considerable overlap and interrelation of the components. In

Chapter 3 the details of the experimental testing program are given. The several phases of the program are outlined, together with trends shown in the results.

The theoretical analysis begins with a short column analysis, a topic treated by Chapter 4 of this work. This chapter briefly outlines the theory and gives some results of the study undertaken. At the end of this chapter it is also possible to make some conclusions about the relative importance of some of the factors considered, and in particular, their effects upon section behavior. In Chapter 5 the long column analysis is introduced. A discussion of the theory involved, with emphasis on the modifications to existing theory required for this purpose, is followed by a parametric study of some of the variables inherent in the study.

Chapter 6 is an attempt to reconcile the theory developed and the experimental results available. By means of such a comparison, conclusions are possible about the adequacy of the theory, and also the need for further experimental data. Chapters 7 and 8 provide opportunities respectively for suggestion of areas in which future research might be fruitful, and dissertation conclusions (an important part of which is design recommendations).

In references to the available literature, the particular work being referenced has been given a number in parentheses, which refers to the work listed by that number in the list of references contained in this dissertation. The references are listed in order of appearance in the dissertation.

2. PREVIOUS WORK

2.1 Introduction

The problem of overall column buckling has been recognized for a long time, and history records many attempts to solve this problem both experimentally and analytically. There is, therefore, an extensive body of literature with some reference to the subject of this dissertation. The problem is further compounded by the fact that the scope of this work includes theoretical and experimental investigation into a number of topics related to the axial load behavior of columns. In restricting the scope of this literature survey it has been necessary to include important historical references, for these have a major role in determining the explicit and implicit assumptions behind methods of approach to the problem of the axial load behavior of fabricated tubular columns. For example, many of the techniques utilized, both theoretical and experimental, have been used elsewhere for other purposes, and it is necessary to have some appreciation of those previous conclusions in order to begin a re-evaluation of the techniques as applied to the problem at hand.

In arranging this survey of previous work, an attempt has been made to group the subject matter such that it corresponds to the work to be presented and discussed in subsequent chapters of this dissertation.

2.2 Short Column Analyses

As discussed in Chapter 1, a typical, long, fabricated tubular column is highly discontinuous in that its behavior and properties are substantially different at different locations along its length. Thus, it was considered that an essential prerequisite to any analysis of the behavior of such a column was an investigation of the particular properties which characterize the behavior of a particular cross section of the column. Not only would such a short-column analysis become a building block in a long column analysis, but it was anticipated that the short column analysis would be able to indicate the relative importance of some of the factors contributing to column performance.

In a short column, or column of unit length, it is possible to consider the influence of residual stresses on section behavior. The changes induced by these stresses on section behavior are observed by derivation of the nonlinear moment-axial load-curvature (M-P-Φ) curves for various combinations of axial load and biaxial bending moment applied to the section. The technique used for this investigation was the tangent stiffness method. Santathadaporn and Chen (1) reported use of this method for analyzing I-sections, noting that the method has also been used by Gurfinkel (2) and Harstead et al. (3) in other specific instances.

Santathadaporn and Chen (1) also reported that residual stresses, inherent in member manufacture, had been included in section analysis. However, these residual stresses were considered to be

present in only one direction, that is, the longitudinal column direction, whereas a fabricated tubular column was thought to have significant residual stresses present in at least two perpendicular directions. The tangent stiffness method as previously reported had, therefore, to be extensively modified in order to include stresses in two perpendicular directions, as well as the interaction between perpendicular stresses.

Another approach to the derivation of M-P-Φ curves for tubular sections has been reported by Wagner et al. (4,5). This method is based on a similar open-form solution technique, but, once again, residual stresses have been included only in a direction parallel to that in which a column is loaded, that is, the longitidunal column direction.

At this point it is also appropriate to note that there have been other attempts to derive M-P-Φ curves of tubular sections analytically, as these provide useful checks for parts of the M-P-Φ curves derived in this investigation. One such method is that by Ellis (6), although this work suffers along with other such attempts from its inability to include the effects of residual stresses. From a different approach, Chen and Atsuta (7) presented a method by which interaction curves for various doubly-symmetric sections - including hollow tubes - could be calculated using both lower bound and upper bound theories. This method could predict only the ultimate strength of perfect cross sections. Since it was confidently expected that ultimate section strength would not be affected by

the presence of residual stresses, the ultimate strength values derived in this reference were used to check "plateau" values of derived M-P-Φ curves. [Chen and Atsuta (8) subsequently modified this method to allow predictions to be made for nonsymmetrical sections composed of rectangular elements.]

2.3 Tubular Column Buckling, Manufacturing and Design Specifications

Before considering the biaxial buckling of tubular columns, it is necessary to briefly trace the development of a simple buckling theory, and note the specific applications to fabricated tubular columns.

During the twentieth century the derivation of column buckling curves hinged on the development of a buckling theory for columns in the inelastic buckling range. In 1947, Shanley (9) introduced the tangent modulus buckling concept, but from the late 1940's it became apparent that the inclusion of residual stresses was essential for the accurate prediction of buckling loads. Many experimental programs were conducted, including many at Lehigh University (for example, 10 and 11), and there followed development of empirical or semi-empirical relationships to define a column buckling curve based on the available set of experimental test data.

In 1976 edition of the Structural Stability Research Council (SSRC) Guide (12) contains a good coverage of developments in column buckling design, clearly illustrating the reasons why there has been a change from the use of one column buckling curve in the 1966

edition of the same guide to the concept of multiple column buckling curves. Reference is made to work done at Lehigh University (13) and work of the European Convention for Constructional Steelworks (14, 15). Curves are suggested for tubular columns, but with little experimental evidence to support them. It is clear that for some time (16) concern over the lack of available experimental data for the proposed curves has been expressed. Oil industry design codes (17,18) rightly put more emphasis on the local buckling problem of cylinders than on the overall buckling problem.

Manufacturing imperfections are known to be significant in determining the buckling loads of cylindrical shells. Thus the American Petroleum Institute (API) specifies (19) tolerances for out-of-straightness and out-of-roundness of prototype columns.

2.4 Long Column Analysis

The problem of inelastic beam-column behavior of long columns has also been studied extensively both analytically and experimentally. Many researchers have made contributions to both experimental and computational areas of investigation. Thus some work mentioned in this discussion also has relevance to experimental investigations discussed in Section 2.6.

The phenomenon of inelastic lateral torsional buckling of beam columns, particularly wide flange sections, prompted Fukumoto and Galambos (20) to attempt solutions to lateral torsional buckling equations using finite difference techniques. They were primarily

concerned with the reduction in predicted buckling strength caused when lateral torsional buckling initiates premature failure. By 1971 Chen (21,22) had made considerable progress towards the inelastic buckling prediction of laterally loaded columns. It is fortunate indeed that the closed section used in tubular columns has such high torsional rigidity that lateral torsional buckling is not considered a problem.

Chen and Atsuta (23) reported in 1972 that the general response of elastic-plastic beam-columns could be obtained with relative ease using an equivalent column concept and column curvature curves. Previously, most solutions had been obtained by numerical computations (24). Santathadaporn and Chen (25) then used the concepts of tangent stiffness to produce load-displacement curves for steel H-columns. Consideration was given to both proportional and non-proportional loading, and for these sections, torsion is an important consideration. To clarify the necessity for three-dimensional analyses of doubly symmetric, open sections, Tebedge et al. (26) compared an experimental test result to a two-dimensional in-plane tangent modulus prediction of column strength and a three-dimensional load-deflection approach. They showed that the two-dimensional analysis gave adequate predictions of maximum column load for such sections, but that, because of residual stresses and yield strength. variations, a three-dimensional analysis was required to adequately predict load-deflection behavior. With this established, Tebedge and Chen (27) and Ross and Chen (28) extended the derivations using

the tangent stiffness technique to provide design criteria for H-columns and I-columns, respectively, under biaxial loadings. These are currently included in design recommendations (29,12).

While these developments were taking place, finite element methods were being used to determine stability of beam columns (for example, 30), and the literature was being searched for available relevant experimental data (for example, 31).

In Switzerland, Vinnakota and associates (32,33) developed finite difference techniques for determining stability of beam-columns and deriving maximum strength interaction curves.

It is noted that in all the foregoing, the analyses have been undertaken for open cross sections in which residual stresses, if included, have been in the longitudinal column direction. Furthermore, column properties have either been constant or varying in a linear manner (34) along a column length. Thus a fabricated tubular column, with properties which may vary in a highly irregular manner along its length, may not necessarily be adequately modelled by such analyses.

As has been noted, the closed section provided by tubular columns enables the torsion problem to be neglected. Thus the behavior of long fabricated tubular columns is considered to be adequately modelled using an iterative technique, such as the Newton-Raphson iterative technique, provided that nonlinear material properties may be considered. This method was used successfully by

Virdi and Dowling (35) on a member of constant section properties along its entire length, and would therefore require modification before being applicable to the problem of manufactured tubular columns.

Another method which has been applied to long tubular beam-columns in order to predict load carrying capacity (4) is Matlock's recursive solution technique (36). While this application allows gradual plastification of sections along a column length, it has not yet been applied to columns in which section properties vary along the column length.

2.5 Residual Stress Measurement

The existence of residual stresses in steel sections due to their manufacture has been known for a long time, and much effort has been expended measuring these stresses. It is beyond the scope of this discussion to attempt a comprehensive listing of types of residual stress measuring apparatus used, or even of all the used to which these have been put. Rather, a brief survey is given of representative types and occasions of use, with rather more attention concentrated on the types of residual stress measuring technique used in this work.

The principle of measuring residual stresses by hole-drilling was suggested by Mathar in 1934 (37), who recognized that the release of strain at a surface could be some measure of residual strain release at the bottom of a hole. At first, there were difficulties

in measuring this strain release at the surface, as Mathar used mechanical extensometers for this work. During the 1940s the method was developed qualitatively rather than quantitatively, by watching crack patterns in a brittle lacquer painted on the steel surface as they developed around a gradually deepening bored hole (38), but by 1950 the concept of using electric resistance strain gages was established (39). By 1955, some theoretical basis for the method had appeared (40), although it is perhaps significant that, in measuring residual stresses caused by autofrettage in gun bores in 1963, Davidson et al. (41) used a technique of gradual destruction in which they gradually turned the bore on a lathe. They were, however, still measuring strain release on a surface due to residual strain release at the bottom of the cut.

Nonetheless, the method of hole drilling was fully established theoretically for isotropic plates by 1966 (42) and for orthotropic materials by 1970 (43), with proprietary apparatus marketed before 1972 (44,45). The principal advantages of the method are its semi-destructive nature; and its ability to measure stresses in two perpendicular directions, enabling derivation of principal stress directions. The method is, however, limited in its ability to accurately measure residual stress very near the surface of the plate. Since the method had proved capable of determining residual stresses on a porcupine shaft (46), it was decided to attempt its use on the fabricated tubular columns under study. The method proved very suitable for measuring circumferential residual stresses in

such a column, particularly as these stresses have significant variation through the thickness of the wall.

In 1888 Kalakoutsky (47) reported on a method of determining longitudinal stresses in bars by slitting strips from the bar and measuring their change in length. From this has developed the sectioning technique for determining residual stresses in which a short length of section is physically dissected slowly, and differences in strain are noted from readings taken before and after dissection. A good summary and explanation of the method is given by Tebedge et al. (48) as a result of work at Lehigh University. In fact, while acknowledging the fact that it is a destructive method of measurement, the report concludes that the method is both more accurate and more foolproof than a number of other methods, and is adequate, accurate and economical when longitudinal residual stresses only in structural members are important. The method has been used successfully on I- and H-sections by Tebedge et al. (26), on welded box shapes by Tall (10), and in thin cold-formed rectangular sections by Sherman (49).

For a more complete examination of possible methods of residual stress determination the reader is referred to Tebedge et al. (50). It is also noted that not all residual stress determinations are made on completed members, as Ostapenko and Gunzelman (51) reported derivation of such stresses in tubular columns by taking strain measurements induced during fabrication from measurements before and after such fabrication.

2.6 Previous Experimental Research on the Buckling of Fabricated Tubular Columns

While axial testing of columns has been undertaken for many years, building a substantial body of experimental data on overall column buckling behavior, such tests have rarely been conducted on fabricated tubular steel columns. As is explained below, there are inherent difficulties of scale in the testing of such columns, which have only been partially solved in the experimental investigation described in this work.

During the 1930s, the University of Illinois was interested in both the local buckling (52) and, as an accompanying concern, the overall buckling of fabricated tubular columns (53). This interest appears to have arisen as a result of a trend toward the use of fabricated tubular columns as supports for elevated storage tanks. The results reported in at least one of the references cited may have some direct comparison with the results reported in this work.

A number of column buckling tests have been reported on small-scale tubular specimens, including some in aluminum (54) and some in steel (55). Such tests typically use specimens up to about 2.5 m (8 ft) in length and about 0.15 m (6 in) in outside diameter, to provide specimens of relatively large slenderness ratio. However, there are several problems when the results of such tests are extrapolated to provide design data for large-scale, fabricated tubular columns such as are commonly used in offshore oil drilling structures.

Some such small-scale testing has been conducted on seamless specimens, thus ignoring the longitudinal residual stress effects thought to be a significant parameter in prototype column buckling. Furthermore, such specimens are commonly manufactured by an extrusion process, which avoids the incidence of discontinuous section properties along a column length. On the other hand, other test specimens have been manufactured with wall thicknesses so small that circumferential residual stress patterns have probably been lost, and the use of such thin walls would have unknown effects on the longitudinal residual stress pattern.

One test sequence which has avoided some of these problems was that of Bouwkamp (56) who tested specimens up to 9 m (30 ft) in length and 0.2 m (8 in) in diameter. Even here, however, it does not seem to have been possible to consider the effects of staggered longitudinal welds, nor any other factors, such as yield strength variations, which lead to varying section properties along the length of a column.

There have been several good "state-of-the-art" papers published on overall buckling, local buckling and the interaction of these phenomena (57,58,59). Recently there has also been interest in the investigation (60) into the feasibility of spirally-wound tubular column manufacture.

Since overall column buckling will involve column bending, it is appropriate to note that experimental investigations into bending

of fabricated tubular columns have been continuing (61) with varying geometric constraints being attempted. Furthermore, it is certain that the investigation reported herein has been enriched by a parallel investigation conducted concurrently at Lehigh University into the local buckling behavior of fabricated tubular steel columns (62,63).

3. EXPERIMENTAL INVESTIGATION

3.1 Introduction

This chapter outlines the experimental program undertaken as part of this investigation. The object of the program was to obtain reliable estimates of residual stresses present in fabricated tubular columns and data relevant to the strength and behavior of typical, full-sized, fabricated tubular columns.

Included among preliminary tests were those on stub columns for measuring residual stresses. Ten full-sized column specimens were tested in axial compression under essentially pinned-end conditions. These columns had nominal slenderness ratios ranging from 39 to 83. Preliminary tests have been reported in detail (64,65) as have column test results (66,67,68,69). This chapter therefore is concerned primarily with collating results in a form useful for the subsequent theoretical studies, and explaining the origin of experimental data used in subsequent theoretical modelling.

After outlining the scope of the testing program, this chapter considers supplementary tests as a unit, before considering residual stress measurements and long column testing, with particular emphasis on initial imperfections of columns, experimental technique, and results obtained.

3.2 Scope of Test Program

As explained in Chapter 1, the cold-rolling process by which short columns or "cans" are formed introduces circumferential residual stresses which vary through the thickness of the wall of the tubular section, while the longitudinal welding process introduces longitudinal residual stresses. These stresses maintain their importance in prototype columns for such columns are typically used without any form of stress relief. In preliminary testing, particular attention was focussed on the magnitudes and distributions of these residual stresses, on the premise that accurate values were essential to the adequate derivation of moment-axial load-curvature (M-P-Φ) curves (see Chapter 4). These measurements were undertaken on a short column of about 1.2 m (45 in) in length.

Three stub column tests were undertaken on short "cans" of the same diameter and wall thickness as prototype columns in order to allow prediction of buckling loads for long columns. Each stub column test yielded a separate column buckling strength curve. Further supplementary tests, in the form of yield strength tests on flat tensile coupons were also conducted. The importance of determining yield strengths of steel used in the columns is underscored by the dependence of yield strength values obtained on the method of testing.

The ten full-sized column specimens tested varied in length from 5.5 m (18 ft) to 11.0 m (36 ft) and had outside diameters of either 0.38 m (15 in) or 0.56 m (22 in). The nominal wall thickness

for all specimens was 8 mm (5/16 in). This combination of sizes resulted in columns having a nominal slenderness ratio in the range from 39 to 83 (at diameter-to-thickness ratios of 48 and 70). All stub columns and long columns were tested in the 5,000,000 pound universal testing machine in Fritz Laboratory.

3.3 Supplementary Tests

The purpose of this section is to discuss the common supplementary tests conducted as part of this investigation, and these include stub column tests and tensile coupon tests. The residual stress measurements are to be presented and discussed under a subsequent heading.

When the tubular columns were manufactured, four "cans", or short specimens, were set aside for stub column tests. These were two 0.38 m (15 in) diameter specimens each about 1 m (40 in) long and two 0.56 m (22 in) diameter specimens about 1.2 m (45 in) long. Since steel from two heat lots was used in the manufacture of the long column specimens, this allowed one stub column specimen from each heat lot in each diameter considered. However, one specimen was diverted to residual stress measurement and three stub column specimens were tested. The experimental method used for stub column testing is given in references 70 and 71.

The stub columns were all tested in the 5,000,000 pound universal testing machine in Fritz Laboratory, Lehigh University. Figure 3.1 indicates the positions of measuring apparatus in a

typical setup. Basically, five electric resistance strain gages were mounted on each specimen at mid-height, each oriented to measure axial strain. These were placed at 45°, 135°, 180°, 225° and 315° from the longitudinal weld in the can. Other instrumentation included two 254 mm (10 in) Whittemore gages to measure mid-height axial strains (both on, and diametrically opposite to, the longitudinal weld), and four dial gages measuring the relative movement between the machine heads (total overall axial compressive movement).

A qualitative series of results is shown in the photographs and diagrams of Figs. 3.2 through 3.6. There were noticeable differences in failure mode between specimens. Figures 3.2 and 3.3 show progressive yielding of Specimen 1 [0.38 m (15 in) diameter and 0.91 m (36 in) long]. These show first a diagonal shaped yielding pattern progressing to a primary buckle 50 mm to 75 mm (that is, 2 to 3 in) from the base of the specimen with a series of smaller buckles (up to 7) extending along the length of the specimen, with approximately even spacing. Specimen 2 [0.38 m (15 in) diameter and 0.91 m (36 in) long], shown in Fig. 3.4, had a similar failure sequence but showed a much reduced tendency to form secondary buckles along the can length.

The unusual feature of Specimen 3 [0.56 m (22 in) diameter and 1.17 m (45 in) long], shown in Figs. 3.5 and 3.6, is that the final buckle formed at a distance from one end of the specimen. A slight upturn in the buckle at the circumferential location of the longitudinal weld was also visible.

Despite the differences in failure mode, all three specimens gave remarkably similar prediction of column buckling strength (Fig. 3.7). (The critical load P_s is defined in Fig. 3.18.) Table 3.1 gives the essential stub column performance data. Column buckling curves were derived from a static stub column stress-strain curve using the tangent modulus technique, in which the column critical buckling stress, σ_{cr}, is given by

$$\sigma_{cr} = \frac{\pi^2 E_t}{\left(\frac{KL}{r}\right)^2} \qquad (3.1)$$

where

E_t = tangent modulus of elasticity

$\frac{KL}{r}$ = column effective slenderness ratio

A series of typical tensile coupon tests was also conducted to determine steel tensile properties. Two heat lots of steel were used in column manufacture, and thus Table 3.2 records material tensile properties as recorded by various testing procedures. The mill report furnished by the steel manufacturers gives relatively high values of yield strength because of the typically high strain rates used in testing of coupons. The "static" laboratory tests were conducted using a common laboratory procedure (72,73), while the commercial laboratory tests used a common industrial procedure. The major difference between the "static" and "commercial" test procedures was that the latter used a higher maximum strain rate. The use of a higher strain rate produced slightly higher values of dynamic yield strength and elastic modulus of elasticity, E, but

these two tests have identical values of static yield strength. In Table 3.2 the dynamic and static yield strength values derived experimentally are given as σ_{yd} and σ_{ys}, respectively.

3.4 Residual Stresses

Measurements were made of residual stresses in both longitudinal and circumferential directions. Many different methods of measuring these have been attempted, with varying degrees of success. The history of methods used here is described in Section 2.5.

The longitudinal residual stress determination was made by a destructive relaxation method, a slicing technique in which the central portion of a stub column specimen was dissected into bars. Measuring the distance between two points in each bar, both before and after dissection, enabled the strain release during dissection to be computed at that location. Figure 3.8 shows the dissection of the specimen and Fig. 3.9 shows representative selections of dissected pieces. Basically, the outside surface of the column at mid-height was marked out in "bars" of 12 mm (0.5 in) width and 280 mm (11 in) length. A Whittemore strain gage of nominal 254 mm (10 in) gage length was then used to measure the strain release as the bar was cut from the column specimen. Because of the expense of the total dissection of all 144 possible bars, incomplete dissection was performed. After dissection, no significant "bowing" of the dissected strips was observed. Some twisting of the strips very near the weld location was observed, but this was assumed to have a negligible effect on the longitudinal strain readings.

The method adopted here for presentation of the measured longitudinal residual stress distribution is shown in Fig. 3.10. For presentation purposes it is assumed, as shown in Fig. 3.10(a), that the specimen is cut diametrically opposite the weld and folded out to give the flat surface given in Fig. 3.10(b). Symmetry of the residual stress distribution about the weld location is assumed. Thus, only half of the surface of Fig. 3.10(b) is required and the results are presented on a surface shown in Fig. 3.10(c). Measurements were, however, taken from points all around the specimen circumference.

The longitudinal residual stress distribution obtained using the slicing method is presented in Fig. 3.11. The curved solid line is a good fit to the experimental results (shown dotted), and it also has the form predicted by Marshall (16). [Marshall predicted that the longitudinal residual stress distribution would be characterized by a region of high tensile stress (probably of material yield strength or greater) near the weld, and area of alternating compressive and tensile stress as one moved away from the weld around the column circumference. He further predicted that the magnitudes of stress peaks would decrease as one moved away from the weld.]

The dashed lines are a straight-line approximation suggested as a simplified alternative (and used in subsequent theoretical analyses - see Chapters 4 and 5). If X_θ is the distance from the weld (measured around the tube circumference), R is the mean radius of the tubular section, σ_L is the longitudinal residual stress at

a point on the circumference, and σ_y is the material yield strength, then the following values may be adopted as the base values in a straight-line approximation:

$$\begin{aligned}
\frac{\sigma_L}{\sigma_y} &= 1.0 \quad \text{at} \quad \frac{X_\theta}{R} = 0 \\
\frac{\sigma_L}{\sigma_y} &= 0 \quad \text{at} \quad \frac{X_\theta}{R} = 0.15 \\
\frac{\sigma_L}{\sigma_y} &= -0.3 \quad \text{at} \quad \frac{X_\theta}{R} \approx 0.3 \\
\frac{\sigma_L}{\sigma_y} &= 0 \quad \text{at} \quad \frac{X_\theta}{R} = 1.0 \\
\frac{\sigma_L}{\sigma_y} &= 0.1 \quad \text{at} \quad \frac{X_\theta}{R} = 1.2 \\
\frac{\sigma_L}{\sigma_y} &= 0 \quad \text{at} \quad \frac{X_\theta}{R} = 2.0
\end{aligned} \tag{3.2}$$

In Eq. 3.2 the ratio $\frac{\sigma_L}{\sigma_y}$ is positive for longitudinal residual stresses in tension, and negative for residual stresses in compression. Reference 74 suggests that the approximation may be adequate for column radii up to a maximum of about 380 mm (15 in); that is, for radii in excess of this value, R should be taken as 380 mm (15 in) in Eq. 3.2. This seems reasonable when it is considered that a finite amount of heat is added to a "can" in the longitudinal welding process. Thus the residual stresses would, for greater than a certain column radius, have a finite range of influence, or, in other words, would induce residual stresses only up to a certain

distance from the longitudinal weld. Reference 74 also suggests that there may be a minor dependence of the $\frac{\sigma_L}{\sigma_y}$ ratio on the yield strength of the material and the welding procedure used.

Circumferential residual stresses were measured by a hole-drilling technique (44,45) in which surface measurements were taken of the strain release due to drilling at the base of a small diameter hole in the tubular wall. These tests, essentially non-destructive in nature, were conducted on the some stub column specimen as was subsequently dissected for longitudinal residual stress measurements. Figure 3.12 gives the results obtained from these tests. No significant variation in circumferential residual stresses was found at different locations on the cross section. Figure 3.12(b) indicates typical experimental results. The testing technique was known to have a limited range of validity such that results near the surface as well as those taken near the centerline of the tube were thought to contain possible inaccuracies. Thus the straight-line approximation is shown dotted in these areas. The hole-drilling experiment was conducted on both inside and outside surfaces of the tubular column specimen. Figure 3.12(c) shows the average circumferential residual stress pattern obtained, and it is compared with a simple assumption in Chapter 4.

3.5 Long Column Testing: General

In the long column testing program, ten long column specimens were tested. It was considered important that the columns be

fabricated using a method resembling as closely as possible that used to fabricate prototype columns for use in real structures. The maximum nominal length of the columns was restricted by the height capacity of the 5,000,000 pound universal testing machine in Fritz Engineering Laboratory (about 12 m, or 40 ft), and the minimum column diameter was controlled by the minimum diameters which could be rolled using the manufacturer's rolling machines. Thus the column specimens tested varied in length from 5.5 m (18 ft) to 11.0 m (36 ft) and in diameter from 0.38 m (15 in) to 0.56 m (22 in).

Table 3.3 gives a detailed list of specimens supplied for testing. The wall thickness of all specimens was 7.9 mm (5/16 in). Given the nominal column length and the outside diameter of each specimen, the nominal slenderness ratio (L/r) can be computed, along with the diameter-to-thickness ratio (D_o/t).

The specimens were fabricated in accordance with the requirements of the American Petroleum Institute Specifications (19). The sections used to form the columns were rolled from ASTM A36 steel plate in which the original milling direction was perpendicular to the longitudinal axis of the finished columns. Two heat lots of steel were included in the specimens and the properties of these, as found in various tensile coupon tests, is recorded in Table 3.2.

An important feature of these tests was the use of spherical bearing heads at each end of each specimen during testing, in an attempt to provide pinned-end conditions. Not only was this an attempt to ensure the maximum value of column effective length

factor, K, was obtained, but it also allowed valuable information on column behavior to be collected. Reference 75 describes testing of pinned-end columns for the case where the buckling direction is well defined. Typically, I- and H-sections have such well defined buckling directions, and in such circumstances it may be possible to use cylindrical end blocks. However, tubular columns are not amenable to the accurate prediction of the buckling direction, and the use of spherical bearing heads allowed each column specimen to adopt its preferred buckling direction without hindrance from end conditions. The buckling direction of each column was noted.

Despite the use of spherical bearing heads, it was, in practice, impossible to attain a true pinned-end support condition, because of unavoidable frictional resistance to head rotation. (Head rotation in two perpendicular directions was monitored continually during most tests.) It then became necessary to determine an effective length factor, K, for positioning the buckling test result on a column buckling curve. Electric resistance strain gages were mounted on each specimen at quarter points along the specimen length and near each end. An approximation to the true column effective length, or at least to the range of K values possible, was found by plotting the curvatures measured along the column length in two perpendicular directions. Of course, since a curvature measurement requires strain measurements diametrically opposite each other on the column circumference, each considered position along the column length needed four strain gages (to allow determination in two perpendicular planes). Each strain gage

measured longitudinal column strain. The range of K values obtained using this approach is given in Table 3.3.

3.6 Long Column Testing: Initial Imperfections

It seemed initially that there may be at least two types of initial, geometric, manufacturing imperfection which may have had significant influence on column strength and behavior - namely, column out-of-roundness and column out-of-straightness. Out-of-roundness measurements were made on one fabricated tubular column specimen and it was found that, in general, there was less than one percent difference between two perpendicular diameters at a particular position along the column length, which was considered negligible. These measurements were, therefore, not made on subsequent specimens. It was concluded that out-of-roundness was not a significant parameter in the column performance, due to a high degree of accuracy in manufacture. (Furthermore, if there was any local deviation from the circular, such as at the weld location, the effects of this would be reduced by the forced matching which takes place during manufacture when the cans are joined with circumferential welds.)

The American Petroleum Institute has specifications (19) for the maximum allowable out-of-straightness of a prototype fabricated tubular column. These specifications allow 3 mm (1/8 in) in 3 m (10 ft) (or one part in one thousand) with the restriction that out-of-straightness must not exceed 9 mm (3/8 in) in 12 m (40 ft) (or

7.5 parts in ten thousand). It was considered that out-of-straightness may be a critical parameter in the prediction of column behavior. In particular, it was likely to be a determining factor in the buckling direction of the column. Considerable effort was therefore devoted to the measurement of these imperfections.

The first problem encountered in measuring out-of-straightness of a tubular specimen is the establishment of perpendicular diametrical planes on which these measurements could be taken. It would be desirable to establish one of these planes such that measured out-of-straightnesses measured in this plane were the maximum that could be measured for that specimen. An attempt was therefore made to find a plane of maximum out-of-straightness by rolling each specimen on a flat surface until a position of unstable equilibrium was reached. The longitudinal welds, however, hampered this process because they tended to protrude slightly from the outside diameter of the specimen. In general, one of the diametrical planes was established close to these weld locations. (The welds in the long column specimens supplied tended to be staggered at about 180° between adjacent cans.) The actual out-of-straightness of each specimen was measured with the specimen in an upright position using a theodolite. When a ruler was held against the specimen at discrete locations along the specimen [usually at 0.6 to 1.0 m (that is, 2 to 3 ft) intervals], a reading through the theodolite established the distance of the outside of the specimen from vertical line traced by the theodolite rotating about a horizontal axis.

The resulting out-of-straightness profiles are reported in Reference 67, along with other long column performance data. In general, the API specified tolerances for out-of-straightness have not been exceeded. Furthermore, there seems to be a trend for the out-of-straightness on a diametrical plane nearly parallel to that including most longitudinal welds to be greater than that on the perpendicular diametrical plane.

3.7 Long Column Testing: Experimental Technique

The use of strain gages at quarter points and at the ends for determining column effective length is mentioned above. For convenience, these gages were mounted on the perpendicular diametrical planes established for taking out-of-straightness measurements. However, this instrumentation will only allow measurement of axial strains (and thus curvatures).

It was also desired to measure lateral deflections of each specimen during loading. In particular it was decided to observe column behavior by measuring lateral deflection at quarter points, and it was thought necessary also to monitor the end rotations of the spherical bearing blocks. Since longitudinal planes had been established for out-of-straightness measurements, and used for effective length determinations, the same planes were used to measure lateral deflections. Measurements of lateral deflection did, however, provide some problems. First, the direction of lateral movement during loading and at buckling was unpredictable (and could

well vary as axial load was increased). Furthermore, the situation was complicated by the desire to measure deflection at a point on a curved surface. Each of these problems contributed to the fact that the customary method of measuring deflection by placing a dial gage against a prepared flat surface was inappropriate. These problems were solved to an adequate degree of accuracy by constructing a frame on the testing machine at quarter points along the specimen length, such that a long, horizontal wire could be connected at one end to a deflection-measuring apparatus (attached to the frame) and at the other end to a point on the column specimen. The wire used to make each such connection was of the order of 1.6 to 2.0 m (that is, 5 to 6 ft) long, allowing the assumption to be made that any movement of the specimen perpendicular to the wire produced a negligible effect on the gage reading. The gage could thus be taken to be measuring deflections unidirectionally. The deflections were measured electronically at quarter points along the specimen by potentiometers, using four at each level, equally spaced around the tubular column circumference. Further, a manual technique was also carried out by using dial gages at mid-height only. Again, four dial gages were used equally spaced around the column circumference. Figure 3.13 shows photographs of this measuring system.

Measurement of spherical bearing head rotations also presented a minor problem. Rotations in two perpendicular directions of the bottom bearing block could be readily measured manually with a dial gage and spirit level apparatus (see Fig. 3.14). Using this system

the slope of the base plate could be measured relative to a steel arm which was maintained horizontal with the aid of the spirit level.

However, this same procedure was impractical for the measurement of top head rotation because measurements were needed to be made at a potition not readily accessible at an elevation of up to 12 m (40 ft). This problem was solved with the use of two plumb bob-type rotation gages in which the curvature of a sheet metal plumb bob support was measured with electric resistance strain gages. A separate calibration of the gages was required. Two such gages were required to measure rotation in two perpendicular directions.

Alignment of each test specimen also requires some comment. Ideally, alignment is a geometric condition in which the center of each end of the specimen being tested is aligned with the center of the spherical bearing block at that end. This is quite different to a stub column test in which alignment may be ensured by a process of trial-and-error loading until equal straining is noted at points on a section circumference. For these tests, the best possible alignment was obtained and then the unintentional end eccentricities noted. These noted eccentricities are recorded in Table 3.4, but it is clear that these are approximations only to the true end eccentricities. (The sign convention used in Table 3.4 is illustrated in Fig. 3.17.) The method of measurement did not allow very accurate determination of end eccentricities, although the results do show that the eccentricities observable tended to be very small. The end eccentricities, of course, could be considered as the source of an unintended,

applied bending moment which was proportional to the applied axial load. Observations were, however, made of axial strains at low axial loads to ensure that no gross end eccentricities were being introduced, and frequently it was found that little, if any bending curvature was being generated.

The axial load was applied in increments, with the size of the increments varying depending on how close to the expected buckling load was the applied axial load. After each increment of load had been applied the column specimen was left to attain equilibrium, if necessary, and the static readings of column behavior (axial strain, lateral deflection and end rotation) noted.

3.8 Long Column Testing - Results and Discussion

The axial load-lateral deflection curves obtained from measurements taken at mid-height of each specimen have been reported in Ref. 67. It was characteristic that for most specimens some lateral movement was observable at approximately seventy to eighty percent of the recorded maximum column axial load. Furthermore, buckling was a sudden phenomenon, coupled with an almost instantaneous adoption of relatively large lateral deflections. Frequently, deflections in this post-buckling range were difficult to measure.

It can be seen from Table 3.5 that there were two modes of buckling failure observed on specimens tested - a general inelastic instability (shown in Fig. 3.16a) characterized by general yielding of the specimen material at the failure location and little cross

sectional distortion, and an interactive instability (shown in Fig. 3.16b) characterized by high cross-sectional distortion, occurring at a very localized cross section at the time of buckling. Examination of Table 3.5 shows that interactive buckling was the final failure mode for all specimens of 0.56 m (22 in) outside diameter, and that general inelastic instability characterized the sections of smaller outside diameter. Furthermore, the axial load-lateral deflection curves of Ref. 67 show that the interactive instability (characterized by high localized cross-sectional distortions) leads to a rapid, catastrophic reduction in load-carrying capacity of a column, while the reduction in load-carrying capacity for those members buckling in a general inelastic instability mode tends to be much more gradual, with a higher proportion of the buckling load capacity retained at relatively large lateral deflections.

Figure 3.15 shows one of the columns after testing. The specimen shown is Specimen 10, and the photograph clearly shows the specimen to be over three stories in height. Furthermore, the location of interactive buckling failure is clearly visible just above midheight.

It appears that the transition from general inelastic instability as the buckling failure mode to the interactive buckling failure mode occurs at a (D_o/t) ratio in the range of 50 to 70 for all slenderness ratios tested. The maximum column strength will be shown in subsequent plots to be apparently independent of the failure mode, although it is recognized that the failure mode has an important role in post-buckling behavior of columns.

Table 3.6 shows pertinent column specimen buckling loads, derived experimentally. Figure 3.18 defines both "static" axial buckling load, P_s, and "dynamic" axial buckling load, P_d, as obtained during testing. The "static" buckling load is essentially the maximum static load the column sustained corresponding to a zero strain rate, whereas the "dynamic" buckling load is taken as the maximum load the specimen sustained during loading. The dynamic-to-static maximum load ratios varied in the range $(P_d/P_s) = 1.02$ to 1.07. The difference between these "static" and "dynamic" loads was noticeable only as the axial load applied to the column specimen approached the column buckling load, and the higher ("dynamic") load was the load reached when the incremental load had been applied to the column. Then, as the column adopted its equilibrium lateral deflection profile (which probably involved some inelastic straining of the material), the applied load on the column tended to drop slightly to its "static" value. Table 3.6 also gives the column buckling loads as a function of the appropriate stress values.

The test results are presented in graphical form for comparison with various column buckling curve design proposals. Figure 3.19 shows these results plotted on a basic AISC-CRC Ultimate Strength Curve. This curve is the basis of allowable axial stresses for columns given by the 1969 Specification of the American Institute of Steel Construction (76). Figure 3.19 is plotted on a "static" loading basis, with "static" column buckling loads and static yield strength values used. The "barbell" plotted for each test reflects the uncertainty in effective lengths of specimens at buckling. It

should be noted that the AISC-CRC Ultimate Strength curve was developed mainly on the basis of buckling tests conducted on hot-rolled, wide-flange steel shapes. The present comparison shows that these fabricated tubular members tested also apparently exhibited a strength close to that implied by the AISC-CRC column curve for the range of column effective length tested, although it is by no means possible to say that this curve is a lower bound of experimental results.

Figure 3.20 compares the "static" column buckling loads obtained experimentally to the ultimate strength column curve "a" proposed by Bjorhovde (13). In the range of column effective length tested this curve shows only minor changes from the AISC-CRC column buckling curve. However, even in this range the multiple column curve gives slightly higher predicted buckling loads than the AISC-CRC column curve and this is further removed from being a lower bound to experimental results.

This graphical comparison is not complete without reference to Fig. 3.7, where the experimental results are superimposed on the column curves predicted by stub column test results. In the range of column effective lengths tested, the stub column predictions appear to give a good lower bound to observed results.

4. SHORT COLUMN ANALYSIS - THEORY AND RESULTS

4.1 Introduction

As a prelude to a long-column buckling analysis of a fabricated tubular column, a nonlinear analysis of a column section of unit height was undertaken. (It is also proven that only by derivation of the behavior of such a section under axial load and biaxial bending moment could the relative importance of the various residual stresses in such a section be gaged.)

The purpose of the investigation described in this chapter was thus to derive bending moment-axial load-curvature curves (that is, M-P-Φ curves) for the section with various combinations of applied loads and residual stresses considered. Of particular importance is the inclusion of residual stresses in two perpendicular directions. The curves derived represent the behavior of the section subject to the applied loads, and, by varying the combinations of residual stresses considered, the relative importance of these factors could be determined.

In this chapter the mathematical formulation of the derivation of the M-P-Φ curves is briefly introduced, followed by a discussion of the method by which stresses in two perpendicular directions are included, recognizing the need to allow interaction between these stresses. Since the experimental derivation of residual stresses is considered in Chapter 3, the residual stress assumptions are treated only briefly here, although some mention of the basis of these

assumptions is important for interpretation of the results. The chapter concludes with sections describing means of verification of the results, and a summary of the results obtained, with appropriate conclusions.

4.2 Mathematical Formulation

The basic theoretical derivation of short column behavior is given here briefly for completeness. The method is known as the tangent stiffness method, and this formulation is based on that used by Santathadaporn and Chen (1), among a number of investigators. This introduction is necessary in order to appreciate the modifications presented subsequently.

For a biaxially loaded column the appropriate generalized stresses for use in analysis are the perpendicular bending moments M_x and M_y and the axial force P. The corresponding set of generalized strains are bending curvatures Φ_x and Φ_y and axial strain ϵ_o. The following force and deformation vectors are thus defined:

$$\{f\} = \begin{Bmatrix} -M_x \\ M_y \\ -P \end{Bmatrix} \tag{4.1}$$

and

$$\{X\} = \begin{Bmatrix} \Phi_x \\ \Phi_y \\ \epsilon_o \end{Bmatrix} \tag{4.2}$$

The generalized stresses and strains are shown is Fig. 4.1 in positive direction. The orientation of the x- and y-axes is defined by the location of the longitudinal weld, marked arbitrarily in Fig. 4.1. The object of the analysis is to derive the deformation history of the cross section given its loading history.

Since the behavior of the section depends on the previous load history of the section, especially when some parts of the section are behaving inelastically, it is possible only to establish the relationship between infinitesimal generalized force increments, $\{\dot{f}\}$, and the corresponding infinitesimal generalized deformation increments $\{\dot{X}\}$.

Santathadaporn and Chen (1) showed that the following relationship between $\{\dot{f}\}$ and $\{\dot{X}\}$ may be derived for the structure:

$$\begin{Bmatrix} -\dot{M}_x \\ \dot{M}_y \\ -\dot{P} \end{Bmatrix} = \begin{bmatrix} Q_{11} & Q_{12} & Q_{13} \\ Q_{21} & Q_{22} & Q_{23} \\ Q_{31} & Q_{32} & Q_{33} \end{bmatrix} \begin{Bmatrix} \dot{\Phi}_x \\ \dot{\Phi}_y \\ \dot{\epsilon}_o \end{Bmatrix} \tag{4.3}$$

in which Q_{ij} is defined as

$$\begin{aligned} Q_{11} &= \int E\, y^2\, dA \\ Q_{22} &= \int E\, x^2\, dA \\ Q_{33} &= \int E\, dA \\ Q_{12} &= Q_{21} = \int E\, x\, y\, dA \\ Q_{13} &= Q_{31} = -\int E\, y\, dA \\ Q_{23} &= Q_{32} = -\int E\, x\, dA \end{aligned} \tag{4.4}$$

Equation 4.3 may be rewritten as

$$\{\dot{f}\} = [Q]\ \{\dot{X}\} \tag{4.5}$$

The above set of simultaneous equations was derived for the whole cross section. However, the integral expressions of Eq. 4.4 may only be evaluated directly for the entire cross section as long as no part of that section is exhibiting inelastic behavior. As soon as any part of the section deforms inelastically, the integrals may not be calculated directly, because the modulus of elasticity, E, then changes at different parts of the section.

To overcome this problem the section is divided into elemental areas, as shown in Fig. 4.2. Each elemental area, or fiber has an elemental area dA and is at a distance x from the y-axis and at a distance y from the x-axis. Provided that deformation compatibility is enforced for all elements of a cross section, the expressions of Eq. 4.4 may be evaluated for each elemental area in turn, where each elemental area has an "effective" modulus of elasticity, and the integrals may be expressed as summations of these contributions from all elemental areas composing the section.

For the special case when the entire cross section is within the elastic stress range, it can be seen that

$$Q_{ij} = 0 \quad (i \neq j) \tag{4.6}$$

The moment-curvature relationships are derived by varying only one of the variables of $\{\dot{f}\}$ at one time (that is, creating a known

$\{\dot{f}\}$) and iterating to a solution for $\{\dot{X}\}$. The addition of $\{\dot{X}\}$ to $\{X\}$ yields a new $\{X\}$. This process continues until the known applied loads $\{f\}$ are in equilibrium with the displacements $\{X\}$.

In order to provide a reference for moment calculation it is usual to calculate the fully plastic bending moment of a tubular cross section, M_p, given by

$$M_p = Z_p \sigma_y \tag{4.7}$$

where Z_p = plastic section modulus, which, for a tubular section is

$$Z_p = \frac{D_o^3}{6}\left[1 - \left(1 - \frac{2t}{D_o}\right)^3\right] \tag{4.8}$$

In Eqs. 4.7 and 4.8, σ_y = material yield strength

t = wall thickness of cross section

D_o = outside diameter of cross section.

Similarly, a reference for curvature calculation is required, and this is taken to be the curvature at first yield of a cross section under uniaxial bending, for which the appropriate curvature is

$$\Phi_{yy} = \frac{2}{D_o}\left(\frac{\sigma_y}{E}\right) \tag{4.9}$$

Just as for moment and curvature, it is desirable that a reference load and a reference strain are available for axial load and axial strain respectively. For axial load, the reference load, P_y, is taken to be the load at which the cross section is completely yielded when no other loads are applied, that is,

$$P_y = \sigma_y A \tag{4.10}$$

If there were no other loads on the section, then, for an elastic-perfectly plastic material, the load P_y would be reached at the reference axial strain ϵ_y given by

$$\epsilon_y = \frac{\sigma_y}{E} \tag{4.11}$$

It must also be predetermined the order in which loads are applied to a section, remembering that it is desired to eventually trace a moment-curvature curve. For the purposes of this investigation it was decided to first apply the required axial load (P), and, of course, compute equilibrium deformations as this was done. Then the moment about the x-axis (M_x) was similarly applied, the axial load remaining constant, and a new set of equilibrium deformations was derived. Because of the possibility of inelastic section behavior as the above axial load and bending moment were applied, it was necessary to apply the loads in a step-wise, incremental manner as outlined by the theory. Both axial load and moment about the x-axis were then held constant, and the moment-curvature relationship for a gradually increasing applied moment about the y-axis (M_y) was developed in a step-wise manner.

4.3 Inclusion of Two-Dimensional Stresses

In order to include both longitudinal and circumferential residual stresses in the analysis it was necessary to introduce a two-dimensional material yielding criterion. Of the number of such

theories available, the Tresca yield criterion was chosen because of its relative simplicity. (One alternative available is to use the Von Mises yield criterion, but, since the maximum difference between these two criteria is eight percent, the choice of yield criterion is not considered to be critical.) It was assumed that the thickness of a tube wall was small, so that no significant radial stresses could be sustained. This assumption allowed the investigation to be considered as a plane stress analysis.

With the section divided into elemental areas as described in Section 4.2, each elemental area was then considered to be subjected to a two-dimensional state of stress, which may be different from the state of stress of other elemental areas, and which could be determined uniquely given the loading on the section and the initial residual stress patterns. The situation was complicated by the fact that stresses in perpendicular directions were linked by an effect similar to a Poisson's ratio effect, so that changes in stress in one direction may affect stresses in a perpendicular direction. To be strictly accurate the Poisson's ratio effect should be considered to operate during both elastic and inelastic behavior of an elemental area. However, the Poisson's ratio effect will be smaller during elastic behavior than during inelastic behavior. To allow for this, provision would need to be made for a variable factor, depending on whether each elemental area was behaving elastically or inelastically. While it is possible to include this, it was considered that the section behavior could be adequately modelled if it was assumed that there was no significant Poisson's ratio effect while the

material remained elastic. The rationale for this assumption was based on the fact that the Poisson's ratio effect could be considered a second order effect, but the verification of it depends on the results obtained, and these are influenced greatly by the magnitudes of the perpendicular stresses, in particular, by the magnitudes of circumferential residual stresses.

Once an elemental area of the section had yielded, a change in the applied longitudinal stress (whether by application of axial load or of bending moment) causes a change in the circumferential residual stress, where possible, by an effective Poisson's ratio, assumed to have a value of 0.5. This interaction is only effective when either the longitudinal stress is tensile and the circumferential stress is compressive, or vice versa.

It is now appropriate to consider a possible stress history of an elemental area of a cross section on the Tresca yield diagram of Fig. 4.3. There are a variety of possibilities which may occur during the loading history of this elemental area and most of these are self-evident. However, the solution technique for one of the more complex possibilities is shown for example purposes in Fig. 4.3. Assume that the combination of circumferential and longitudinal residual stresses is such that the initial stress state of the elemental area is represented by point A. Now, assume further that a compressive load is being applied to the elemental area (for example, by the application of axial load), such that the stress combination of the element moves along AB while the element remains elastic. At

point B the element reaches first yield. As loading of the element is continued, still in compression, along path BC there is a relieving of circumferential residual stress as well as a continuing reduction in the effective modulus of elasticity for the elemental area (see below). If load was applied such that the element continued to be loaded in compression, the stress state would eventually be represented by point E, at which point the circumferential residual stress has been completely relieved and the elemental area is not able to sustain any more compressive load.

However, it may be that application of compressive load to the elemental area ceases at point C on Fig. 4.3. This could happen if the applied load was changed, for example, from applied axial load to applied bending moment. Under these circumstances it is possible that, after point C, a tensile incremental load is being applied to the elemental area. The stress history would then follow line CD, for the elemental area is then unloading elastically in the longitudinal direction while the circumferential residual stress remains unchanged after point C. Since the area is now behaving elastically it once again has a full elastic modulus of elasticity.

Another problem which had to be considered was the continuing reduction in the effective modulus of elasticity as the section was loaded along line BCE of Fig. 4.3. As an approximation, it was assumed that this effect could be modelled by adopting an effective modulus of elasticity which varied as shown in Fig. 4.4. The point B in Fig. 4.3, the stress state at first yielding of the element,

may be represented by σ_a, the first yielding stress, in Fig. 4.4. The small step in the modulus of elasticity assumed at the material yielding strength was adopted in order to ensure that full yield strength is finally reached for the element. The basis of the assumed variation of modulus of elasticity (given in Fig. 4.4) is somewhat pragmatic. It is consistent with the knowledge that the effective modulus of elasticity must decrease as the stress is increased above the first yield stress, σ_a, and that, when the axial stress reaches material yield strength the effective modulus of elasticity must be zero. However, the bilinear variation adopted is merely an assumption consistent with these known phenomena.

A brief comparison of the complications introduced by the inclusion of two-dimensional stresses with those when only uniaxial stresses are considered leads to a greater understanding of the power of this approach. If one considers only uniaxial stresses and further makes the assumption that the section material performs in an elastically-perfectly plastic manner (a common assumption for steel) then the evaluation of the expressions of Eq. 4.4 becomes relatively simple. As the integral expressions are derived by summation of the expressions for each elemental area over the entire cross section, each element has a modulus of elasticity equal either to the elastic value or to zero, depending on whether or not the material of that elemental area has yielded. For such materials, an elemental area cannot contribute further to section load-carrying capacity once it has yielded (unless, of course, there is a load

reversal), and so its contribution is simply not included in the integral summations over the cross-sectional area.

While still considering uniaxial stresses, it is possible without difficulty to abandon the elastic-perfectly plastic material yielding assumption, and use instead, perhaps, a gradual transition from elastic to plastic material behavior. Whatever assumption for material yielding was adopted, however, it would need to be predetermined in the form of a stress-strain diagram.

The work reported here contributes a further step in this progression in that stresses in two perpendicular directions are now considered. It is not possible, now, to predetermine the axial stress-axial strain diagram which would be followed by an elemental area, since each elemental area has its unique stress-strain diagram, which may differ from that followed by other elemental areas on the cross section. The particular stress-strain diagram followed by a particular elemental area is dependent on the two-dimensional stress state of the element. All the work in this investigation had the capacity to consider the effects of two-dimensional stresses, but the above comparison with earlier uniaxial stress investigations gives a better indication of the complexity of the method and the power of the approach.

4.4 Inclusion of Residual Stresses

The problem of the inclusion of residual stresses in the analysis is vital, as it is this factor which renders the problem

non-trivial. Furthermore, the modification to previously reported investigations (discussed in Section 4.3) which enables the effects of two-dimensional stress states to be included, was prompted by a perceived need to allow for residual stresses to be included in two perpendicular directions.

It is the purpose of this section to discuss briefly the particular residual stress patterns included in the analysis, although, for the most part they are the product of experimental results presented in Chapter 3 of this thesis. It has been a relatively recent development that the residual stress patterns likely in a fabricated tubular column could be determined reasonably accurately, and this explains the relatively diverse theoretical approximations of residual stresses used by other investigators (see, for example, Ref. 4).

In those cases where a longitudinal stress pattern was used in this analysis, it was of the form shown in Fig. 4.5, which corresponds to the measured longitudinal residual stress pattern presented in Chapter 3. For convenience, the measured stress distribution has been reduced to a series of straight line approximations.

The inclusion of circumferential residual stresses presented a somewhat more difficult problem. The most obvious approach was to include the circumferential residual stress pattern measured and presented in Chapter 3, but there was also a desire to indicate whether in fact the particular circumferential residual stress pattern adopted had any significant affect on the moment-curvature

curve derived. For this reason another similar circumferential residual stress pattern was also used, and this second pattern was derived from a very brief "first approximation" of the phenomena involved. There were thus two distinct circumferential residual stress patterns assumed at different stages of the investigation, and these are distinguished below as the measured circumferential residual stress pattern (experimentally derived) and the assumed circumferential residual stress pattern (an assumed distribution, based on "first approximation" conditions).

It is necessary here to outline the basis of the assumed circumferential residual stress pattern, since it is used for comparison purposes in the results. Of course, it is not intended that the assumed circumferential residual stress pattern be taken as the correct circumferential residual stress pattern, as it is much more likely that the measured circumferential residual stress pattern reflects the true residual stress situation in a fabricated tubular column. When flat plate is cold-rolled to form a cylindrical "can" it was assumed that fully-plastic deformation was induced in the material, with a resulting stress distribution through the thickness of the wall of the tubular column shown in Fig. 4.6(a). It was then assumed that the rolled plate was released, and allowed to "spring back". This process was taken to consist of an elastic unloading process which induced a stress distribution through the column wall similar to that shown in Fig. 4.6(b). The maximum fiber stress was taken as 1.5 σ_y (where σ_y is the yield strength of the material), because it was considered that all of the bending moment

applied to the plate in the rolling process must be released during the "spring back" phenomenon. Addition of the stress distributions shown in Figs. 4.6(a) and 4.6(b) yielded the distribution shown in Fig. 4.6(c), which was the assumed circumferential residual stress distribution.

A comparison of measured and assumed circumferential residual stress patterns is presented in Fig. 4.7. It can be seen that the two distributions differ considerably, and also that the measured distribution is not in bending moment equilibrium as is the assumed distribution. It is noted, however, that any free body cut from the fabricated tubular section is in complete moment and force equilibrium, as is the entire cross section. Although not an accurate assessment, the ability to include an "assumed" circumferential residual stress distribution permits study of the effects of the magnitudes of circumferential residual stresses on derived M-P-Φ curves.

4.5 Verification of the Analysis

This section is concerned with use of available methods to verify, as far as possible, the results obtained from this analysis. In all cases, the assumed properties of the specimen were:

D_o = outside diameter of the tube = 560 mm (22.0 in)

t = wall thickness = 7.93 mm (5/16 in)

σ_y = material yield strength = 248 MPa (36.0 ksi)

However, since the results were nondimensionalized, they were not affected by the section properties assumed. These section properties

were adopted for they were the specified properties of some specimens tested in the experimental test program reported in Chapter 3.

The first verification is the shape factor of the moment-curvature curve for a perfect thin-walled tube, that is, the ratio of plastic moment to first yield moment for a member with moment applied in only one direction, and with no applied axial load. The empirically verifiable value for shape factor of 1.27, was indeed derived.

Another check for a tubular cross section with no residual stresses included is the analytical expressions reported by Ellis (6), which allow derivation of moment-curvature curves. For completeness, the analytical expressions derived by Ellis are included here.

Ellis assumed the stress state of a cross section, and proceeded from this to derive the applied loads and deformations of the section. The three possibilities of stress state considered are shown in Fig. 4.8 and correspond to:

(i) entire cross section behaving elastically (Fig. 4.8a),

(ii) one zone of the section behaving inelastically (Fig. 4.8b), and

(iii) two zones of the section behaving inelastically (Fig. 4.8c).

In the diagrams of Fig. 4.8, each of the possibilities of stress state is given in terms of a diagram showing zones of material inelasticity and of assumed stress diagrams. An elastic-perfectly plastic stress-strain diagram has been assumed for the material.

In Fig. 4.8 the intermediate stresses σ_1 and σ_2 are defined, and in these expressions use is made of the plastic moment, M_p, given in Eq. 4.7, and the yield load of the section, P_y, given in Eq. 4.10.

For case i, elastic material behavior throughout the section, the following relationships are valid:

$$\frac{P}{P_y} = \frac{\sigma_1 - \sigma_2}{2} \tag{4.12}$$

$$\frac{M}{M_p} = \frac{\pi}{8}(\sigma_1+\sigma_2) \tag{4.13}$$

and

$$\frac{1}{\rho} = \frac{M}{M_p}\frac{4}{3\pi} \tag{4.14}$$

where $\frac{1}{\rho}$ is a nondimensional curvature given by

$$\frac{1}{\rho} = \frac{E}{3\,\sigma_y} R\,\Phi_y \tag{4.15}$$

and R = mean radius of the tubular section.

For case ii, plastic material behavior in one zone only, the following relationships are given by Ellis:

$$\frac{P}{P_y} = -\left[1 - \frac{(1+\sigma_2)}{\pi(1+\sin\theta)}\left\{\sin\theta\left(\theta + \frac{\pi}{2}\right) + \cos\theta\right\}\right] \tag{4.16}$$

where θ is defined in Fig. 4.8(b),

$$\frac{M}{M_p} = -\left[\frac{(1+\sigma_2)}{(1+\sin\theta)}\left\{\frac{\sin\theta\,\cos\theta}{4} + \frac{\theta}{4} + \frac{\pi}{8}\right\}\right] \tag{4.17}$$

and $$\frac{1}{\rho} = -\frac{(1+\sigma_2)}{3(1+\sin\theta)} \tag{4.18}$$

for case iii, plastic material behavior in two zones, the following relationships are produced:

$$\frac{P}{P_y} = \frac{2\beta}{\pi} + \frac{2}{\pi}\left(\frac{\sin\theta}{\sin\theta-\sin\beta}\right)(\theta-\beta) + \frac{2(\cos\theta-\cos\beta)}{\pi(\sin\theta-\sin\beta)} \tag{4.19}$$

where β is defined in Fig. 4.8(c),

$$\frac{M}{M_p} = -\cos\beta - \frac{\sin\beta(\cos\theta-\cos\beta)}{(\sin\theta-\sin\beta)} - \frac{(\theta-\sin\theta\cos\theta-\beta+\sin\beta\cos\beta)}{2(\sin\theta-\sin\beta)} \tag{4.20}$$

and $$\frac{1}{\rho} = \frac{-2}{3(\sin\theta-\sin\beta)} \tag{4.21}$$

A comparison of the moment-curvature relationships derived using the tangent stiffness method and using Ellis' equations shows that for the load cases considered, the curves derived are virtually identical, a good confirmation of the method.

Another check, this time of the ultimate plateaux of the moment-curvature curves, is available. Chen and Atsuta (7) tabulated interaction curves for perfect hollow circular sections using exact interaction relations for doubly symmetric sections. The values of ultimate load combinations tabulated represent the plateau of the moment-axial load-curvature curves derived in this analysis.

4.6 Results and Discussion

A representative sampling of results obtained from this analysis is presented in Fig. 4.9 through 4.12. The following nondimensional

ratios are used in the graphs:

$$m_x = \frac{M_x}{M_p} \tag{4.22}$$

and

$$p = \frac{P}{P_y} \tag{4.23}$$

where M_x and P are the applied bending moment about the x-axis and applied axial load respectively, while M_p and P_y are defined in Eqs. 4.7 and 4.10 respectively. The term M_y is used to denote an applied bending moment about the y-axis, with the corresponding curvature Φ_y, so that the graphs presented are a nondimensional form of applied moment about the y-axis versus a nondimensionalized curvature about the y-axis. For the purpose of comparison only, all curves presented were derived with the longitudinal weld in the same position on the section, that is, on the y-axis where the y-coordinate of its location has its largest positive value.

As expected, for a particular combination of applied p and m_x (as defined in Eqs. 4.22 and 4.23), the M-P-Φ curves, whether including residual stresses or not, are all asymptotic to the same ultimate plateau value. For the purposes of clear presentation the curves of Figs. 4.9 through 4.12 have been presented with offset origins to clearly separate curves of individual load combinations.

In Fig. 4.9 nearly every load combination has four graphs plotted. Typically these are: the curve with no residual stresses included (perfect tube), with longitudinal residual stresses only included, with longitudinal and measured circumferential stresses

included, and with longitudinal and assumed circumferential residual stresses included.

While not affecting ultimate moment plateaux, residual stresses tend to affect the knee portion of the moment-curvature curves where they produce greater curvature for a given applied moment than the curvature of a perfect tubular section. This effect is primarily observable at applied moments M_y greater than about sixty percent of the ultimate moment capacity for that particular load combination. Furthermore the effects of residual stresses seems to be cumulative, in that the M-P-Φ curves are affected more with residual stresses included in two perpendicular directions than when residual stresses are included in a direction only parallel to the direction of section loading.

The magnitude of residual stresses included also has an effect. As was clear from Fig. 4.7, the assumed circumferential residual stress distribution tends to have larger residual stress magnitudes than the measured circumferential stresses (depending somewhat on location within the cylinder wall). In all cases it was noted that the use of the assumed circumferential residual stresses in conjunction with longitudinal residual stresses led to a greater effect on the knee portion of the moment-curvature curve than when measured circumferential residual stresses were used in conjunction with longitudinal residual stresses. While this result might have been anticipated, this investigation is the first opportunity to verify it.

Another trend which is not new, but which is confirmed in this study, is that the effects of residual stresses tend to become less pronounced as larger combinations of p and m_x are applied.

Perhaps one of the more surprising results of this study is that the residual stresses, as measured and reported in Chapter 3, have a relatively minor effect on section bending properties. This leads to the conclusion that it may not really be necessary to include all residual stresses in the column buckling analysis to be reported in Chapter 5, where applied axial loads are a substantial proportion of the section yield load P_y. This suggestion is a result of the observed tendency for less effect on the knee portion of the M-P-Φ curves as applied loads are greater and also due to the relatively localized and small residual stress values. In practice, although the long column analysis has the capacity to include circumferential residual stresses, all results have been obtained using longitudinal residual stresses only, as discussed in Chapter 5.

5. LONG COLUMN ANALYSIS - THEORY AND RESULTS

5.1 Introduction

As a prelude to the development of a theoretical model for the behavior of long fabricated tubular columns, reference is made in this dissertation to a long column testing program (Chapter 3) and a theoretical investigation of the cross section of a short tubular column (Chapter 4). In this chapter the theory is outlined for the model of a long fabricated tubular column, and a brief study is undertaken to determine theoretically the dependence of column behavior on various parameters. The results of such a long column model are the ability to model an individual long column and its behavior, and also the derivation of a long column buckling curve. The derivation of such a column buckling curve would allow subsequent comparison with other predictions and also with available experimental data. These comparisons are considered in Chapter 6. This chapter derives the theoretical bases on which subsequent comparisons are to be based.

Before commencing the theoretical derivation considered herein, it is desirable to reemphasize the difficulties to be overcome by this analysis. The first problem, that of residual stresses (in two perpendicular directions), was considered in Chapter 4 in the discussion of a short tubular column, but, of course, the capacity of including residual stresses must be an integral part of the long column behavior consideration also. The situation is further complicated by the fact that the fabricated tubular column does not

have uniform properties along its length. The fact that the column is made up of a number of short "cans" (as explained in Chapter 1) introduces the possibility of different sections along the column having different behavior characteristics because of the weld staggering. Furthermore, it is common practice in the manufacture of prototype, long, fabricated tubular columns to include steel from different heat lots, which introduces the possibility of sections having different material properties as well as different behavior properties. These properties, both material and behavior, would clearly vary in a highly discontinuous manner along the length of a column, which makes it impossible to consider the column to be modelled in the same way as has previously been done. It has been common practice to consider a column to have constant properties along its length, or uniformly varying properties along its length.

Another important determinant of long column behavior is out-of-straightness. In order to adequately model real long column behavior it is necessary to be able to include an essentially-random, measured out-of-straightness distribution along the column length (in two perpendicular directions). To allow consideration of changes in material and behavior characteristics along a column length, as well as a highly variable out-of-straightness distribution, it was decided to use a second-order Newton-Raphson iterative technique, in which discrete locations, or stations, along the column length are considered. At each station independent section properties may be considered. The out-of-straightness can also be specified independently at each considered location.

It is necessary also to briefly consider the limitations placed on this analysis by the method assumed. First of all, the method will not allow any consideration of post-buckling behavior, as the second-order Newton-Raphson iterative technique uses the concept of vanishing stiffness as the criterion for ultimate, axial load of a column. Furthermore, distortion of the cross section has not been considered in the analysis (and may not be readily included). While it is true that considerable cross-sectional distortion was noticed in some long column specimens tested (see Chapter 3), the observable distortions occurred during post-buckling behavior. It was thus assumed that the assumption of no cross-sectional distortion would not affect the pre-buckling behavior, nor computation of buckling loads. Based on experimental results, it was considered that there were no significant deviations from perfect tubular column roundness introduced during manufacture, and thus in the method reported here it has been assumed that all sections along a tubular column are perfectly round and remain so throughout the loading history of the column.

The development considered in this chapter has also ignored any affects of the circumferential welds between "cans". Of course, such welds will introduce residual stresses in each end of each can. However, the induced residual stresses will be circumferential in direction (that is, perpendicular to the direction of loading), and are likely to be highly localized. In Chapter 4 it was discovered that circumferential residual stresses tend to have a second-order

effect on column behavior. Experimental evidence, composed of visual evidence of long column tests suggests that the circumferential welds between cans were not responsible for premature column buckling (and may, indeed, have had the reverse effect). For, all these reasons the assumption that circumferential welding has no effect on column behavior or strength appears reasonable.

In this chapter the theoretical development of the analytical method is traced, followed by available verification of the analysis. Derivation of upper and lower bounds of a theoretical column buckling curve (as a result of the inclusion of residual stresses) is an important result of this analysis. Tangent modulus predictions of column buckling are also included in an attempt to decide whether such predictions, considered satisfactory for I- and H-sections, are satisfactory indications of column strength for long fabricated tubular columns. A short study follows in which various parameters which may influence column behavior and performance are varied and the effects noted. These factors include the dependence of column buckling load on the initial fabricated out-of-straightness of a column, the effect of varying the number of stations considered along the column length, and the effect of the proportion of column length considered to behave inelastically. The chapter concludes with a discussion of the possibility of refining the upper and lower bounds of column buckling curve previously derived.

5.2 Theoretical Development

In order to derive the axial load versus lateral deflection behavior of an imperfect tubular column, with fabrication imperfections included, use was made of the second-order Newton-Raphson iterative procedure for systems of nonlinear equations. This method uses the concept of vanishing stiffness as the criterion for ultimate column axial load, thereby precluding examination of post-buckling behavior.

This method of column analysis has been reported by Virdi and Dowling (35), but, since substantial alterations to the theory have been necessary for the analysis of a long fabricated tubular column, the derivation is treated in some detail here. The basic approach of this method can readily be described. If a lateral deflection profile is assumed for a column, then curvatures at discrete points along the column may also be derived. With the use of an appropriate moment-axial load-curvature curve, the curvature at each section can be transformed to a bending moment at that section. When the section moment is divided by the section axial load, and any initial displacements subtracted, a new, updated deflection profile is obtained.

Up to this point it has been assumed that conditions remained unchanged during the updating process. The Newton-Raphson iterative procedure allows inelastic effects and end restraints to be included, by means of a Jacobian matrix. The original deflection profile, the updated deflection profile and the assembled Jacobian matrix are all used to derive an improved deflection profile, which is then compared

to the initial assumption. This resulting improved deflection profile is used as the new assumed deflection profile and the process is repeated until satisfactory iterative stabilization has been achieved.

With this brief outline of the technique it is possible to outline the derivation in more mathematical terms. For a given column, under a given combination of end loads, there may be a varying curvature all along the column length, and such curvatures cause internal bending moments which are in equilibrium with the applied external forces. If, at a station s, within the column length (defined by Fig. 5.1): M_{xs} and M_{ys} are the two perpendicular section bending moments; e_{xs} and e_{ys} are the corresponding initial eccentricities of the centroid of the section from the effective line of action of the applied load, and u_s and v_s are the x- and y-deflections respectively of this point of the column, then

$$M_{xs} = P(e_{xs}+u_s) \tag{5.1}$$

$$M_{ys} = P(e_{ys}+v_s) \tag{5.2}$$

It is usual to assume that the small deflection theory holds, such that total curvatures in the x- and y-planes may be defined as

$$\Phi_x = -\frac{\partial^2 u}{\partial x^2} \tag{5.3}$$

and

$$\Phi_y = -\frac{\partial^2 v}{\partial y^2} \tag{5.4}$$

respectively.

If u_o and v_o are the initial deflections (out-of-straightnesses) of the column in an unloaded state, the initial curvatures may be written as

$$\Phi_{ox} = - \frac{\partial^2 u_o}{\partial x^2} \tag{5.5}$$

and

$$\Phi_{oy} = - \frac{\partial^2 v_o}{\partial y^2} \tag{5.6}$$

and the net section curvatures due to loading as

$$\varphi_x = \Phi_x - \Phi_{ox} \tag{5.7}$$

and

$$\varphi_y = \Phi_y - \Phi_{oy} \tag{5.8}$$

If it is assumed that discrete points are chosen at which to evaluate the second-order differential expressions of Eqs. 5.3 through 5.6, and that these points are at an equal spacing, h, then the finite difference operators yield expressions of the form

$$\Phi_{xs} = - \frac{\partial^2 u_s}{\partial x^2} = \frac{1}{h^2}\left[-u_{s-1} + 2u_s - u_{s+1}\right] \tag{5.9}$$

where u_s deflection in the x-direction, close to the exact solution, at node s. This approach was used by Virdi and Dowling (35).

For the analysis of fabricated tubular columns, however, the assumption of a constant interstation distance, h, is not satisfactory. The lengths of the short "cans" from which a long column is fabricated, are of highly variable length, and thus it is desirable to have a variable interstation length. In the following derivation it may be assumed that the section properties of a

particular station are identical to the section properties of locations close to that station. It could then be considered that the section behavior of a station represents the behavior of a short column of which the station considered is near the mid-height. This gives an alternative point of view from which to approach the necessity of allowing a variable interstation distance.

If the varying interstation distances are defined as shown in Fig. 5.2, then Eq. 5.9 may be rewritten in the form

$$\Phi_{xs}^{\,k} = -\frac{\partial^2 u_s}{\partial x^2} = \frac{2}{h_s+h_{s-1}}\left[-\frac{u_{s-1}^{\,k}}{h_{s-1}} + u_s^{\,k}\left(\frac{1}{h_s}+\frac{1}{h_{s-1}}\right) - \frac{u_{s+1}^{\,k}}{h_s}\right] \tag{5.10}$$

where the superscript k has been added as a reminder that this is an iterative process, and that this could be considered to be the result after the (k-1)-th iteration. An analogous expression, using v instead of u, can be derived for y-direction curvature (i.e., for $\Phi_{ys}^{\,k}$).

Next, it is necessary to make use of the moment-axial load-curvature (M-P-Φ) relationships for station s. The development of these has already been considered in Chapter 4, and so it is not necessary to deal with their derivation here. Since the section axial load, P, and the curvatures φ_{xs} and φ_{ys} are known, the relevant stress resultants, $M_{xs}^{\,k}$ and $M_{ys}^{\,k}$, are derived using the appropriate M-P-Φ relationship. In practice, of course, it is not necessary to trace a whole M-P-Φ curve to obtain the stress resultants. Rather, with the curvatures given (and axial strain value computed from the

known axial load), it is possible to sum the effects over elemental areas of the cross section at each station, and compute the stress resultants directly.

Application of Eqs. (5.1) and (5.2) leads to new deflection vectors,

$$U_s^k = \frac{M_{xs}^k}{P} - e_{xs} \tag{5.11}$$

and

$$V_s^k = \frac{M_{ys}^k}{P} - e_{ys} \tag{5.12}$$

The Newton-Raphson iterative technique is used to compute a better solution for u_s^{k+1} and v_s^{k+1}, given by

$$u_s^{k+1} = u_s^k - (I_m - J)^{-1} \{u_s^k - U_s^k\} \tag{5.13}$$

and

$$v_s^{k+1} = v_s^k - (I_m - J)^{-1} \{v_s^k - V_s^k\} \tag{5.14}$$

where I_m is a unit matrix and J is a Jacobian matrix to be defined below. For the next iteration u_s^k and v_s^k are replaced by u_s^{k+1} and v_s^{k+1} respectively, and the iterative procedure repeated until, for a particular iteration r,

$$|u_s^r - U_s^r| \leq \epsilon \quad \text{for all s} \tag{5.15}$$

and

$$|v_s^r - V_s^r| \leq \epsilon \quad \text{for all s} \tag{5.16}$$

where ϵ is an arbitrarily selected small value.

Now, the Jacobian, J, has terms defined as

$$J_{ij} = \frac{\partial W_i}{\partial w_j} \tag{5.17}$$

where {W} and {w} are defined as

$$\{W\} = \begin{Bmatrix} U_1 \\ V_1 \\ \vdots \\ U_s \\ V_s \\ \vdots \\ U_{n+1} \\ V_{n+1} \end{Bmatrix} \text{ and } \{w\} = \begin{Bmatrix} u_1 \\ v_1 \\ \vdots \\ u_s \\ v_s \\ \vdots \\ u_{n+1} \\ v_{n+1} \end{Bmatrix} \tag{5.18) and (5.19}$$

For derivation of the elements of the Jacobian matrix, the total change in function {W} is separated into two components

$$\frac{\partial W}{\partial w} = \frac{\partial C}{\partial w} + \frac{\partial R_t}{\partial w} \tag{5.20}$$

where C defines the contribution of changes in curvature, and R_t defines the contribution of end restraints.

From Eq. (5.10) the various contributions due to curvature may be computed. In the following discussion, the superscript k has been deleted for clarity, although it is to be understood that

the expressions derived are for the k-th iteration in the iterative process. Considering a station, s, well away from the ends, Eq. (5.10) gives

$$\frac{\partial \varphi_{xs}}{\partial u_{s-1}} = \frac{-2}{h_{s-1}(h_s+h_{s-1})} \tag{5.21}$$

$$\frac{\partial \varphi_{xs}}{\partial u_s} = \frac{2}{h_s\, h_{s-1}} \tag{5.22}$$

and

$$\frac{\partial \varphi_{xs}}{\partial u_{s+1}} = \frac{-2}{h_s(h_s+h_{s-1})} \tag{5.23}$$

and thus

$$(-h_{s-1})\frac{\partial \varphi_{xs}}{\partial u_{s-1}} = (-h_s)\frac{\partial \varphi_{xs}}{\partial u_{s+1}} = \frac{h_s\, h_{s-1}}{(h_s+h_{s-1})}\frac{\partial \varphi_{xs}}{\partial u_s} = \frac{2}{h_s + h_{s-1}} \tag{5.24}$$

A small change, Δ_{xs}, in the x-deflection of node s produces a change in the curvature φ_{xs} and thus in both the total curvature at that section (that is, the vector sum of the curvature components) and in the direction of this resultant. Thus, in that portion of the column loading history in which a section behaves inelastically, both moment components M_{xs} and M_{ys} are affected by the small change in the x-deflection of node s to, say, M_{xs}' and M_{ys}'. If U_s' and V_s' are the deflection values obtained from Eqs. (5.11) and (5.12) respectively, and the corresponding new deflection values are C_{xs}' and C_{ys}', then

$$\frac{\partial C_{xs}}{\partial u_s} = \frac{C_{xs}' - U_s'}{\Delta_{xs}} \tag{5.25}$$

and
$$\frac{\partial C_{ys}}{\partial u_s} = \frac{C_{ys}' - V_s'}{\Delta_{xs}} \tag{5.26}$$

From Eq. (5.24) and its analogous expression in the y-z plane

$$-\frac{(h_s+h_{s-1})}{h_s}\frac{\partial C_{xs}}{\partial u_{s-1}} = \frac{\partial C_{xs}}{\partial u_s} = -\frac{(h_s+h_{s-1})}{h_{s-1}}\frac{\partial C_{xs}}{\partial u_{s+1}} = \frac{C_{xs}' - U_s'}{\Delta_{xs}} \tag{5.27}$$

and
$$-\frac{(h_s+h_{s-1})}{h_s}\frac{\partial C_{ys}}{\partial u_{s-1}} = \frac{\partial C_{ys}}{\partial u_s} = -\frac{(h_s+h_{s-1})}{h_{s-1}}\frac{\partial C_{ys}}{\partial u_{s+1}} = \frac{C_{ys}' - V_s'}{\Delta_{xs}} \tag{5.28}$$

There are also two equations analogous to Eqs. (5.27) and (5.28) which are derived when a small change, Δ_{ys}, is made in the y-deflection at node s. For completeness, these expressions are given as

$$-\frac{(h_s+h_{s-1})}{h_s}\frac{\partial C_{xs}}{\partial v_{s-1}} = \frac{\partial C_{sx}}{\partial v_s} = -\frac{(h_s+h_{s-1})}{h_{s-1}}\frac{\partial C_{xs}}{\partial v_{s+1}} = \frac{C_{xs}'' - U_s''}{\Delta_{ys}} \tag{5.29}$$

and
$$-\frac{(h_s+h_{s-1})}{h_s}\frac{\partial C_{ys}}{\partial v_{s-1}} = \frac{\partial C_{ys}}{\partial v_s} = -\frac{(h_s+h_{s-1})}{h_{s-1}}\frac{\partial C_{ys}}{\partial v_{s+1}} = \frac{C_{ys}'' - V_s''}{\Delta_{ys}} \tag{5.30}$$

where U_s'' and V_s'' are the new expression derived from Eqs. (5.11) and (5.12) respectively, and C_{xs}'' and C_{ys}'' are the new deflection values derived to correspond to C_{xs}' and C_{ys}'. Now, the column deflections at the two ends are zero. Thus,

$$u_1 = v_1 = u_{n+1} = v_{n+1} = 0 \tag{5.31}$$

and derivatives with respect to these deflections need not be considered. Comparison of Eq. (5.19) with Eqs. (5.27) through (5.30) shows that derivatives of the function C with respect to

w_i are all zero for $3 \leq i \leq 2s - 4$ and $2s + 3 \leq i \leq 2n$, as these w_i do not influence the curvature at station s. The components of the Jacobian matrix formed by curvature components are thus confined to a limited band close to the major diagonal.

The end restraint effect terms, corresponding to the second term of Eq. (5.20) may be derived with reference to Fig. 5.3 where the appropriate quantities in the x-z plane are defined, for the top of the column (end A). There are similar quantities readily defined in the y-z plane at end A of the column, as well as in both planes at the bottom of the column (end B). Using Fig. 5.3, it can be shown that the slope in the x-z plane at end A, Ψ_{xa}, is given by

$$\Psi_{xa} = \frac{u_2(h_1+h_2)^2 - u_3 h_1^2}{h_1 h_2(h_1+h_2)} \tag{5.32}$$

from which

$$\frac{\partial \Psi_{xa}}{\partial u_2} = \frac{h_1 + h_2}{h_1 h_2} \tag{5.33}$$

and

$$\frac{\partial \Psi_{xa}}{\partial u_2} = \frac{-h_1}{h_2(h_1+h_2)} \tag{5.34}$$

There are eight deflection values in the end-slope calculations, u_2, u_3, v_2, v_3, u_{n-1}, u_n, v_{n-1}, v_n, and a change in any one of these will cause a change in some restraining moment, which will in turn affect e_{xs} and e_{ys} at all sections. The moment-end rotation characteristics of the end restraint (that is, of the form of Fig. 5.4) are now necessary. In practice, where this capability has been used in this dissertation, it has consistently been assumed that the

moment-end rotation relationship is linear, but there is no necessity that this always be so. The adoption of a moment-end rotation characteristic permits derivation of the values of

$$\frac{\partial M_{xa}}{\partial \Psi_{xa}} = \frac{M_{xa}' - M_{xa}}{\delta \Psi_{xa}} \tag{5.35}$$

where M_{xa}' represents the end moment in the x-z plane, including correction for a restraining moment, corresponding to a net slope of $(\Psi_{xa} + \delta\Psi_{xa})$. From this

$$\frac{\partial M_{xa}}{\partial u_2} = \frac{\partial M_{xa}}{\partial \Psi_{xa}} \frac{\partial \Psi_{xa}}{\partial u_2} = \frac{(M_{xa}'-M_{xa})}{\delta \Psi_{xa}} \frac{(h_1+h_2)}{h_1 h_2} \tag{5.36}$$

and

$$\frac{\partial M_{xa}}{\partial u_3} = - \frac{(M_{xa}'-M_{xa})}{\Psi_{xa}} \frac{h_1}{h_2(h_1+h_2)} \tag{5.37}$$

The incremental bending moment $(M_{xa}'-M_{xa})$ causes a change in the value of station moments M_{xs}, which then produces a change in the computed value of U_s, as defined by Eq. (5.11). The contributions to the second term of Eq. (5.20) are now expressed as

$$\frac{\partial R_{xs}}{\partial u_3} = \left(1 - \frac{s-1}{n}\right) \frac{\partial M_{xa}}{\partial u_3} = -\left(1 - \frac{s-1}{n}\right) \left(\frac{M_{xa}' - M_{xa}}{\delta \Psi_{xa}}\right) \frac{h_1}{h_2(h_1+h_2)} \tag{5.38}$$

and

$$\frac{\partial R_{xs}}{\partial u_2} = - \frac{(h_1+h_2)^2}{h_1^2} \frac{\partial R_{xs}}{\partial u_3} \tag{5.39}$$

There are similar experssions to Eqs. (5.38) and (5.39) for changes in slope at the end A in the y-z plane. For example, Eq. (5.38) becomes

$$\frac{\partial R_{ys}}{\partial v_3} = -\left(1 - \frac{s-1}{n}\right)\left(\frac{M_{ya}'' - M_{ya}}{\delta\Psi_{ya}}\right)\frac{h_1}{h_2(h_1+h_2)} \qquad (5.40)$$

There are also a completely analogous set of expressions for end restraint at the end B, in both x-z and y-z planes.

5.3 Verification of the Analysis

The process of verifying an analysis such as this is not readily accomplished, beyond such elementary checks as that the buckling load is less than the section yield load, and that results appear reasonable. However, there is a valuable check on the lateral deflection profile which may readily be obtained in the elastic range of column behavior, and this involves solving the fourth-order differential equations governing column behavior. If the lateral deflection of a column w (which is a function of z, the axial direction of the column), then the performance of the column is governed by

$$EI\frac{\partial^4 w}{\partial z^4} + P\frac{\partial^2 w}{\partial z^2} = -P_o\frac{\partial^2 w_o}{\partial z^2} \qquad (5.41)$$

where E = modulus of elasticity

I = moment of inertia of the section

P = applied axial load

w_o = initial lateral deflection of the column.

The solution to such an equation has two parts - a complimentary solution, w_c, and a particular solution, w_p. If these portions of the solution are considered to have the form

$$w_c = A_1 \cos kz + B_1 \sin kz + C_1 z + D_1 \tag{5.42}$$

and

$$w_p = (G_1 + G_2 z + G_3 z^2) z^2 \tag{5.43}$$

where A_1, B_1, C_1, D_1, G_1, G_2, and G_3 are constants, then the general solution can be shown to have the form

$$w = w_c + w_p \tag{5.44}$$

which becomes

$$w = A_1 \cos\left(\sqrt{\frac{P}{EI}}\, z\right) + B_1 \sin\left(\sqrt{\frac{P}{EI}}\, z\right) + C_1 z + D_1 + \frac{0.64\, z^2}{L^2} \tag{5.45}$$

This expression was evaluated for a perfect tubular cross section with an initial out-of-straightness profile defined by a half-wave sine curve, and compared to the results obtained from the developed analysis. The solution of the differential equations, of course, leads to a continuous column lateral deflection profile, whereas the developed analysis gives lateral deflections only at discrete locations. Nonetheless, the agreement between results obtained using the two methods was excellent, and on this basis it was assumed that the method was verified at least in the elastic range of column behavior. A comparison of the two methods is not presented diagrammatically because such a comparison would show no measurable difference between the lateral deflection profiles obtained by each method.

5.4 Tangent Modulus Predictions for Comparison

As a result of extensive research into the buckling behavior of columns over the last 30 years (summarized in Ref. 77), it was discovered that in many instances, the buckling load of real columns could be reliably predicted by use of the tangent modulus theory. In fact, in 1952, the Column Research Council (since 1976 known as the Structural Stability Research Council) issued a memorandum to this effect (78). Subsequent studies into the buckling of built-up shapes such as H-sections and welded-box shapes (79) showed that the magnitude and distribution of residual stresses within a cross section was the major factor in determining the strength of straight, axially-loaded columns. Furthermore, it seemed that despite the fact that real, manufactured columns were not straight, the ultimate axial load which could be carried by a real column was accurately predicted using the tangent modulus concept, provided that appropriate residual stresses were included. In other words, it did not seem to matter that the theory predicted buckling loads for straight columns and that real columns had some initial, fabricated out-of-straightness profile. Rather the residual stress effects which had to be included seemed to be a more important determinant of column strength.

With this background, it is clear that it would be desirable to ascertain whether the tangent modulus buckling prediction is still an indication of the buckling strength of fabricated tubular columns. It is not proposed to give details of the tangent modulus

concept or its use here, as these are referred to in Ref. 77 and Chapter 4 of Ref. 24, where particular details are given on the inclusion of residual stresses. In the cited references, the basic equations are applicable to any cross-sectional shape, but they have been used in particular for analyses of I- and H-shapes and rectangular box sections. By this method, a column buckling curve may be derived by plotting the tangent modulus buckling load, P_{TM}, as a fraction of the yield load of the section, P_y (see Eq. 4.10), versus the function, λ, where λ is defined as

$$\lambda = \sqrt{\frac{I_e/I}{P_{TM}/P_y}} = \frac{1}{\pi}\sqrt{\frac{\sigma_y}{E}}\frac{KL}{r} \qquad (5.46)$$

where I = moment of inertia of the section

I_e = moment of inertia of the "elastic core" of the section.

Using the longitudinal residual stress distribution plotted in Fig. 4.5 (a straight-line approximation to the measured distribution discussed in Chapter 3), the tangent modulus predictions shown in Fig. 5.5 were obtained. The curves indicate that there is not a great deal of difference between the tangent modulus predictions and the Euler elastic buckling curve with a cut-off at the yield load. It is also clear that there is some dependence of buckling load upon the orientation of the bending axis with respect to the longitudinal weld.

5.5 Variations of Ultimate Column Load with Location of Longitudinal Welds

In order to present typical results obtained using the theory developed and explained in Section 5.2, a number of pinned-end columns were chosen with no applied end moments (end eccentricity of load) or end restraints. (In practice, it was noted that the inclusion of end restraints may considerably affect the amount of computational effort required to obtain convergence in the deflection pattern.) Each column was divided into eight segments of equal length, which meant that nine stations were required along a column length. The columns differed only in length, and were selected in order to represent different portions of the tangent modulus buckling curve (Fig. 5.5). One column had a λ value of 0.34, corresponding to the region where the buckling load is approximated by the yield load. Two more columns had λ values of 0.76 and 0.96, corresponding approximately to the abrupt transition between yield plateau and elastic Euler buckling curve. A fourth column had a λ value of 1.54, which meant that it could be expected to buckle as an elastic buckling phenomenon. In all results presented in this Chapter it has been assumed that the material is of constant yield strength along the column length.

A half-period sinusoidal out-of-straightness pattern was specified for each column, and the maximum out-of-straightness (at mid-height) was taken to be 0.001 x (column length). This maximum out-of-straightness was derived from current fabrication specifications (19), which, in general, specify this value, but with some restrictions.

In order to further reduce the computational effort it was assumed that the affects of circumferential residual stresses (induced during plate rolling) were negligible. This assumption was introduced at the close of Chapter 4. At that point it was suggested that, because it is expected that the applied load combination will be relatively high at column buckling, the assumption that circumferential residual stresses had a negligible affect appeared reasonable. This was further discussed in Section 5.1. Nonetheless, the theoretical development reported here does include the capacity to consider the affects of circumferential residual stresses. This capacity however, has not been fully utilized in the interests of economy.

Another simplifying assumption was that inelastic column behavior could be adequately monitored by allowing only the three central sections (or "cans") to perform inelastically. (The theoretical development allows section inelasticity to be considered at all stations, but at considerable extra expenditure of computational effort.) This assumption does allow the formation of plastic "hinges" at locations where they might be expected, and the other sections are assumed to maintain completely elastic behavior throughout their loading history. In order to facilitate comparisons, it was further assumed that the material used in column fabrication was of uniform yield strength, but provision was made in the development for material yield strengths to vary independently at each station.

Figures 5.6(a) and 5.6(b) define an elevation and a central section (that is, with inelastic performance capability) respectively of an analyzed column. The x_o defined in Fig. 5.6(a) is the initial mid-height column out-of-straightness in the x-direction. Unless otherwise stated, the initial out-of-straightness in the y-direction (y_o) has been taken to be equal to x_o, with the result that the maximum mid-height column out-of-straightness, δ_m, is given by $\delta_m = \sqrt{2}\, x_o$.

For each column tested it was discovered that, for a given constant, initial out-of-straightness profile, the column buckling load showed some dependence on the circumferential location of the longitudinal welds. For this reason, computations were made with the longitudinal welds at all stations aligned at the same circumferential location, with the assumption that this would provide the limiting conditions. It is recognized, of course, that this is not what happens in practice, since manufacturing specifications specify minimum staggering of welds between "cans". The process of varying all longitudinal welds along a column around the tubular circumference produced the curves of Fig. 5.7. The two solid lines plotted in Fig. 5.7 are the upper and lower bounds determined by this process of placing the longitudinal welds at various locations on the circumference, while with the welds at other circumferential locations the buckling loads fell between these limits. In each column tested the upper bound was achieved when all longitudinal welds were located at the point on the column circumference corresponding to the "outside" of the initial out-of-straightness profile.

In other words, the upper bound was achieved when the longitudinal weld at each station was at an angle given by $\theta = \frac{\pi}{4}$ in Fig. 5.6. The lower bound was derived when all longitudinal welds were diametrically opposite the location which produced the upper bound of column buckling load (that is, $\theta = -\frac{3\pi}{4}$ at all stations). The data on which the theoretical curves of Fig. 5.7 were based is given in Table 5.1.

One comparison which can readily be made in Fig. 5.7 is the comparison between column buckling loads predicted using this theoretical development, and the loads predicted by tangent modulus theory. It seems that tangent modulus predictions are not an adequate indicator of long column buckling loads for tubular columns, even though longitudinal residual stresses have been included in tangent modulus predictions. However, this comparison is really not valid in that tangent modulus theory concerns itself with the axial load at which initially straight fabricated tubular columns reach their ultimate load capacity. On the other hand, the analysis reported here considers fabricated tubular columns which have an appreciable, pre-determined initial out-of-straightness profile. The curves derived and presented in Fig. 5.7 indicate that longitudinal residual stresses do have a significant effect on column buckling load, as it is this effect alone which provides the difference between upper and lower bounds of column buckling loads.

5.6 Variations of Ultimate Column Load with Column Out-of-Straightness

Up to this point, the discussion has centered on the buckling load derivation of a column with a sinusoidal initial out-of-straightness profile with a maximum initial, mid-height out-of-straightness of δ_m, where δ_m is given by:

$$\delta_m = 0.001 \times (\text{column length}) \tag{5.47}$$

In Section 3.6 the basis for this in fabrication specifications was presented, with the recognition that, as the column gets longer, the allowable initial out-of-straightness decreases somewhat. Nonetheless, the curves presented in Fig. 5.7 were developed with the maximum initial out-of-straightness allowed by fabrication specifications (i.e., $\delta_m = 0.001 \times$ column length), since it was thought that these would be of most use to a designer.

It is now desirable to relax the restriction that a particular column has the maximum allowable initial out-of-straightness, and to study the effects of varying initial out-of-straightness on column buckling behavior. The first study undertaken thus is rather in the nature of a check on the theoretical method developed than the discovery of trends in column buckling. Figure 5.7 clearly indicated that the tangent modulus buckling load predictions were not good indicators of the strength of imperfectly straight fabricated tubular columns. However, it might reasonably be expected that the accuracy of such predictions would be substantially improved as initial out-of-straightness was decreased. In order to verify

this three columns with no residual stresses included were studied, and the variation in column buckling load noted as initial out-of-straightness was decreased. The results of this study are shown in Fig. 5.8, where it can be seen that the buckling load does indeed tend to the tangent modulus prediction as out-of-straightness is decreased. Of necessity, the analysis developed cannot consider a perfectly straight column, as such a column is not in a biaxial bending state, and instead an analysis of this needs a bifurcation study. Nonetheless, the approximation to zero initial out-of-straightness may be made. In two cases shown on Fig. 5.8, the line is dotted near the zero out-of-straightness line (that is, the y-axis) to indicate the trend to tangent modulus prediction under that condition.

As a continuation of this study, it is possible to examine the effects of residual stresses and variations in initial out-of-straightness. For this study two columns were chosen, having λ values of 0.96 and 1.54, and the results are plotted in Figs. 5.9 and 5.10, respectively. It is noted that there is a general trend toward increasing column buckling load as column initial out-of-straightness is decreased. This observation confirms that a designer is being conservative if he uses the curves of Fig. 5.7, which were derived under conditions of maximum allowable out-of-straightness (Eq. 5.47). Just as under conditions of maximum allowable out-of-straightness, Figs. 5.9 and 5.10 indicate that there continues to be a range of column buckling loads as out-of-straightness is decreased (designated by shaded areas), depending on the locations

of longitudinal welds. The various labels of Figs. 5.9 and 5.10 may be explained by reference to Fig. 5.6. The symbols θ_4, θ_5 and θ_6 represent angles θ (Fig. 5.6b) at stations 4, 5 and 6 (Fig. 5.6a), respectively. Since the assumption had been made that it was adequate to allow inelastic section behavior only at the three central stations (that is, stations 4, 5 and 6), the locations of the longitudinal weld at these stations defines the locations of the longitudinal weld at all required stations.

In Fig. 5.9, however, it seems that the trend toward increasing buckling load as out-of-straightness is decreased, is not in a uniform manner. This is particularly obvious for the case when all the longitudinal welds are at a position defined by $\theta = \frac{\pi}{4}$ (see Section 5.5). It would seem in this instance that the column out-of-straightness profile tends to make the column deflect laterally in one direction, while the longitudinal weld tends to make the column deflect laterally in the diametrically opposite direction. As initial column out-of-straightness is decreased the ability of the column to deflect in the direction defined by the out-of-straightness profile is decreased. It was noted that, for this particular case, with a very small initial out-of-straightness profile, the longitudinal weld forced deflection in its preferred direction.

5.7 Variation of Theoretical Assumptions

In the discussion reported in this chapter there have been a number of assumptions which have been made in the interests of

economy, but with no demonstrable basis except intuition and experience. Such theoretical modelling assumptions, it is hoped, have had no significant effect on the results obtained. It is the function of this section to briefly examine two of these assumptions - namely, the assumption that nine stations along a column length is sufficient to model column performance, and the assumption that the column buckling load could be accurately obtained when only the central three stations (out of the nine considered) were permitted to behave inelastically. For both investigations a column with pinned-ends and a λ value of 0.96 was selected. For each examination a half-wave sinusoidal initial out-of-straightness profile was prescribed, although two curves were traced - one for a maximum initial out-of-straightness equal to the maximum permitted (Eq. 5.47), and the other for a maximum initial out-of-straightness equal to half the maximum permitted. In all cases longitudinal residual stresses were included at each station, and the weld location at each station was considered to be at the worst possible location - in other words at an angle given by $\theta = -\frac{3\pi}{4}$ in Fig. 5.6.

The results of the study into the variation of column buckling load with number of stations considered along the column length are presented in Fig. 5.11. In presentation of such results it is very difficult to increase the number of stations considered along the column and still maintain a constant proportion of the column which may be considered to have inelastic performance capabilities. It was desired to maintain such a constant proportion in order to, if

possible, separate these two effects. In Fig. 5.11 it can be seen that there is some variation in the proportion of the column with inelastic performance capability, given as $\left(\frac{\Delta L_i}{L}\right)$, but this variation has been kept to a minimun. As expected, the trend in Fig. 5.11 is for a decreasing buckling load as the number of stations is increased. This may be attributed to the fact that a better approximation to the sinusoidal initial out-of-straightness profile is attained as the number of stations is increased. However, as had been hoped, such decreases are small, and amount to a maximum of about five percent of the buckling load over the whole range of number of stations considered. As the initial out-of-straightness profile is decreased, from the maximum value permitted to half the maximum, the values plotted indicate that there is even less variation of column buckling load with number of stations considered. It must be recognized that there is a vast increase in computational effort required to calculate maximum column axial load when the number of stations considered increases from 6 to 16 (the limits considered), as it typically takes more iterations for adequate stabilization of the iterative process as more stations are considered. In view of this fact, it was concluded that the assumption of nine stations along the column length was an adequate assumption for the derivation of column buckling loads.

The study of the variation of column buckling load with changes in the proportion of the column length having inelastic performance capability yielded the results shown in Fig. 5.12. In each case the

central station (that is, station 5) was considered to have inelastic performance capability. As greater proportions of the column were considered to have this capability, the stations above and below the mid-height station gained this capacity in a symmetrical manner. Thus when three stations had inelastic performance capacity they were stations 4, 5 and 6, while when five stations had such capacity they were stations 3, 4, 5, 6 and 7. Figure 5.12 shows that the variation of column buckling load with number of stations with inelastic performance capability was truly negligible. On these grounds too, it was then considered that the assumptions implicit in Fig. 5.7 were quite satisfactory.

These studies of theoretical variants in the column buckling analysis are referred to again in Section 6.3 where the conclusions reached here are verified in the analysis of the strength and behavior of a prototype long column specimen.

5.8 Refinement of Bounds of Column Buckling Curve

In the discussion of the column buckling predictions of Fig. 5.7 presented in Section 5.5 it was explained that the upper and lower bounds of expected column buckling load were dependent on the location of the longitudinal welds on the column circumference. In particular, the upper bound was derived when all welds along a column length were in the most favorable location on the column circumference (that is, $\theta = \frac{\pi}{4}$ at all stations), and the lower bound was derived when all welds were in the least favorable location (that is, $\theta = -\frac{3\pi}{4}$ at all stations).

With these upper and lower bounds determined it was thought desirable to decide whether it would be possible to trace the variation of column buckling strength as the location of the longitudinal weld in one (say central) "can" was varied around the column circumference. It would be expected that the results obtained would lie within or on the upper and lower bounds already determined.

Such a study was conducted on a column with a λ value of 0.96, and the study was conducted three times - once the column had the maximum permitted out-of-straightness (Eq. 5.47), once it had half the maximum permitted out-of-straightness, and once it had ten percent of the maximum permitted out-of-straightness. In each case the column performance was considered to be adequately monitored by using nine stations along the column length, with the central three stations having inelastic performance capabilities (that is, stations 4, 5 and 6 in Fig. 5.6a). The location of the longitudinal weld at stations 4 and 6 was assumed to be constant at the least favorable location (that is, $\theta_4 = \theta_6 = -\frac{3\pi}{4}$), and the longitudinal weld at the central station taken to be at varying locations on the column circumference. The results of this study indicated that there was no significant advantage to be derived from variation of the longitudinal weld in merely one can. In most instances the improvements notes were within experimental limits (as determined by supposedly symmetrical results), and as expected, the variations were much less than the difference between upper and lower bounds determined and presented in Fig. 5.7.

On the basis of these tests it was concluded that there were no appreciable benefits to be derived from the study of the variations in column buckling load with the variation in the location of the longitudinal weld around the column circumference. It seemed preferable to limit the specifications to overall bounds, depending on whether welds as a group tended to be in favorable or unfavorable circumferential locations.

There is, however, another reason why such an attempt may be of little benefit to designers. In order to be able to take advantage of exact predictions of column buckling strength the designer would need to know and control both the exact circumferential location of all welds and the initial out-of-straightness profile. In practice the designer has no control over either of these factors. The out-of-straightness profile is essentially an accidental or random outcome of the fabrication process, while the locations of the longitudinal welds are largely left to the fabricators. While there are certain restrictions placed on fabricators (usually in the form of "minimum stagger" requirements or the requirement that the weld in a certain "can" not be in a certain location, in order to facilitate subsequent joining to other members), there is still a wide latitude allowed in the positioning of longitudinal welds. For all these reasons, any attempt to refine the upper and lower bounds of Fig. 5.7 appears to be neither possible nor desirable.

6. COMPARISONS AND DISCUSSION

6.1 Introduction

In this dissertation so far the results of an experimental test program have been presented and an extensive theoretical analysis has been developed, both for analyzing a section behavior and predicting the behavior of a long fabricated tubular column. These two investigations, experimental and theoretical, have in general, proceeded separately except where experimental measurements (such as residual stress distributions) could be used in theoretical analysis. At some point, however, it is necessary to consider just how good the developed theoretical analysis is. One intention of this chapter is to present as many comparisons as practicable in an attempt to reach some conclusion on this question. Such comparisons, however, are fraught with many difficulties, and so the attempts at verification of the analyses are by no means exhaustive.

It is further desirable to deduce, as far as possible, any design recommendations which may be of use to designers and which seem to be a logical outgrowth of this work. Some of these have already emerged from the theoretical work reported in earlier chapters of this dissertation, but it is anticipated that a number of further such conclusions will emerge from this discussion.

For convenience, this discussion has been divided primarily into two sections - namely attempts to verify the analysis undertaken, and comparisons of derived column buckling curves with other possible

design curves. The attempts to verify the analysis are further subdivided into two parts - a direct plotting of available experimental data on derived column buckling curves, and attempts to model the behavior of individual columns.

6.2 Theoretical Column Buckling Curve and Observed Experimental Results

One of the quickest and easiest attempts to verify the theoretical analysis of this dissertation is the plotting of available test data on the column curves derived. Figures 6.1 and 6.2 present such results. The experimental data of Fig. 6.1, plotted as barbells to reflect uncertainty over column effective length, are the experimental values obtained from the testing program reported in Chapter 3. Static yield strength values have been used, along with the maximum static axial load measured, P_s (see Fig. 3.18). This comparison has been used in order to preserve the consistency between theory (derived under static considerations) and experiment. (If dynamic yield strength values are used, along with maximum "dynamic" axial load measured [P_d in Fig. 3.18] then the experimental results tend to indicate a more serious situation, with the experimental points being plotted at a lower proportion of the yield load, P_y.) Comparison of Figs. 6.1, 3.19 and 3.20 shows that the lower bound of the theoretical buckling curve is a more conservative approximation to experimental data than either the AISC-CRC column curve or the multiple column curve "a". Consideration of Fig. 6.1 alone indicates that the lower bound of the theoretical

buckling curve seems to be a good lower bound of observed experimental results for the range of column effective length tested. The fact that experimental results tend to be clustered rather towards the upper bound of theoretical buckling curve could be due to a combination of factors. Among these could be the effect of weld "staggering" between cans along the length of the column, and probably more importantly, initial out-of-straightness of a fabricated column being less than the maximum allowed by fabrication specifications. This is discussed in more detail below.

The presentation of Fig. 6.2 is somewhat more suspect. The comparison is presented between predicted column buckling curve and the results obtained by Wilson (53) in 1937. There are several factors which indicate that this comparison may not be valid for at least some specimens. First of all, the tests were not conducted under pinned-end conditions but rather the specimens merely were located between two surfaces. Each surface (or head of the testing machine) was aligned to the plane of the end of each column initially and then fixed. There remains, therefore, much doubt about the real column effective length. The results have been plotted on the assumption that the effective length factor, K, was somewhere between 0.5 and 1.0 (that is, end conditions were somewhere between fixed and pinned). While these may indeed be the limits of effective length factor, it does not seem possible to further restrict the value.

However, probably the major difficulty with Wilson's results is that, especially for the short columns tested, it seems more likely that the columns exhibited failure by local shell buckling, rather than by overall column buckling. One indication of this possibility is that the diameter-to-thickness ratios $\left(\frac{D}{t}\right)$ of specimens tested ranged from 69 to 194. Furthermore, many specimens exhibited the familiar checkerboard buckling pattern characteristic of shell buckling. For all these reasons it is not thought that the comparison of Fig. 6.2 is very good, and it is included here only for completeness.

There is another reason for approaching the comparison of Figs. 6.1 and 6.2 with some lack of confidence. It is recalled (see Chapter 5) that the predicted column buckling curves were developed for a set of circumstances involving some restricted assumptions. Among these assumptions were the assumption that material of identical yield strength was used throughout the column length and that each column had a half-wave sinusoidal out-of-straightness profile, with the maximum out-of-straightness, at mid-height, equal to the maximum permitted under manufacturing specifications (Eq. 5.47). The assumption of uniform material yield strength has certainly been violated by the test program reported in Chapter 3, although it appears to have been satisfied in Wilson's testing program. However, the much more important out-of-straightness assumption has been violated by both testing programs. Of course, real fabricated tubular columns exhibit an

almost random out-of-straightness profile. This would lead to the expectation that real fabricated tubular columns would have a buckling load greater than, or equal to, the buckling load predicted for columns having an assumed half-wave sinusoidal out-of-straightness profile.

6.3 Theoretical Modelling of the Behavior of Individual Columns

An attempt to confirm the validity of the theoretical analysis is also possible by modelling the behavior of individual columns. In the analysis described in previous chapters much effort has been expended introducing various capabilities to the analysis. For example, in addition to the capability of considering any defined initial column out-of-straightness profile, the analysis also permits varying section behavior, both in terms of different material properties at different stations and different circumferential locations of the longitudinal weld. Using these capabilities it should, therefore, be possible to adequately model the behavior of individual columns. Not only should it be possible to predict the actual static column buckling load but it should also be possible to obtain lateral mid-height deflection values closely corresponding to the observed values during the experimental testing program.

There are, however, a number of factors which complicate such attempts to verify the analysis. First of all, there is the consideration that, even if there was some mistaken assumption in the analysis, it might still be possible to make a reasonable prediction

of column strength if a sufficient number of discrete locations was considered along the column length. The concentration must therefore be on attempts to provide accurate but also economical solutions. A related problem concerns the veracity of the measured results. While it is true that the measured static column buckling load is probably very close to the true static column buckling load, the measurements of lateral mid-height deflection could readily have an experimental error of about 0.5 mm (0.02 in). Under such circumstances, an approximate agreement between theory and experiment is the best that can reasonably be expected.

In order to briefly clarify the means by which actual column specimens were modelled theoretically, reference is made to Fig. 6.3. On the left hand side of Fig. 6.3 is a diagram of a typical column specimen. As the diagram indicated, the column is made up of short "cans", with the longitudinal weld staggered between cans. Furthermore, there exists the possibility that the column is fabricated using cans formed from steel of different yield strength. The next two diagrams of Fig. 6.3 indicate that one of the input variables is the measured column out-of-straightness profile, in two perpendicular directions. While these variations have no predetermined mathematical description (since they are an essentially random fabrication variable), they are nonetheless known, having been measured prior to column testing.

The two diagrams on the right hand side of Fig. 6.3 indicate the theoretical model assumptions. In general, it is considered desirable

to consider the station location to be near the center of a short column of which its behavior can be considered representative. In other words, it is preferable for short column "cans" to terminate as far as possible from station locations. Of course, it is perfectly possible for there to be more than one station located within a column "can" and frequently this option is adopted. (In such a case the two or more stations within the length of the can would have identical material and behavior properties.) Thus Fig. 6.3 indicates just one possible discretization of the column, out of an infinite number of such possibilities. However, the discretization of Fig. 6.3 is probably the coarsest discretization which could be expected to yield reliable results, and it does clearly indicate the desirability of allowing variable interstation distances, h. The model diagrams of Fig. 6.3 also indicate that the accuracy of the assumed initial column out-of-straightness profile is highly dependent on the number of stations considered, since out-of-straightness may be specified only at station locations.

In attempting to model column specimen performance it rapidly became clear that end conditions were extremely important. Not only did possible imperfections in pinned-end conditions have an influence, but also the end eccentricities contributed significantly to column strength and behavior. Although some values of end eccentricity of column specimens tested are given in Table 3.4, it is not considered that these were very accurate measurements, but merely gave an indication of the order of magnitude of the probable end eccentricity. For this reason, modelling was attempted with a

high degree of latitude in end eccentricities considered. It was concluded that, if experimental column strength and behavior data could be adequately predicted using any combination of end eccentricities of the order of the available data, then it could be considered that the method was verified.

Tables 6.1 to 6.9 present the results of such modelling attempts. In each table the results are presented for the modelling of one individual long column test specimen. This specimen may be from the testing program reported in Chapter 3 or from Wilson's series of long column buckling tests. The results compared are lateral deflection at mid-height of the column, at representative loads, and static failure (or buckling) load of the column. It was considered that a valuable indicator of column behavior was the lateral deflection at mid-height, and in particular the direction in which the columns were deflecting. For this reason in each table the deflection angle, α, is computed for comparison of experimental and model results. In these tables, the deflection angle, α, is defined as

$$\alpha = \tan^{-1}\left(\frac{\text{y-movement}}{\text{x-movement}}\right) \qquad (6.1)$$

The results shown in Tables 6.1 to 6.9 can readily be considered in three categories. In the first category are Tables 6.1 to 6.4, representing the tests of long column specimens 3, 4, 6 and 10, respectively, as reported in Chapter 3. For these specimens adequate column modelling could readily be achieved provided that some eccentricity of applied loads at the column ends was permitted. In the second category are Tables 6.5 and 6.6, representing specimens

7 and 8, More care was needed in modelling these specimens, which were considered to be important because they had the largest nominal slenderness ratio of any specimens tested in the testing program discussed in Chapter 3. It appeared that inclusion of possible end eccentricities alone was not sufficient for adequate modelling of the behavior of these specimens. In category three are Tables 6.7 to 6.9, representing modelling attempts of Wilson's test results, in which separate problems were encountered. This provides an introduction for the results discussed.

In Table 6.1 the results of two distinct discretizations of long column specimen number 3 are presented. This was the only column for which this was attempted. The comparison of the two models provides an excellent indication that a relatively good determination of long column strength may be achieved with a relatively coarse column discretization. Not only are the predictions of column buckling load identical and within two percent of the experimental column buckling load, but also the predictions of column buckling direction are very close to each other. As further indication the range of deflection directions encompassed by the two predictions includes the buckling direction observed experimentally. Even the magnitudes of deflection values predicted at the specified load (very close to the buckling load) are in excellent agreement, both with each other and with the experimental results. This result is taken to be an added confirmation of the analytical study reported in Section 5.7.

In Table 6.2 the results of three modelling attempts are presented to illustrate the modelling method used in subsequent column analysis. In general a column was first analyzed under the assumption that there were no end eccentricities. In the case of this long column specimen (specimen number 4), this yielded a buckling load much higher than the experimental results indicated. In models 1, 2 and 3, therefore, a gradually increasing end eccentricity was considered in such a manner that both the column buckling load and lateral mid-height deflection predictions were improved. Model 3, included as an example, indicated that this process eventually yields worse results, and that, for this analysis, model 2 is the best prediction.

Tables 6.3 and 6.4 represent the results of modelling attempts for long column test specimens 6 and 10, respectively. The results indicate that excellent column modelling is to be expected by consideration of possible end eccentricities. It seems very likely that, by a trial-and-error process, it would be possible to obtain modelling results even closer to the experimental results than has been achieved in models reported in Tables 6.3 and 6.4. For these four columns then, comprising the first category of column modelling, a theoretical model has been derived which predicts the column buckling load to within two percent. Furthermore, the direction of lateral movement at mid-height of a column has been predicted, in general to within about 0.2 radians (about 10°), with the discrepancy rising to 0.4 radians (about 20°) in only one case presented. It is

considered that, for these four column specimens modelled, the model developed is an excellent, economical method to predict fabricated tubular column strength and behavior. It is further concluded that an even closer agreement between experimental data and theoretical model results could be achieved if more analytical effort was expended.

The column specimens modelled in Tables 6.1 to 6.4 had nominal slenderness ratios $\left(\frac{L}{r}\right)$ in the range of 39 to 60. However, there were two columns tested in the long column test program reported in Chapter 3 that had larger nominal slenderness ratios. These were specimens 7 and 8, and the results of modelling attempts of these specimens is shown in Tables 6.5 and 6.6, respectively. Both of these columns had nominal slenderness ratios of 83. Accurate modelling of these columns, comprising the second category of results considered, was not possible by the simple device of considering only end eccentricities. Furthermore, when no end eccentricities were considered (Model 1 in both tables), the predicted buckling load was 10 to 12 percent less than the buckling load measured experimentally. It was, therefore, considered that some other factor was operative in affecting the behavior of these column specimens. It was considered a possibility that the end bearing blocks had some frictional resistance to rotation. As noted in Chapter 5, the analytical method does allow for consideration of end restraint, and so this possibility could be verified. For convenience, the program considers the rotation resistance of the

ends to be identical in both perpendicular directions and identical at both ends. (While there is no theoretical basis for this, and it would be readily possible to abandon the assumption, there seems little to be gained thus, as there appears no reasonable basis on which to differentiate the various frictional resistances.) When this rotational resistance was assigned to the ends of the column specimens, still with no end eccentricities considered, the prediction of column buckling load improved dramatically. For specimen 7 (Model 2, Table 6.5) an exact determination of experimental buckling load could be achieved by the model, while the equivalent value for specimen 8 (Model 2, Table 6.6) was within six percent of the experimental buckling load. However, this still left the problem of buckling direction. For specimen 8 (Table 6.6) the buckling direction was in agreement with experimental data to within about 0.4 radians (about 20°), which could be considered acceptable. However, for specimen 7 (Table 6.5) the discrepancy was much larger, and considered unacceptable.

The possibility of including both rotational resistance, at the ends and end eccentricities is now examined. The results of such modelling attempts appear in Model 4 of Table 6.5 for specimen 7, and in Model 3 of Table 6.6 for specimen 8. These results indicate that very acceptable results may be achieved when both end eccentricities and rotational resistance of the ends is allowed. Not only are the predictions of column buckling load still very close to experimentally observed values, but the estimates of direction of

lateral movement at mid-height are also much improved. The results for Specimen 7 (Table 6.5) are less conclusive, but it is noted that even experimental results show a marked change of direction of lateral movement as the axial load is increased from 2046 kN (460 kips) to 2210 kN (497 kips), a condition also noted by the theoretical model. (Even the experimental results, showing such small values of measured lateral deflection, must be considered with discretion, for they are subject to considerable experimental error, and may well be a misleading indicator of the true direction of column lateral movement at mid-height.) Furthermore, it seems that slight adjustments to the end eccentricities and/or end moment resistances considered could produce even closer agreement between theory and experiment. The results shown in Table 6.6 are more conclusive evidence that the experimentally observed strength and behavior of specimen 8 can be readily produced theoretically.

It was, therefore, concluded that for these two long specimens modelled in Tables 6.5 and 6.6, a good theoretical model of experimental results could be obtained. However, such modelling requires more care than for previously considered columns of smaller slenderness ratio. In particular, it seems that, in addition to end eccentricities previously considered, the possibility of some rotation resistance of the end bearing blocks needs to be allowed.

In the third category of modelling conditions some of the results obtained by Wilson (53) are considered. These results are presented in Tables 6.7 to 6.9, and represent the modelling of test

specimens A1, A2, and B1, respectively, as reported by Wilson. There are a number of problems associated with modelling these results, and so, just as in Section 6.2, these results are included only for completeness. The first problem, that of end conditions, is mentioned briefly in Section 6.2. As mentioned there, the problem was one of estimating column effective length. For the purposes of individual columns as considered here, the problem manifests itself in an uncertainty over the rotation restraint to be attributed to the ends of a particular column. By a trial-and-error process it was determined that rotational resistances of the order of 11.3 kN-m/rad (100 k-in/rad) gave reasonable results. While considering end conditions, it is appropriate also to note that Wilson does not report any effective end eccentricities, but rather seems to assume that the method of application of applied axial load led to zero end eccentricities. It does not seem possible to make any estimate of the veracity of this assumption.

There is, however, another problem with the results reported by Wilson, and this also is a direct result of a lack of reported data. In particular, the circumferential location of longitudinal welds in "cans" is not reported. It has been considered throughout this dissertation that it is essential to have an accurate indication of the location of longitudinal welds in order to adequately predict the strength and behavior of a particular long fabricated tubular column. Wilson does report the column initial out-of-straightness profile, and so it was first attempted to model the column specimens

using only initial out-of-straightness profiles given. The results of these attempts are presented as model 1 in Tables 6.7 to 6.9, where no residual stresses at all have been considered. As the results show, the theoretical column buckling load differs from the experimental column buckling load by up to thirty-two percent, which was clearly unsatisfactory. As a result, it was concluded that some estimate of the locations of circumferential welds was essential for accurate column modelling. Accordingly, a series of estimates was made as to the circumferential location of longitudinal welds. It was assumed that the welds were always on one of the axes considered, and that the longitudinal welds were "staggered" by 180° between adjacent "cans". Using these assumptions, the analyses reported in Model 2 of Tables 6.7 to 6.9 were produced. The buckling load could now be predicted to within five percent of experimentally derived values in all three cases, which was considered satisfactory. However, there was still the problem of buckling direction. For the models considered the variation between observed and predicted buckling direction was typically of the order of one radian (about 60°), which was considered unsatisfactory. It seemed impractical to pursue this investigation further, but it was concluded that, with further information being available, all indications were that better column modelling was a good probability.

In considering all of Tables 6.1 through 6.9 representing theoretical modelling of nine long column specimens, it seems that adequate theoretical prediction of experimental results of both column strength and behavior can be achieved. In almost all cases

the number of stations considered along the column length was the minimum possible consistent with having one station located in each column "can" (considered essential for good modelling). There is thus no doubt about the fact that accurate modelling may be achieved with a coarse discretization of the column. The column modelling does, however, clearly illustrate two problems which must be considered in experimental testing of long fabricated tubular columns. It seems that end eccentricities and the rotational resistance offered by end blocks may be important determinants of column strength and behavior. For these reasons it is recommended that, in future long column test programs, considerable effort be expended to measure these parameters. Where sufficient experimental information was available, a theoretical model was produced which predicted the buckling strength to within four percent of the observed value. Furthermore, in general, the direction of lateral movement at applied axial loads, approaching the column buckling load, was predicted to within about 0.4 radians (about 20°). (For the one exception to this observation, the experimental results indicate a rapidly changing direction of lateral movement, and experimental results themselves are of such small magnitude as to be subject to considerable experimental error.) The overall good agreement between theory and experiment leads to the conclusion that this modelling of individual column strength and behavior shows a very good verification of the theoretical analysis.

6.4 Comparison of Column Buckling Curves

Having verified the theoretical analysis it remains now to compare the column buckling curves derived with other column buckling curves available. Figure 6.4 presents a graphical comparison of the derived theoretical column buckling curves, the commonly used AISC-CRC column buckling curve, and the proposed column curve "a" (13). As the diagram shows, the range of possible column buckling loads encompassed by the upper and lower bounds of theoretical analyses generally includes the predictions of the other column buckling curves, at least for columns having λ values less than about unity. However, the lower bound of theoretical column buckling curve is somewhat below either of the other buckling curves, which would indicate the possibility of underdesigning a real fabricated tubular column if the design was based on either of the previously proposed curves.

As longer columns are used, with λ values of the order of 1.5, the theoretical analysis indicates that the expected column buckling load could well be consistently less than that predicted by other design curves. There is, however, one qualification which may prove somewhat applicable for columns of this order of λ value. It is discussed (in Section 3.6) that, for long columns (over, say 11 m [40 ft] in length), a somewhat more stringent out-of-straightness criterion is specified by current tubular column fabrication codes. In derivation of the theoretical column buckling curve, a maximum out-of-straightness value given by Eq. 5.47 was used throughout. If

a somewhat reduced column maximum out-of-straightness can be reliably predicted, then it would be expected that predicted column buckling loads would be somewhat increased (see Section 5.6). However, since it cannot be ascertained just where the more stringent out-of-straightness criterion becomes effective (since the λ value is a function of variables other than column length), the uniform maximum out-of-straightness was retained throughout the analysis.

7. SUGGESTIONS FOR FURTHER RESEARCH

7.1 Introduction

As this discussion has progressed a number of areas in which further research would be advisable have appeared. The intention of this chapter is to briefly consider these topics, under the headings of experimental and theoretical research. Of course, such topics are rarely exclusive, but the understanding of physical phenomena usually proceeds by a close inter-relation of experimental and theoretical investigation.

Where possible this chapter suggests methods by which the suggested research might be commenced, but, particularly for theoretical analyses, this is not always possible or appropriate.

7.2 Further Experimental Investigation

The work reported in this dissertation readily leads to at least three areas in which further experimental research is desirable. The first of these concerns the circumferential residual stress measurements undertaken on a fabricated tubular column and reported in Chapter 3. As was clear from Fig. 4.7, the measured residual stress distribution is not yet readily amenable to easy theoretical prediction. It is likely that a considerable advance toward an understanding of the phenomena involved in producing the measured residual stress distribution could be made by examining the residual stresses in a "can" at various stages of fabrication, in particular

after cold-rolling but before longitudinal welding, and possibly, after less than the full number of passes in the longitudinal welding process.

One of the most obvious needs in the area of column buckling is the need to test experimentally typical long fabricated tubular columns, of slenderness ratios as high as possible. As a result of conversations with fabricators, it seems that such columns could be rolled in diameters as small as 0.30 m (12 in). Also the 5,000,000 pound universal testing machine in Fritz Laboratory could probably take specimens up to a maximum of 11.5 m (38 ft) in length. Using a wall thickness of 8 mm (5/16 in), as in the test sequence reported, this gives a nominal slenderness ratio, $\frac{L}{r}$, of 110 as opposed to a maximum of 83 in the testing program reported in this investigation. If normal strength structural steel (ASTM A36 grade is used this gives a λ value of 1.22, whereas if higher strength steel [say, ASTM 50 grade] is used, this gives a λ value of 1.44, and these values are much closer to the desired λ values, and enable a better range of the column buckling curve to be covered).

A further area, which would require both experimental and theoretical investigation, concerns the circumferential welds which join the short column "cans" together in the formation of a long tubular column. In the analysis presented in this dissertation it has been assumed that these welds have no affect on column performance, and experimental evidence suggests that these welds are not weak points in a column. However, at present there is no available

data on the magnitude or distribution of residual stresses introduced by circumferential welding, and so it is not possible to estimate the effect of the welds on long column performance. A logical conclusion of such an investigation might be an indication of whether it was desirable to fabricate a prototype long column from few, long "cans", or from more, but shorter, "cans".

7.3 Further Theoretical Investigation

The investigation undertaken in this work must be considered to be merely a start in leading to the necessary understanding of the strength and performance of tubular steel columns. While this analysis allows an accurate assessment of column axial load behavior, it really does not even begin to enter the fields of tubular column bending, or columns under combined loading. It is true that the introduction of end eccentricities allows end moments to be placed on a column. However, this was not the major intent of the analysis, and it does only permit proportional loading. In order to permit derivation of strength interaction curves it is necessary to be able to consider non-proportional loading. The possibility of biaxial bending of fabricated tubular columns is also worthy of investigation, but is well beyond the scope of the analysis reported here.

Up to this point it has only been considered that the column (or beam-column) is loaded at its ends. However, in use as structural members of offshore oil drilling structures, fabricated

tubular columns might well be, and probably are, subjected to substantial lateral forces, which might arise from ocean forces or the deliberate loading of the structure. At present it does not seem possible to analyze fabricated tubular columns under these conditions, using the method adopted in this investigation.

It is also possible that there is some limitation which ought to be placed on the maximum diameter of long fabricated tubular column for which the family of long column maximum load curves presented in Fig. 5.7 is appropriate. This limitation is a result of the fact that the longitudinal residual stress distribution used in these analyses (and given in Fig. 4.5) is appropriate only for columns of small outside diameter. As noted in Section 3.4, other researchers (for example, Ref. 74) have discovered that for large diameter tubular columns it is more appropriate to specify the longitudinal residual stress distribution in terms of linear distance from the weld rather than angular rotation. In particular, for large diameter tubular columns, this would suggest that the residual stress distribution is more localized near the weld location than would be assumed if the relationship of Fig. 4.5 was adopted. Before the curves of Fig. 5.7 were adopted for use in design of large diameter fabricated tubular columns, it would therefore be desirable to ascertain what effects this changed longitudinal residual stress distribution has on the curves proposed.

8. CONCLUSIONS

8.1 Introduction

In reviewing the scope of this dissertation, which encompasses an experimental portion and two distinct theoretical endeavors, it was considered important to distinguish between the conclusions of this work and the contributions made by this work. For the purposes of this distinction, therefore, the conclusions of this work have been considered to be those results emerging from this work, which also include confirmation of previously established knowledge. On the other hand, the contributions of this work are defined as those aspects of this work which are distinctly new and previously unconfirmed.

Even this distinction however, cannot be considered sufficient in some cases. One example of such a situation is the derivation of moment-axial load-curvature curves. The form of these curves had been well-established for cross sections other than fabricated tubular sections. It was thus possible to confidently predict at least the form of these curves for the fabricated tubular sections analyzed herein although they had never, in fact, been derived. When such curves were produced, they were considered as conclusions rather than contributions.

This chapter concludes with a summary of design recommendations which are an outcome of this dissertation.

8.2 Conclusions

(1) Longitudinal residual stresses in a fabricated tubular column have been measured experimentally. The distribution of these stresses is in general agreement with the expected distribution and with the distribution obtained experimentally using other techniques. This distribution has the form of high tensile stresses near the longitudinal weld (equal to the yield strength right at the weld), with alternating regions of compressive and tensile stress as one moves away from the longitudinal weld around the tubular circumference. Furthermore, as expected, the magnitudes of the stress peaks decrease as one moves away from the location of the longitudinal weld.

(2) The moment-axial load-curvature (M-P-Φ) curves for a fabricated tubular column do indeed have the general form derived for other cross-sectional shapes. Furthermore, the residual stresses are a significant parameter in section performance. The inclusion of residual stresses always influences the knee portion of the M-P-Φ curves, and thus would have an influence on long column strength. As expected the inclusion of residual stresses has a consistent effect on the M-P-Φ curves in the knee portion. This effect is to induce the section to have a larger curvature for a given applied bending moemnt than would be the case had there been no residual stresses.

(3) Accurate estimates of residual stresses are essential to the derivation of accurate M-P-Φ curves. In the case of fabricated

tubular columns, it is essential to have an accurate determination of residual stresses in two perpendicular directions (namely longitudinal and circumferential directions) in order to derive M-P-Φ curves. This conclusion was demonstrated by the significant difference between curves derived using measured circumferential residual stresses and curves derived using assumed circumferential residual stress values.

(4) The effects of residual stresses on M-P-Φ curves tends to be less pronounced as the combination of applied loads is increased. In other words, as the combination of applied loads is increased, the M-P-Φ curves derived for sections with residual stresses included tend to show a reduced deviation from the M-P-Φ curve derived for the same section under the same combination of applied loads, but with no residual stresses included (that is, a perfect tubular section is being considered for comparison).

(5) The second-order Newton-Raphson iterative technique is a viable method by which to analyze the axial load behavior of a column. This method has previously been reported as being used in the analysis of columns with uniform section properties along its length. For such columns it is possible to consider discrete locations at equal spacings along a column length.

(6) Initial imperfections, particularly out-of-straightness of a fabricated tubular column do affect its axial load behavior. In general, the smaller the initial out-of-straightness of the

column, the higher the column buckling load. The effects of section out-of-roundness have been assumed to be negligible because preliminary experimental investigations indicated that column out-of-roundness was a relatively minor initial imperfection, at least for the columns tested in the experimental portion of this investigation.

8.3 Contributions

(1) For the first time, measurements of both typical circumferential and typical longitudinal residual stress distributions, as measured on the same tubular column specimen, are available. These residual stress distributions are not yet readily obtainable by a purely theoretical derivation. While it seems highly likely that some theoretical derivation of the longitudinal residual stress distribution is possible (given perhaps, a heat input to the section during the longitudinal welding process), there remains some considerable doubt about a theoretical derivation of a circumferential residual stress distribution. This contribution is confirmed by the fact that the assumed circumferential residual stress distribution was not a good indication of the measured circumferential residual stress distribution, despite some similarity of form.

(2) A substantial addition to the available body of test data on the strength and behavior of prototype long fabricated tubular columns has been made. Previously available data was

deficient in the range of slenderness ratio covered and in the thoroughness of data reported. Furthermore, the experimental data reported here gives clear indication of the need for more experimental data on the strength and behavior of long, fabricated tubular columns, particularly in the range of higher slenderness ratios than has previous been tested. The necessity of using end conditions approximating as closely as possible to pinned-end conditions has been demonstrated along with the importance of being able to accurately determine the column effective length of specimens tested.

(3) It is noted in Section 8.2, that the effects of residual stresses on the behavior of a section of a fabricated tubular column become less pronounced as the combination of applied loads is increased. Of particular interest in this context is the affect of the inclusion of circumferential residual stresses when a relatively large axial load was applied to the section prior to bending. It was noted, furthermore, that the measured circumferential residual stress distribution was characterized by relatively small stress values, at least when compared with the assumed circumferential residual stress distribution. This may possibly explain the fact that, particularly when the section was subject to a high applied axial load, the measured circumferential residual stress distribution contributed a relatively minor effect on the M-P-Φ curves over and above the effects of the longitudinal residual stress distribution.

Now, in deriving column buckling loads it would be expected that column buckling would take place at an axial load which was a substantial proportion of the column axial yield load. For these reasons, circumferential residual stresses have not been included in the long column analyses. In practice, the analysis has been developed with the capacity to include circumferential residual stresses, but effects of these stresses have been ignored in the interests of economy. It was not possible to make this conclusion prior to the completion of the short column analysis.

(4) The second-order Newton-Raphson iterative technique has been demonstrated to be an appropriate technique by which to analyze the strength and behavior of a column with highly variable properties along its length. The economy of this method is highly dependent on the degree of refinement adopted in modelling the column, and also in the accuracy of initial estimates of the displaced shape of the column under load.

(5) The analytical technique developed has been used to derive upper and lower bounds of a column buckling curve for fabricated columns. These bounds depend on whether the longitudinal weld is in uniformly the best place on the cross section along the entire column length or in uniformly the worst position. For the more realistic case, with staggered longitudinal welds, the buckling load of a column would be expected to lie between the upper and lower bounds derived. For derivation of these curves

it has been assumed that material of constant yield strength has been used along the entire column length (a usual design assumption). If this is not so, it would appear that the yield strength of sections near the mid-height of a pinned-end column would be more likely to be critical values.

(6) The analytical model has also been used to determine the variation of buckling load of a fabricated tubular column with varying column out-of-straightness. As is noted in Section 8.2, column buckling load tends to increase as initial out-of-straightness is decreased. However, this increase does not appear to be in a uniform or predictable fashion, when the longitudinal welding of a fabricated tubular column is considered. Indeed, if the out-of-straightness tends to force the column to deflect laterally in one direction, and the longitudinal welding tends to force the column to deflect in the opposite direction there is the possibility of a "spring-through" deflection. In such circumstances the column at first may deflect in the direction indicated by the out-of-straightness, but the longitudinal weld may dictate the final deflection direction. This phenomenon, however, seems to happen at column out-of-straightnesses substantially less than the maximum allowable under current fabrication specifications.

(7) The upper and lower bounds of column buckling curves derived theoretically appear, in general, to encompass the range of experimental results obtained in the experimental testing

program. In particular, the lower bound of predicted column buckling curve, is a good lower bound to the experimental results obtained. While this is a good indicator of column strength and tends to confirm the theoretical investigation, there is some doubt about whether this means a great deal. The theoretical column buckling curves were derived for columns fabricated from steel of uniform yield strength throughout their length. Furthermore, the assumed analytical columns had an assumed half-wave sinusoidal initial out-of-straightness profile with the maximum out-of-straightness at mid-height equal to the maximum allowed by current fabrication specifications (that is, $\delta_m = 0.001 \times$ [column length]). In practice, the long column specimens supplied did not satisfy the yield strength assumption, but were manufactured such that they had a smaller maximum out-of-straightness than allowed in fabrication specifications. Nonetheless, it seems likely that the yield strength of steel relatively close to the mid-height of the specimen is of more importance than steel near the ends in determining column strength and behavior. Furthermore, the differences between real column out-of-straightness and assumed theoretical column out-of-straightness may have been reduced by the use of column effective length in plotting experimental results. For all these reasons, it was concluded that it was a good confirmation of the analytical model that the experimental results occurred within the bounds of the predicted buckling curve.

(8) The analytical model was further verified by consideration of individual long column specimens as tested. The model allowed actual yield strength variation along the column to be considered as well as weld staggering and measured out-of-straightness profiles, to any desired degree of accuracy. For the column specimens modelled it appeared that end eccentricities albeit unintentional, had a significant effect on column strength and behavior as did rotational resistance of column end conditions. Using end eccentricities of the same order as those measured during the experimental testing program, and where necessary some end rotational resistance, it was possible to produce a model of the column which predicted the observed column buckling load to within two percent, and also predicted the direction of lateral deflection to within about 0.2 radians (about 10°). This importance of end eccentricities and/or end rotational resistance should be given every attention in the future testing of long fabricated tubular columns.

(9) It does not appear to be either practicable or desirable to further refine the upper and lower bounds of expected column buckling loads derived theoretically. Such a refinement was attempted analytically. To do this, a long column with an assumed half-wave sinusoidal out-of-straightness profile was first analyzed with all longitudinal welds at the same location on the tubular circumference for the whole column length. The column was then reanalyzed several times with all conditions identical except that the longitudinal weld in one (central)

portion of the column was considered at a different location on the tubular circumference in each analysis. For all three maximum out-of-straightness values tested, the observed changes in column buckling load were, at best, marginal. For this reason further refinement of the analytical predictions did not appear to be practicable.

Furthermore, the manufacturing process of fabricated tubular columns is such that the circumferential portions of the longitudinal welds along the column length are usually not absolutely fixed by designers. Rather, it is usual for fabrication specifications to include a "minimum stagger" provision, which specifies some minimum offset between the longitudinal welds in successive "cans" along a column length. It would seem, therefore, that refinements of this nature would be of little practical value to designers.

8.4 Design Recommendations

(1) A new range of column buckling curves for use in the axial design of fabricated tubular columns has been proposed. The lower bound of these curves is somewhat more conservative than previously available column buckling curves, but the reduction in predicted column buckling load is never more than about ten percent.

(2) It seems to be important to maintain a high degree of quality control on the initial imperfections introduced during the

fabrication of long fabricated tubular columns. In particular, the current restriction of initial out-of-straightness has been examined. Basically, this restricts maximum out-of-straightness to 0.1 percent of the column length, with slightly more stringent restrictions for longer columns. This value seems to be a reasonable limiting value, for it seems that manufacturers have little trouble meeting the specification, and furthermore at the maximum permissible value there has not been observed any anomalous lateral deflection behavior of columns as loads are increasing at a value near their buckling load.

(3) The practice of staggering welds between successive "cans" of a long column has long been common for reasons other than column strength. From a column strength point of view the benefits of this practice are somewhat more dubious. Nonetheless, although the placing of the longitudinal wled in one "can" has an indeterminate effect in and of itself, the aggregate effect of such staggering is to produce a column which might be expected to have a buckling load exceeding that predicted by the theoretical lower bound column buckling curve. For these reasons, it is recommended that, if the lower bound of column buckling curve be adopted, the practice of weld staggering be continued.

9. NOMENCLATURE

A = cross-sectional area of section

C = curvature contribution to Eq. 5.20

D_o = outside diameter of tubular section

E = modulus of elasticity

E_t = tangent modulus of elasticity

e_{xs} = initial eccentricity in x-direction of centroid of section at station s from effective line of action of applied load

e_{ys} = initial eccentricity in y-direction of centroid of section at station s from effective line of action of applied load

f = generalized force vector (Eq. 4.1)

$\dot{f}$ = change in generalized force vector

h = interstation distance (if constant along a column)

h_s = distance along column between station s and s+1

I = moment of inertia of cross section

I_e = moment of inertia of "elastic core" of cross section

I_m = unit matrix

J = Jacobian matrix

k = iteration number

K = column effective length factor

L = column length

M = bending moment

M_p = plastic bending moment of section

M_x = bending moment about x-axis

M_{xa} = bending moment about x-axis at end A

M_{xb} = bending moment about x-axis at end B

M_{xs} = bending moment about x-axis at station s

M_y = bending moment about y-axis

M_{ya} = bending moment about y-axis at end A

M_{yb} = bending moment about y-axis at end B

M_{ys} = bending moment about y-axis at station s

m_x = $\frac{M_x}{M_p}$

n = number of segments column is divided into

P = axial load

P_d = "dynamic" column buckling load (see Fig. 3.18)

P_s = "static" column buckling load (see Fig. 3.18)

P_{TM} = tangent modulus column buckling load

P_y = column axial yield load = $A \sigma_y$

p = $\frac{P}{P_y}$

Q_{ij} = see Eq. 4.4

R = mean radius of tubular section

R_i = internal radius of tubular section

R_t = end restraint contribution to Eq. 5.20

r = radius of gyration of cross section

s = station number

t = wall thickness of tubular section

U_s = deflection of station s in x-direction, outcome of first iterative process (see Eq. 5.11)

u_o = initial displacement of station s in x-direction, while column in an unloaded state

u_s = deflection of station s in x-direction

V_s = deflection of station s in y-direction, outcome of first iterative process (see Eq. 5.12)

v_o = initial displacement of station s in y-direction, while column in an unloaded state

v_s = deflection of station s in y-direction

W = deformation vector (Eq. 5.18)

w = deformation vector (Eq. 5.19)

w_c = complimentary solution (Eq. 5.44)

w_o = initial lateral deflection of column

w_p = particular solution (Eq. 5.44)

X = generalized deformation vector (Eq. 4.1)

$\dot{X}$ = change in generalized deformation vector

x = distance from y-axis

x_o = initial mid-height out-of-straightness in x-direction (Fig. 5.6)

x_θ = distance from the longitudinal weld (measured around the tubular circumference)

y = distance from x-axis

y_o = initial mid-height out-of-straightness in y-direction

Z_p = plastic section modulus (Eq. 4.8)

α = deflection angle

β = angle (Fig. 4.8)

δ_A = end eccentricity towards A

δ_B = end eccentricity towards B

δ_m = maximum column out-of-straightness

ϵ = arbitrary small value

ϵ_o = axial strain (Fig. 4.1)

ϵ_y = axial strain when section just yielding under axial load only

θ = angle (Fig. 4.8)

θ_i = weld angle at station i (Fig. 5.6)

λ = $\frac{1}{\pi}\sqrt{\frac{\sigma_y}{E}}\frac{KL}{r}$

$\frac{1}{\rho}$ = nondimensional curvature (Eq. 4.15)

σ_{cr} = critical buckling stress

$\sigma_i (i=1,2)$ = material stresses (Fig. 4.8)

σ_L = longitudinal residual stresses

σ_y = material yield strength

σ_{yd} = material "dynamic" yield strength

σ_{ys} = material "static" yield strength

Φ_{ox} = initial curvature in x-direction

Φ_{oy} = initial curvature in y-direction

Φ_x = bending curvature about x-axis (Fig. 4.1) = $-\frac{\partial^2 u}{\partial x^2}$

$\bar{\Phi}_x$ = change in bending curvature about x-axis

Φ_y = bending curvature about y-axis (Fig. 4.1) = $-\frac{\partial^2 v}{\partial y^2}$

$\bar{\Phi}_y$ = change in bending curvature about y-axis

Φ_{yy} = curvature of tubular section at first yield (Eq. 4.9)

φ_x = $\Phi_x - \Phi_{ox}$

φ_y = $\Phi_y - \Phi_{oy}$

Ψ_{xa} = slope in x-direction at end A

Ψ_{xb} = slope in x-direction at end B

Ψ_{ya} = slope in y-direction at end A

Ψ_{yb} = slope in y-direction at end B

10. TABLES AND FIGURES

Table 3.1 Stub Column Failure Data

Specimen	Heat Lot	Outside Diameter m (in)	Length m (in)	Dynamic Ultimate Load kN (kips)	Static Ultimate Load kN (kips)	Maximum Recorded Strain $\mu\varepsilon$
1	II	0.38 (15)	0.91 (36)	3596 (808)	3444 (774)	22600
2	I	0.38 (15)	0.91 (36)	3373 (758)	3222 (724)	14200
3	II	0.56 (22)	1.17 (46)	4589 (1030)	4459 (1002)	7790

Table 3.2 Material Tensile Properties

Origin	Measurement	Heat Lot I	Heat Lot II
Mill Report	Dynamic σ_{yd}, MPa (ksi)	318 (46.1)	328 (47.5)
	Static σ_{ys}, MPa (ksi)	-	-
	E, MPa (ksi)	-	-
"Static" Laboratory Test[a]	Dynamic σ_{yd}, MPa (ksi)	288 (41.7)	321 (46.5)
	Static σ_{ys}, MPa (ksi)	271 (39.3)	308 (44.6)
	E, MPa (ksi)	211,000 (30,600)	212,000 (30,700)
Commercial Laboratory Test[b]	Dynamic σ_{yd}, MPa (ksi)	293 (42.5)	324 (47.0)
	Static σ_{ys}, MPa (ksi)	271 (39.3)	308 (44.6)
	E, MPa (ksi)	214,000 (31,000)	213,000 (30,800)

[a]Maximum Strain Rate = 0.64 mm/min (0.025 in/min)

[b]Maximum Strain Rate = 1.28 mm/min (0.05 in/min)

All specimens taken from plate before rolling.

Table 3.3 List of Long Column Specimen Properties

Specimen No.	Nominal Length, L m (ft)	Outside Diameter, D_o m (in)	Nominal L/r Ratio	Diameter-to-Thickness Ratio, D_o/t	Range of Effective Length Factor, K	Central Can Heat Lot[a]
1	5.5 (18)	0.38 (15)	42	48	0.85-0.95	I, II[b]
2	5.5 (18)	0.38 (15)	42	48	0.95	I, II[b]
3	7.6 (25)	0.38 (15)	60	48	0.88-0.92	II
4	7.6 (25)	0.38 (15)	60	48	0.96	II
5	7.6 (25)	0.56 (22)	39	70	0.60-0.68	II[c]
6	7.6 (25)	0.56 (22)	39	70	0.72-0.76	II[c]
7	11 (36)	0.38 (15)	83	48	0.78-1.0	II
8	11 (36)	0.38 (15)	83	48	0.61-0.69	I, II[b]
9	11 (36)	0.56 (22)	58	70	0.75-0.86	II[c]
10	11 (36)	0.56 (22)	58	70	0.64-0.83	II[c]

[a]The yield stress of Heat Lot II was higher than that for Heat Lot I (see Table 3.2)

[b]Circumferential weld near center, different heat lots on each side

[c]All pipe from steel of Heat Lot II

Table 3.4 Approximate Unintentional End Eccentricities

Specimen	Top Bearing Block		Bottom Bearing Block	
	Eccentricity toward A, δ_x, mm (in)	Eccentricity toward B, δ_y, mm (in)	Eccentricity toward A, δ_x, mm (in)	Eccentricity toward B, δ_y, mm (in)
1	-	-	-	-
2	-	-	-0.07 (0.02)	-0.07 (0.02)
3	-	-	1.6 (0.06)	-2.4 (0.09)
4	-2.2 (0.09)	0	-	-
5	-5.6 (0.22)	5.6 (0.22)	0	0
6	5.6 (0.22)	1.1 (0.04)	1.1 (0.04)	1.1 (0.04)
7	3.4 (0.13)	-3.4 (0.13)	10.7 (0.42)	-4.1 (0.16)
8	6.1 (0.24)	4.1 (0.20)	0	0
9	0.6 (0.02)	1.1 (0.04)	-2.5 (0.10)	-9.6 (0.38)
10	6.9 (0.27)	6.9 (0.27)	3.9 (0.15)	-0.6 (0.02)

Table 3.5 Long Column Failure Behavior Data

Specimen	Failure Mode	Location of Critical Section $\left(\frac{Z}{L}\right)^a$	Maximum Measured Deflection at Mid-Height δ_m, mm (in)	$\left(\frac{\delta_m}{L}\right)$ %
1	General Inelastic Instability	0.48	53 (2.07)	0.96
2	General Inelastic Instability	0.48	57 (2.24)	1.04
3	General Inelastic Instability	0.57	84 (3.31)	1.10
4	General Inelastic Instability then Interactive Instability	0.62	96 (3.79)	1.26
5	Interactive Instability	0.38	79 (3.10)	1.03
6	Interactive Instability	0.82	49 (1.92)	-[b]
7	General Inelastic Instability	0.41	184 (7.26)	1.68
8	General Inelastic Instability	0.64	140 (5.50)	1.27
9	Interactive Instability	0.27	106 (4.16)	-[b]
10	Interactive Instability	0.56	121 (4.77)	1.10

[a] Z is measured from base of specimen

[b] Maximum deflection is closer to a quarter point

Table 3.6(a) Maximum Column Loads

Specimen	Dynamic			Static		
	P_d kN (kips)	P_y[a] kN (kips)	$\frac{P_d}{P_y}$	P_s kN (kips)	P_y[b] kN (kips)	$\frac{P_s}{P_y}$
1	2581 (580)	2674 (601)	0.965	2476 (556)	2523 (567)	0.981
2	2648 (595)	2674 (601)	0.990	2492 (560)	2523 (567)	0.988
3	2403 (540)	2674 (601)	0.899	2270 (510)	2523 (567)	0.900
4	2403 (540)	2674 (601)	0.899	2290 (516)	2523 (567)	0.910
5	4370 (982)	4406 (990)	0.992	4263 (958)	4228 (950)	1.01
6	4361 (980)	4406 (990)	0.990	4112 (924)	4228 (950)	0.973
7	2270 (510)	2674 (601)	0.849	2212 (497)	2523 (567)	0.877
8	2465 (554)	2674 (601)	0.921	2367 (532)	2523 (567)	0.938
9	4272 (960)	4406 (990)	0.970	4183 (940)	4228 (950)	0.99
10	4228 (950)	4406 (990)	0.960	4094 (920)	4228 (950)	0.968

[a]Derived using dynamic yield stresses derived in "Static" Laboratory Tests (see Table 3.2)

[b]Derived using static yield stresses derived in "Static" Laboratory Tests (see Table 3.2)

Table 3.6(b) Maximum Column Loads

Specimen	Dynamic		
	P_d kN (kips)	P_y [c] kN (kips)	$\frac{P_d}{P_y}$
1	2581 (580)	2370 (612)	0.95
2	2648 (595)	2370 (612)	0.97
3	2403 (540)	2370 (612)	0.88
4	2403 (540)	2370 (612)	0.88
5	4370 (982)	4540 (1015)	0.97
6	4361 (980)	4540 (1015)	0.95
7	2270 (510)	2370 (612)	0.83
8	2465 (554)	2370 (612)	0.90
9	4272 (960)	4540 (1015)	0.95
10	4228 (950)	4540 (1015)	0.94

[c]Derived using dynamic yield stresses derived in commercial laboratory tests (see Table 3.2)

Table 5.1 Upper and Lower Bounds of Theoretical Buckling Load for Particular Long Fabricated Tubular Columns Considered

$\lambda = \frac{1}{\pi}\sqrt{\frac{\sigma_y}{E}}\frac{KL}{r}$	Buckling Load / Section Yield Load	
	Upper Bound	Lower Bound
0.34	1.0	0.94
0.76	0.88	0.80
0.96	0.76	0.68
1.54	0.34	0.32

Table 6.1 Comparison of Test Data and Theoretical Model Results for Long Column Specimen 3

Long Column Specimen No. 3				
Length = 7.6 m (25 ft) $\frac{L}{r}$ = 60 O.D. = 0.38 m (15 in)		Test Data	Model 1	Model 2
Model Parameters	Number of Stations No. of stations with Inelastic Capabilities	- -	10 4	7 3
End Eccentricities mm (in)	Top, x-direction Top, y-direction Bottom, x-direction Bottom, y-direction	- - 1.6 (0.06) -2.4 (0.09)	0 0 0 0	0 0 0 0
Failure Load	P_s, kN (kips) $\frac{P_{model}}{P_{expt}}$	2270 (510) -	2230 (508) 0.98	2230 (508) 0.98
Lateral Movement at Mid-Height	At load = 500 kips x-movement, mm (in) y-movement, mm (in) α (radians)	 -1.91 (-0.075) -5.49 (-0.216) 4.38	 -2.03 (-0.08) -5.08 (-0.20) 4.33	 -1.32 (-0.052) -4.95 (-0.195) 4.45

Table 6.2 Comparison of Test Data and Theoretical Model Results for Long Column Specimen 4

Long Column Specimen No. 4					
Length = 7.6 m (25 ft) $\frac{L}{r}$ = 60 O.D. = 0.38 m (15 in)		Test Data	Model 1	Model 2	Model 3
Model Parameters	Number of Stations	-	7	7	7
	No. of stations with Inelastic Capabilities	-	3	3	3
End Eccentricities mm (in)	Top, x-direction	-2.2 (-0.09)	-2.5 (-0.1)	-6.4 (-0.25)	-12.7 (-0.5)
	Top, y-direction	0	0	0	0
	Bottom, x-direction	-	-2.5 (-0.1)	-6.4 (-0.25)	-12.7 (-0.5)
	Bottom, y-direction	-	0	0	0
Failure Load	P_s, kN (kips)	2290 (516)	>2402 (>540)	2349 (528)	2104 (473)
	$\frac{P_{model}}{P_{expt}}$	-	>1.05	1.02	0.92
Lateral Movement at Mid-Height	At load = 510 kips				
	x-movement, mm (in)	12.0 (0.473)	3.30 (0.13)	12.2 (0.481)	-
	y-movement, mm (in)	0.4 (0.015)	1.42 (0.056)	1.83 (0.012)	-
	α (radians)	0.03	0.41	0.15	-
	At load = 460 kips				
	x-movement, mm (in)	3.86 (0.152)	-	4.62 (0.182)	13.0 (0.51)
	y-movement, mm (in)	0	-	1.02 (0.040)	1.3 (0.05)
	α (radians)	0	-	0.22	0.10

Table 6.3 Comparison of Test Data and Theoretical Model Results for Long Column Specimen 6

Long Column Specimen No. 6			
Length = 7.6 m (25 ft) $\frac{L}{r}$ = 39 O.D. = 0.56 m (22 in)		Test Data	Model Data
Model Parameters	Number of Stations No. of Stations with Inelastic Capabilities	- -	6 4
End Eccentricities mm (in)	Top, x-direction Top, y-direction Bottom, x-direction Bottom, y-direction	5.6 (0.22) 1.1 (0.04) 1.1 (0.04) 1.1 (0.04)	0 0 0 0
Failure Load	P_s, kN (kips) $\frac{P_{model}}{P_{expt}}$	4112 (924) -	4040 (908) 0.98
Lateral Movement at Mid-Height	At Load = 900 kips x-movement, mm (in) y-movement, mm (in) α (radians)	 0.53 (0.021) 0.76 (0.030) 0.96	 3.38 (0.133) 1.96 (0.077) 0.52

Table 6.4 Comparison of Test Data and Theoretical Model Results for Long Column Specimen 10

Long Column Specimen No. 10				
Length = 11 m (36 ft) $\frac{L}{r}$ = 58 O.D. = 0.56 m (22 in)		Test Data	Model 1	Model 2
Model Parameters	Number of Stations No. of Stations with Inelastic Capabilities	- -	8 2	8 2
End Eccentricities mm (in)	Top, x-direction Top, y-direction Bottom, x-direction Bottom, y-direction	6.9 (0.27) 6.9 (0.27) 3.9 (0.15) -0.06 (-0.02)	0 0 0 0	2.5 (0.1) 2.5 (0.1) 2.5 (0.1) 2.5 (0.1)
Failure Load	P_s, kN (kips) $\frac{P_{model}}{P_{expt}}$	4094 (920) -	4094 (920) 1.00	3945 (887) 0.96
Lateral Movement at Mid-Height	At load = 860 kips x-movement, mm (in) y-movement, mm (in) α (radians) At load = 910 kips x-movement, mm (in) y-movement, mm (in) α (radians)	 -0.71 (-0.028) -1.63 (-0.064) 4.30 -1.2 (-0.046) -3.1 (-0.121) 4.35	 -0.51 (-0.020) -2.16 (-0.085) 4.48 -0.5 (-0.02) -6.6 (-0.26) 4.64	 - - -3.9 (-0.154) -5.8 (-0.230) 4.12

Table 6.5 Comparison of Test Data and Theoretical Model Results for Long Column Specimen 7

Long Column Specimen No. 7				
Length = 11 m (36 ft) $\frac{L}{r}$ = 83 O.D. = 0.38 m (15 in)		Test Data	Model 1	Model 2
Model Parameters	Number of Stations	-	9	9
	No. of Stations with Inelastic Capabilities	-	3	3
	Rotation Resistance of Ends, kN-m/rad(k-in/rad)	-	0	11.3 (100)
End Eccentricities mm (in)	Top, x-direction	3.4 (0.13)	0	0
	Top, y-direction	-3.4 (-0.13)	0	0
	Bottom, x-direction	10.7 (0.42)	0	0
	Bottom, y-direction	-4.1 (0.16)	0	0
Failure Load	P_s, kN (kips)	2212 (497)	1957 (440)	2202 (495)
	$\frac{P_{model}}{P_{expt}}$	- -	0.89	1.00
Lateral Movement at Mid-Height	At load = 460 kips			
	x-movement, mm (in)	0.30 (0.012)	-	1.68 (0.066)
	y-movement, mm (in)	0.89 (0.035)	-	-1.30 (-0.051)
	α (radians)	1.24	-	5.51
	At load = 497 kips		-	-
	x-movement, mm (in)	-0.76 (-0.030)	-	-
	y-movement, mm (in)	7.11 (0.280)	-	-
	α (radians)	1.68		

Table 6.5 Continued

Long Column Specimen No. 7				
Length = 11 m (36 ft) $\frac{L}{r}$ = 83 O.D. = 0.38 m (15 in)		Test Data	Model 3	Model 4
Model Parameters	Number of Stations	-	9	9
	No. of Stations with Inelastic Capabilities	-	3	3
	Rotation Resistance of Ends, kN-m/rad(k-in/rad)	-	22.6 (200)	11.3 (100)
End Eccentricities mm (in)	Top, x-direction	3.4 (0.13)	0	0.51 (0.02)
	Top, y-direction	-3.4 (-0.13)	0	-0.51 (-0.02)
	Bottom, x-direction	10.7 (0.42)	0	0.51 (0.02)
	Bottom, y-direction	-4.1 (0.16)	0	-0.51 (-0.02)
Failure Load	P_s, kN (kips)	2212 (497)	2246 (505)	2290 (515)
	$\frac{P_{model}}{P_{expt}}$	-	1.02	1.04
Lateral Movement at Mid-Height	At load = 460 kips			
	x-movement, mm (in)	0.30 (0.012)	1.65 (0.065)	-1.42 (-0.056)
	y-movement, mm (in)	0.89 (0.035)	-1.07 (-0.042)	1.07 (0.042)
	α (radians)	1.24	5.71	2.21
	At load = 497 kips			
	x-movement, mm (in)	-0.76 (-0.030)	5.23 (0.206)	0.30 (0.012)
	y-movement, mm (in)	7.11 (0.280)	-3.81 (-0.150)	0.15 (0.006)
	α (radians)	1.68	5.65	0.46

Table 6.6 Comparison of Test Data and Theoretical Model Results for Long Column Specimen 8

Long Column Specimen No. 8					
Length = 11 m (36 ft) $\frac{L}{r}$ = 83 O.D. = 0.38 m (15 in)		Test Data	Model 1	Model 2	Model 3
Model Parameters	Number of Stations	-	10	10	10
	No. of Stations with Inelastic Capabilities	-	2	2	2
	Rotation Resistance of Ends, kN-m/rad (K-in/rad)	-	0	56.5(500)	22.6(200)
End Eccentricities mm (in)	Top, x-direction	6.1(0.24)	0	0	-1.02(-0.04)
	Top, y-direction	4.1(0.20)	0	0	1.02(0.04)
	Bottom, x-direction	0	0	0	-1.02(-0.04)
	Bottom, y-direction	0	0	0	1.02(0.04)
Failure Load	P_s, kN (kips)	2375(534)	2068(465)	2224(500)	2335(525)
	$\frac{P_{model}}{P_{expt}}$	-	0.87	0.94	0.98
Lateral Movement at Mid-Height	At Load = 480 kips				
	x-movement, mm (in)	-2.90(-0.114)	-	-8.66(-0.341)	-3.81(-0.150)
	y-movement, mm (in)	1.02(0.040)	-	7.52(0.296)	3.33(0.131)
	α (radians)	2.80	-	2.43	2.42
	At load = 530 kips				
	x-movement, mm (in)	-4.83(-0.190)	-	-	-
	y-movement, mm (in)	2.44(0.096)	-	-	-
	α(radians)	2.67	-	-	-

Table 6.7 Comparison of Test Data and Theoretical Model Results for Wilson Long Column Test Specimen A1

Wilson Test Specimen A1				
Length = 9.14 m (30 ft) $\frac{L}{r}$ = 84 O.D. = 0.309 m (12.15 in)		Test Data	Model 1	Model 2
Model Parameters	Number of Stations	-	11	11
	No. of Stations with Inelastic Capabilities	-	3	3
	Longitudinal Residual Stresses Included?	-	No	Yes
	Rotation Resistance of Ends, kN-m/rad(k-in/rad)	-	11.3 (100)	11.3 (100)
End Eccentricities mm (in)	Top, x-direction	-	0	0
	Top, y-direction	-	0	0
	Bottom, x-direction	-	0	0
	Bottom, y-direction	-	0	0
Failure Load	P_s kN (kips)	596 (134)	583 (131)	565 (127)
	$\frac{P_{model}}{P_{expt}}$	-	0.98	0.95
Lateral Movement at Mid-Height	At load = 130 kips			
	x-movement, mm (in)	-1.87 (-0.07)	9.45 (0.372)	-
	y-movement, mm (in)	4.57 (0.18)	9.30 (0.366)	-
	α (radinas)	1.94	0.78	-
	At load = 100 kips			
	x-movement, mm (in)	0	5.74 (0.226)	5.00 (0.197)
	y-movement, mm (in)	2.29 (0.09)	3.00 (0.118)	4.47 (0.176)
	α (radians)	1.57	0.48	0.73

Table 6.8 Comparison of Test Data and Theoretical Results for Wilson Long Column Test Specimen A2

Wilson Test Specimen A2				
Length = 9.14 m (30 ft) $\frac{L}{r}$ = 84 O.D. = 0.308 m (12.12 in)		Test Data	Model 1	Model 2
Model Parameters	Number of Stations	-	11	11
	No. of Stations with Inelastic Capabilities	-	3	3
	Longitudinal Residual Stresses Included?	-	No	Yes
	Rotation Resistance of Ends, kN-m/rad(k-in/rad)	-	11.3 (100)	11.3 (100)
End Eccentricities mm (in)	Top, x-direction	-	0	0
	Top, y-direction	-	0	0
	Bottom, x-direction	-	0	0
	Bottom, y-direction	-	0	0
Failure Load	P_s, kN (kips)	489 (110)	547 (123)	507 (114)
	$\frac{P_{model}}{P_{expt}}$	-	1.12	1.03
Lateral Movement at Mid-Height	At load = 100 kips			
	x-movement, mm (in)	7.37 (0.29)	13.2 (0.519)	10.6 (0.417)
	y-movement, mm (in)	15.2 (0.60)	3.30 (0.130)	3.05 (0.120)
	α (radians)	1.12	0.25	0.28
	At load = 80 kips			
	x-movement, mm (in)	5.59 (0.22)	6.71 (0.264)	6.71 (0.264)
	y-movement, mm (in)	14.2 (0.56)	1.80 (0.071)	1.80 (0.071)
	α (radians)	1.20	0.26	0.26

Table 6.9 Comparison of Test Data and Theoretical Model Results for Wilson Long Column Test Specimen B1

Wilson Test Specimen B1				
Length = 9.14 m (30 ft) $\frac{L}{r}$ = 84 O.D. = 0.308 m (12.12 in)		Test Data	Model 1	Model 2
Model Parameters	Number of Stations	-	11	11
	No. of Stations with Inelastic Capabilities	-	3	3
	Longitudinal Residual Stresses Included?	-	No	Yes
	Rotation Resistance of Ends, kN-m/rad(k-in/rad)	-	11.3 (100)	11.3 (100)
End Eccentricities mm (in)	Top, x-direction	-	0	0
	Top, y-direction	-	0	0
	Bottom, x-direction	-	0	0
	Bottom, y-direction	-	0	0
Failure Load	P_s, kN (kips)	522 (117.3)	689 (155)	512 (115)
	$\frac{P_{model}}{P_{expt}}$	-	1.32	0.98
Lateral Movement at Mid-Height	At load = 110 kips			
	x-movement, mm (in)	3.56 (0.14)	-0.25 (-0.010)	-0.25 (-0.010)
	y-movement, mm (in)	-2.54 (-0.10)	-1.22 (-0.048)	-1.47 (-0.058)
	α (radians)	5.66	4.51	4.54
	At load = 80 kips			
	x-movement, mm (in)	2.29 (0.09)	-0.20 (-0.008)	-0.05 (-0.002)
	y-movement, mm (in)	-1.78 (-0.07)	-0.89 (-0.035)	-0.71 (-0.028)
	α (radians)	5.51	4.49	4.64

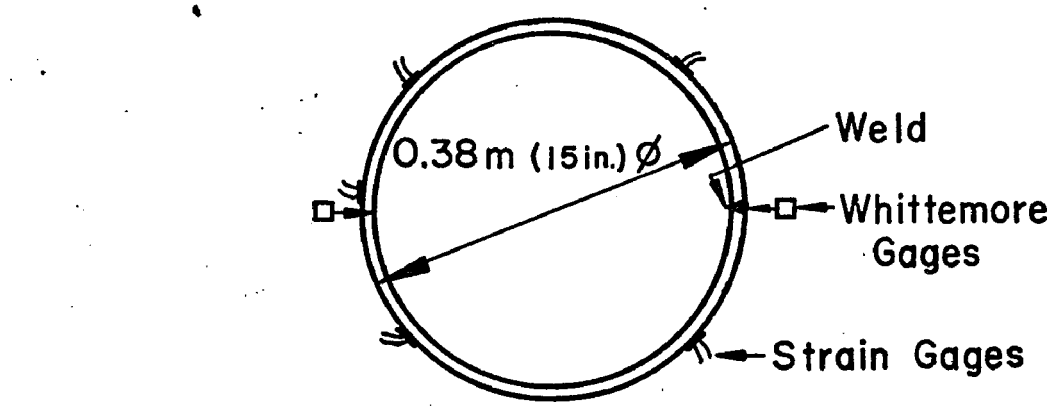

a) Plan

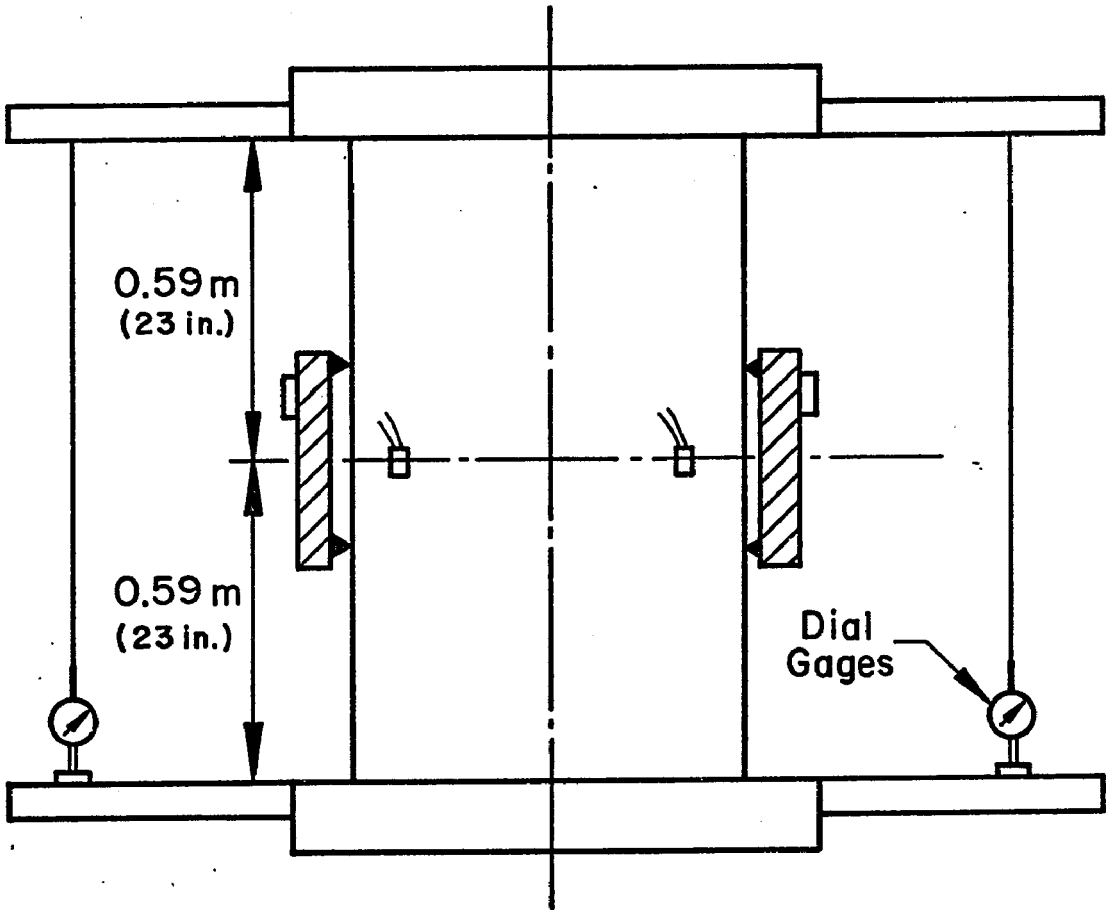

b) Elevation

Fig. 3.1 Diagram of Stub Column Tests

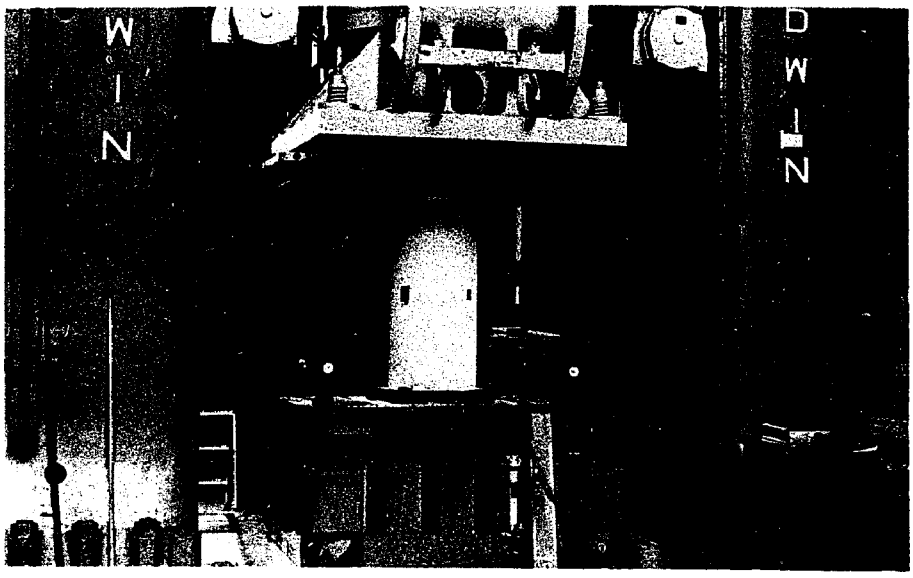

a) Overall View of Specimen in Testing Machine

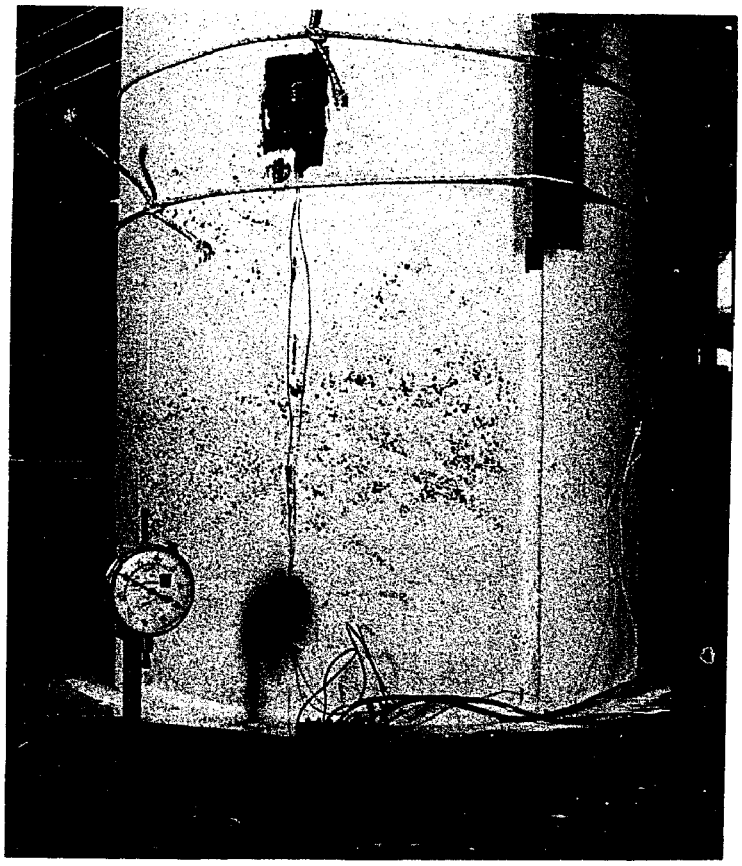

b) Detailed Instrumentation

Fig. 3.2 Typical Stub Column Testing Technique

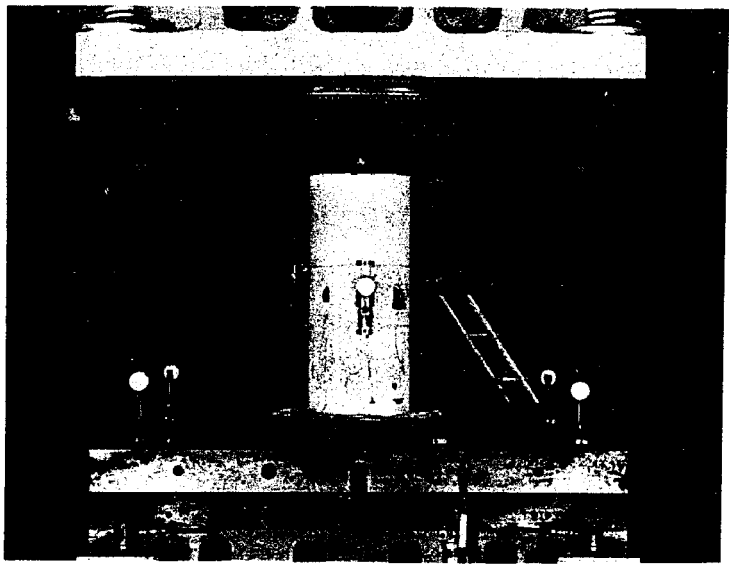

a) Testing Partly Completed

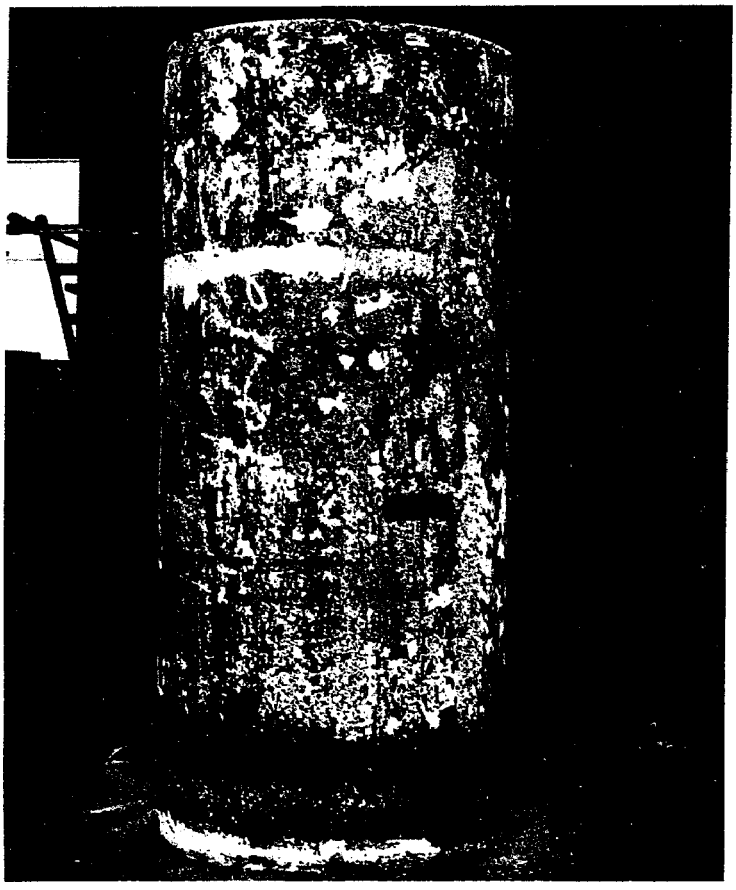

b) After Completion of Testing

Fig. 3.3 Stub Column No. 1 - Testing Photographs

a) Testing Complete - Opposite to Weld

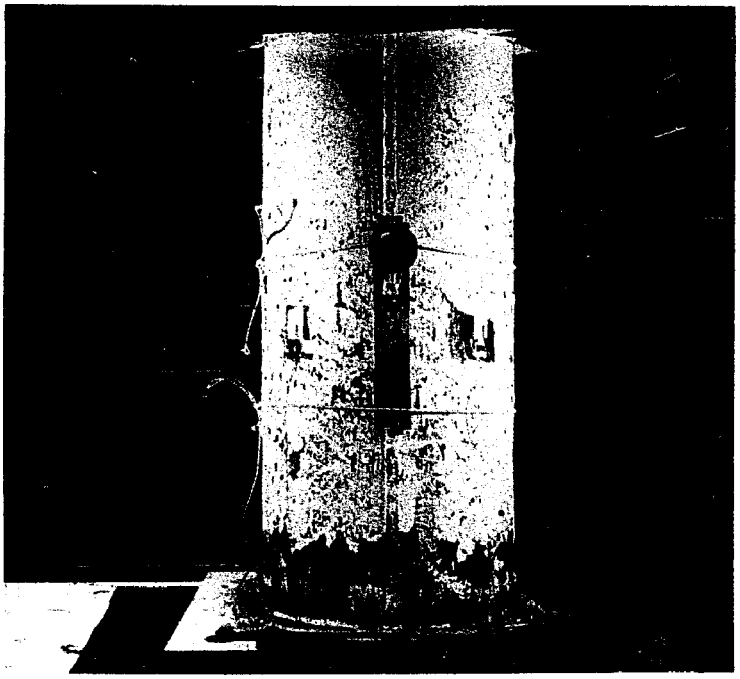

b) Testing Complete - Weld Side of Specimen

Fig. 3.4 Stub Column No. 2 - Testing Photographs

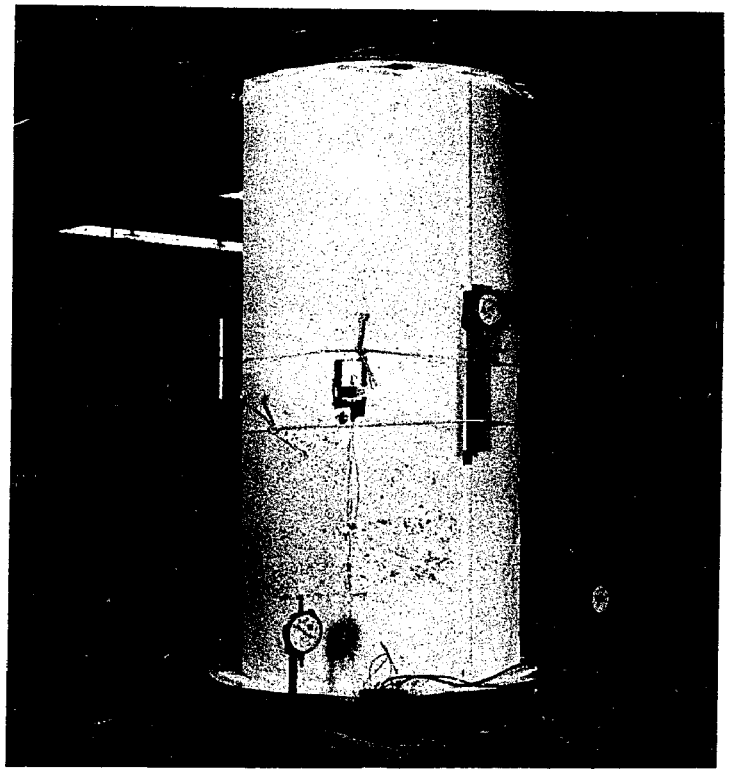

a) Onset of Yield

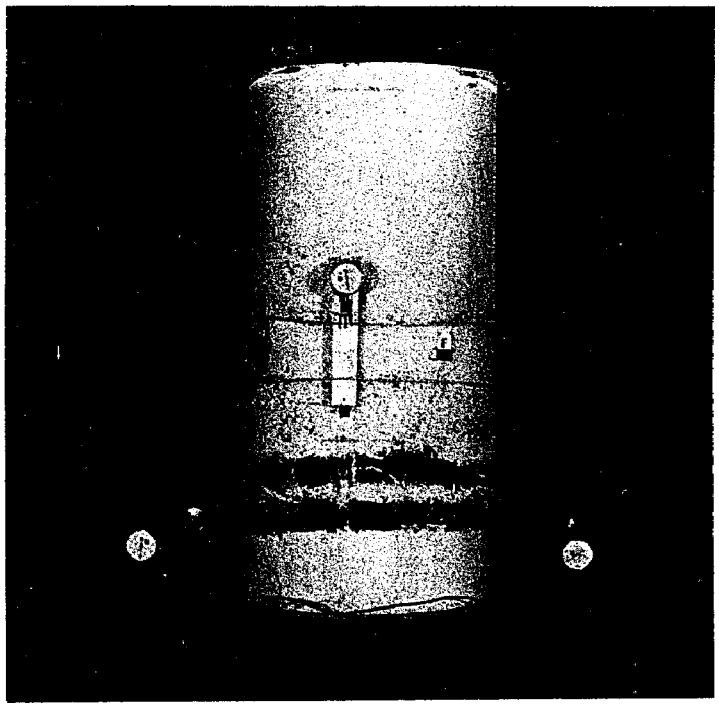

b) Testing Completed

Fig. 3.5 Stub Column No. 3 - Testing Photographs

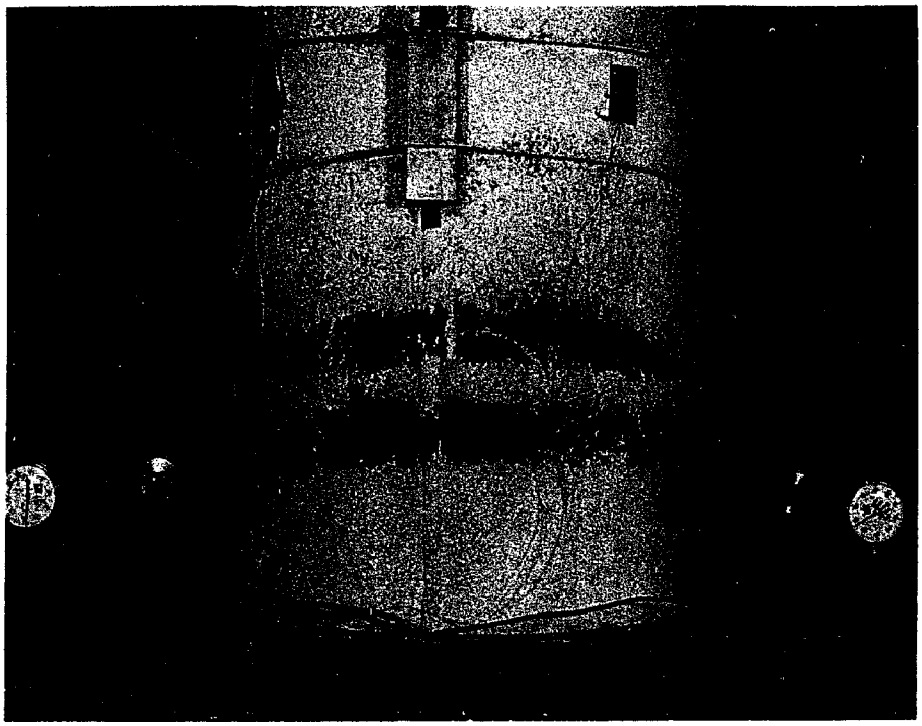

a) Weld Side of Specimen

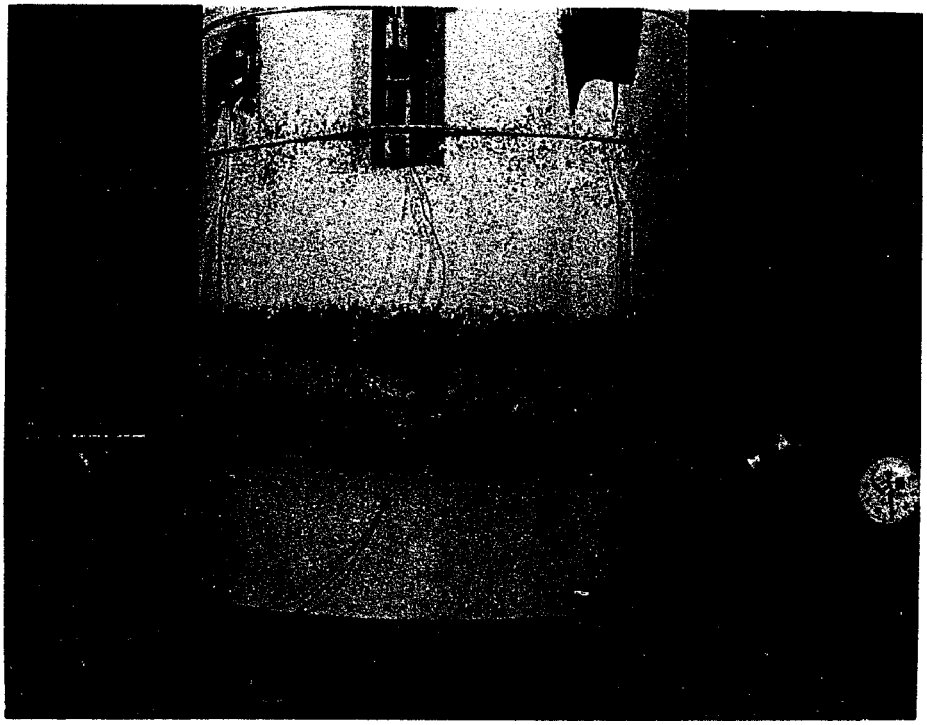

b) Opposite to Weld

Fig. 3.6 Details of Stub Column Specimen No. 3 Failure

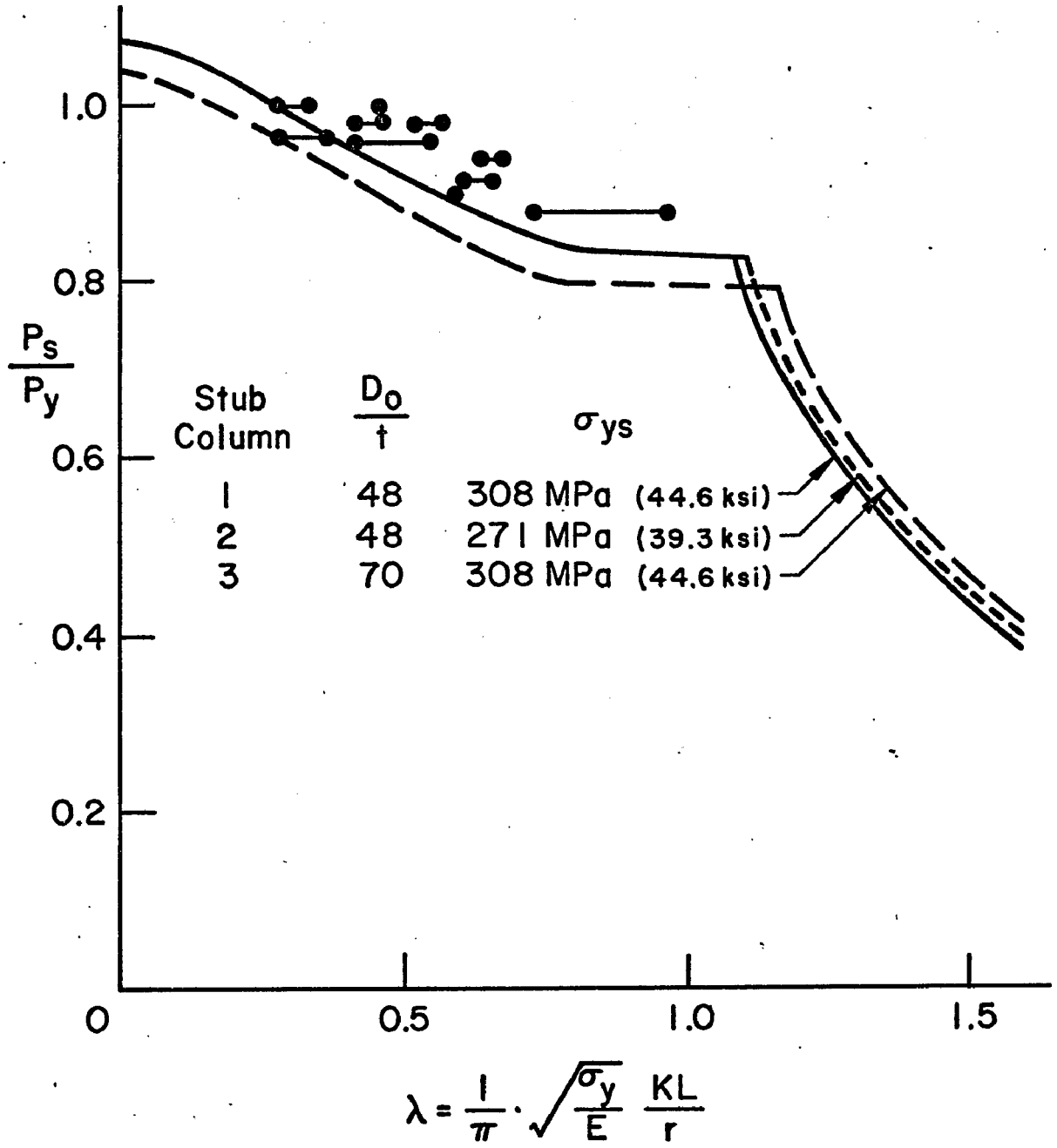

Fig. 3.7 Column Buckling Curves Predicted by Stub Column Tests and Comparison with Long Column Test Results

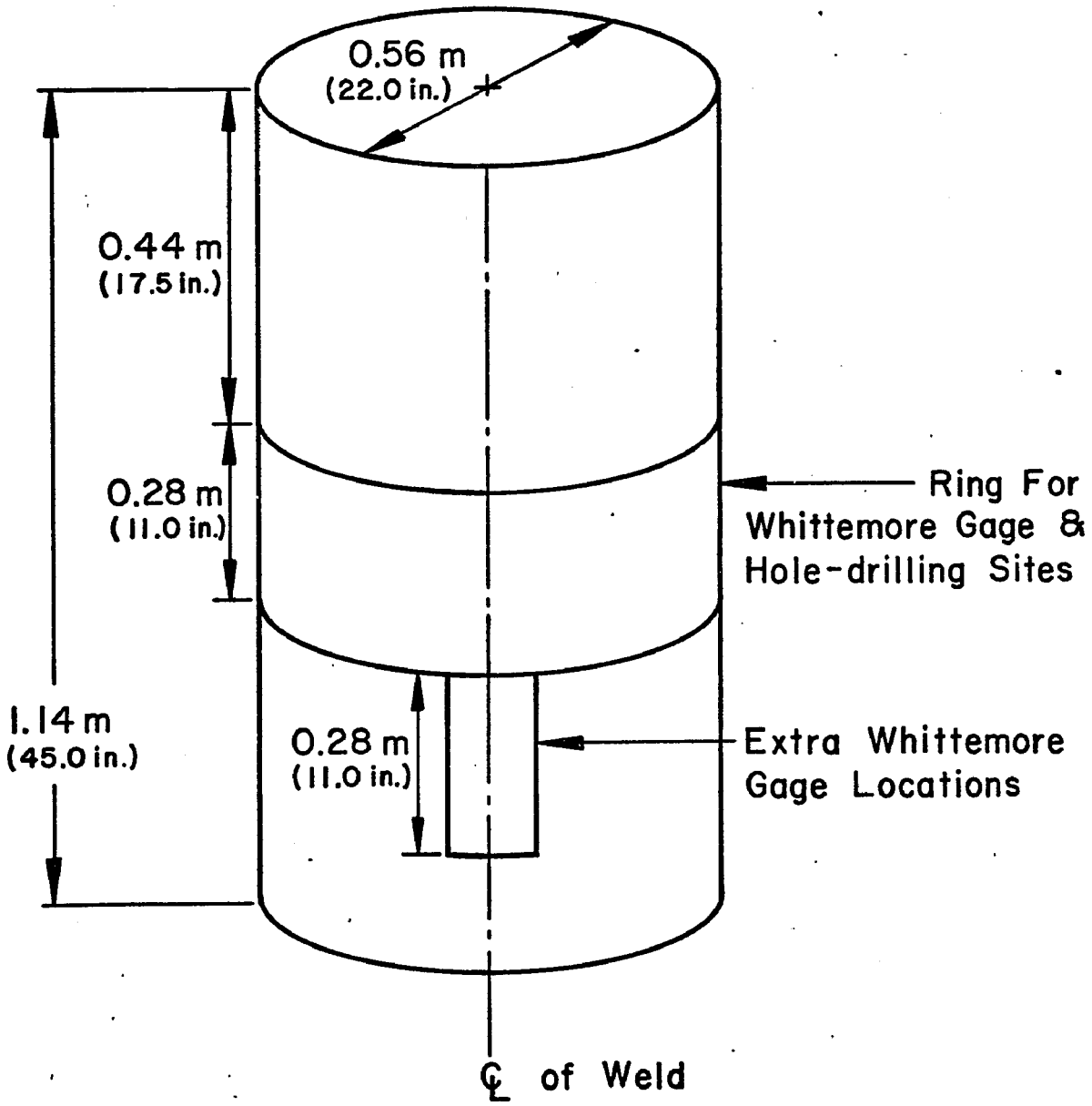

Fig. 3.8 Layout of Stub Column Dissection for Residual Stress Measurements

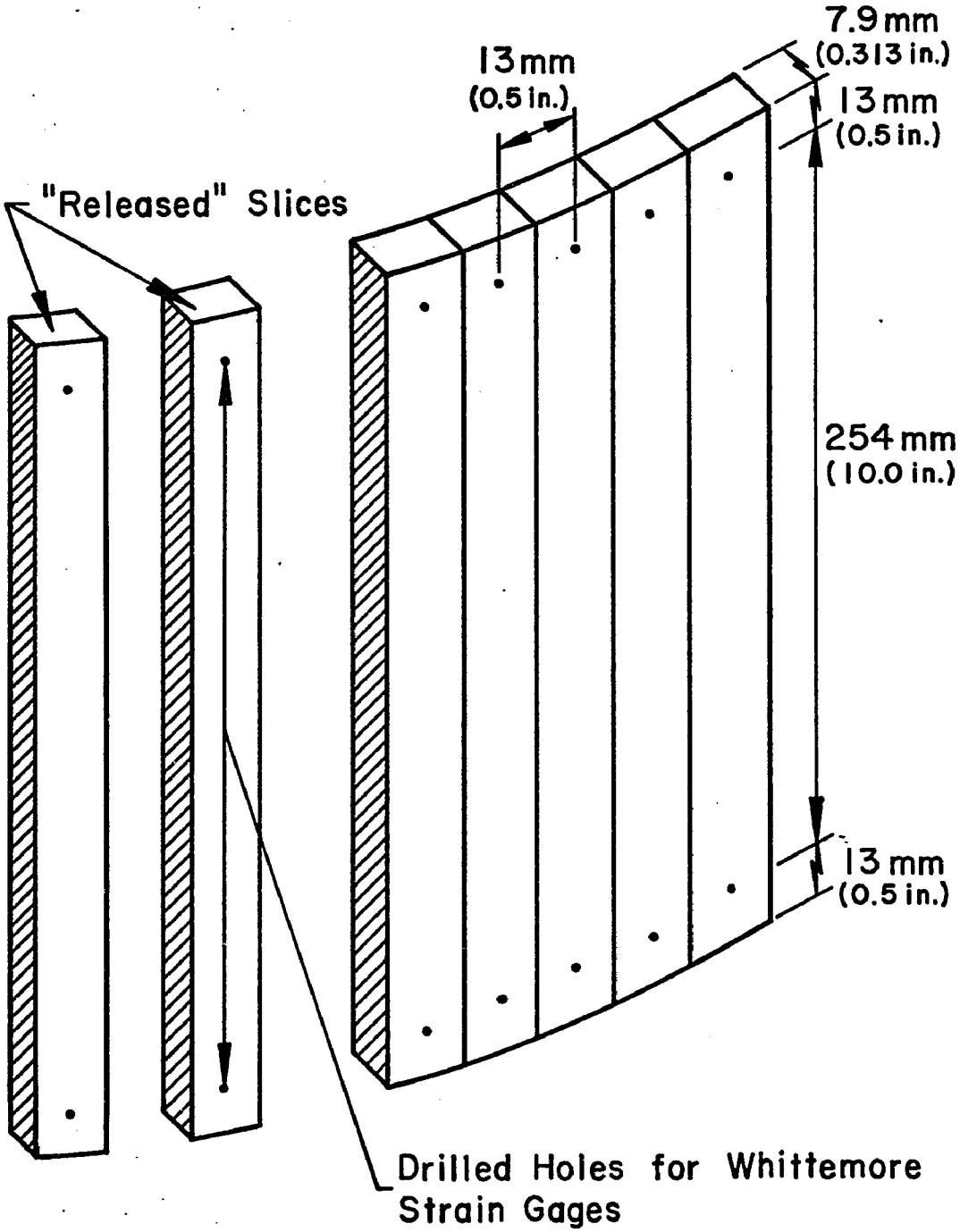

Fig. 3.9 Cutting of Bars for Longitudinal Residual Stress Measurement

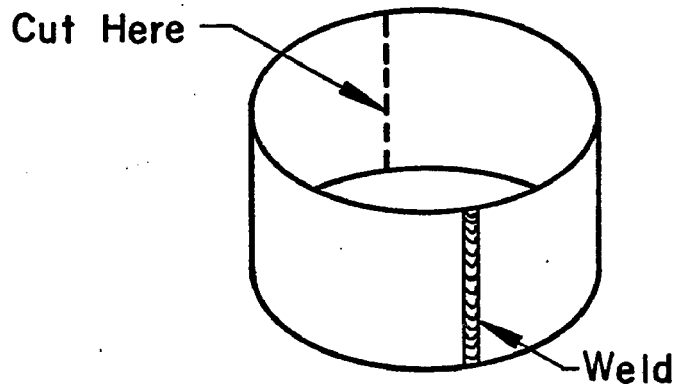

a) Cutting a cylindrical tube for flat presentation

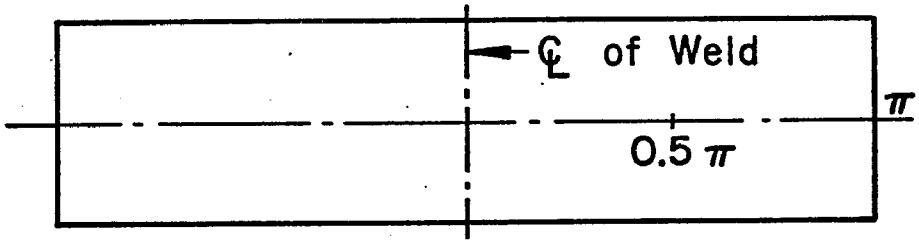

b) Flat projection of surface of a cylindrical tube

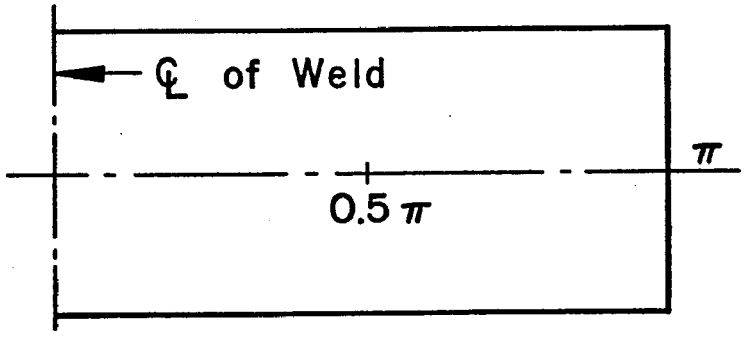

c) Half of projection of surface of cylindrical tube

Fig. 3.10 Presentation of Results of Longitudinal Residual Stress Measurements

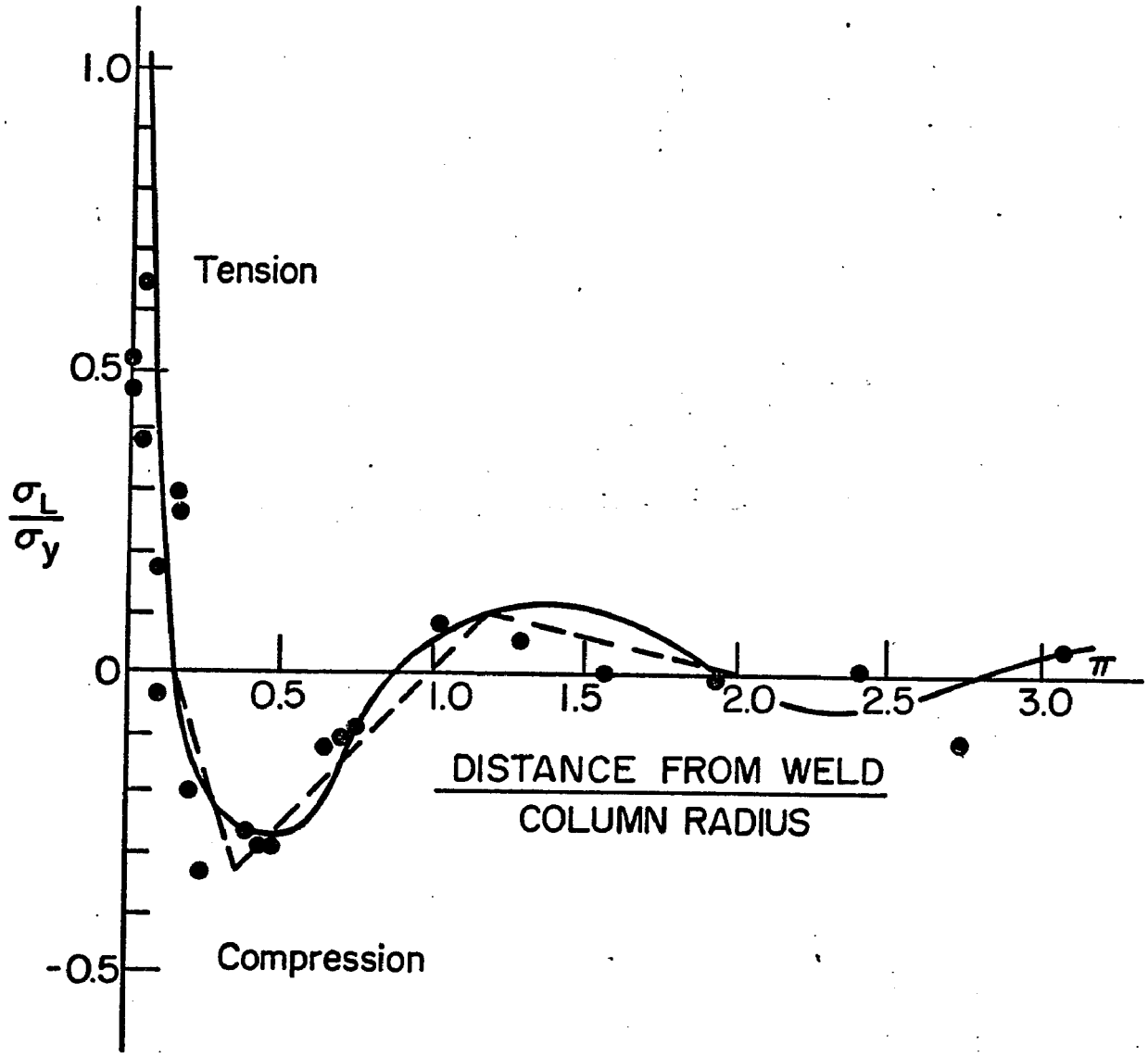

Fig. 3.11 Longitudinal Residual Stress Distribution Obtained from Slicing Method

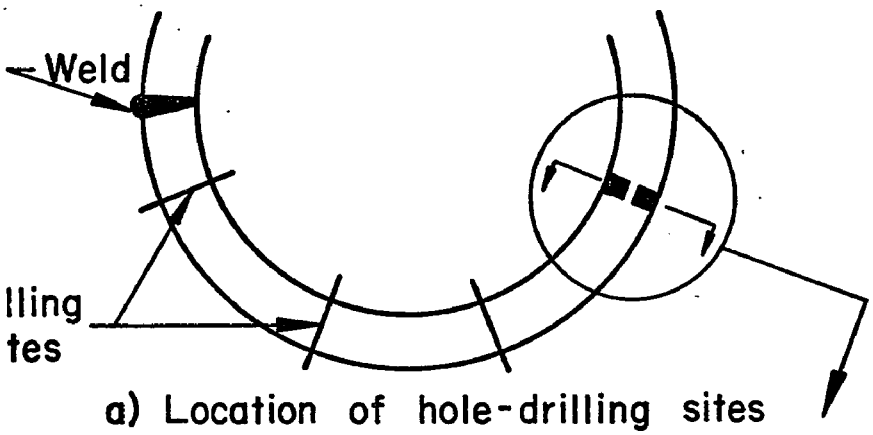

a) Location of hole-drilling sites

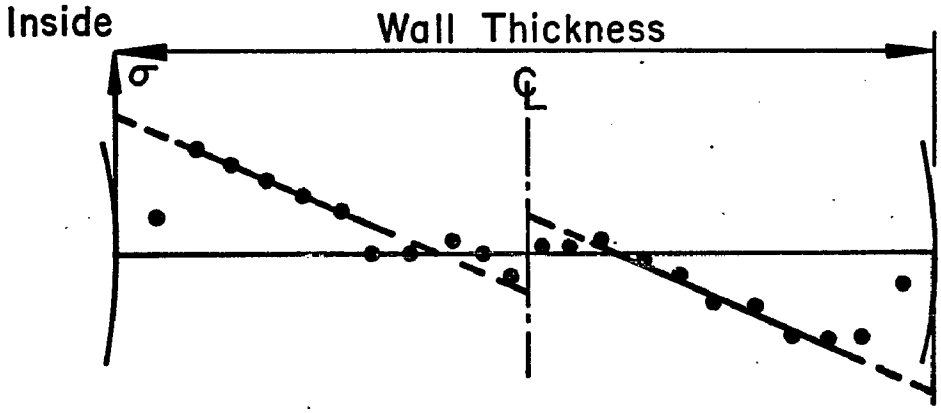

b) Typical hole-drilling circumferential residual stress results

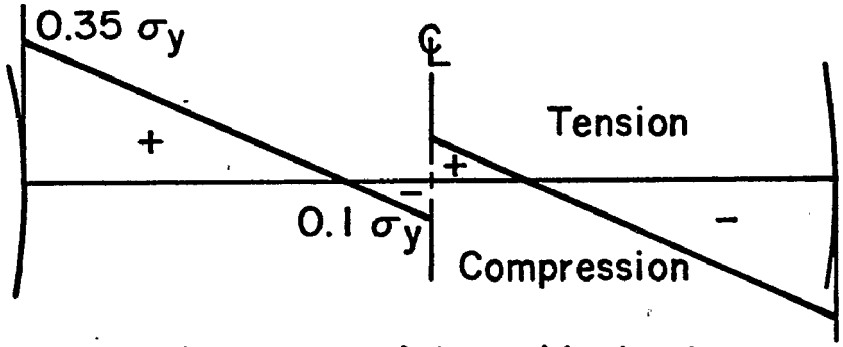

c) Average circumferential residual stress pattern

Fig. 3.12 Circumferential Residual Stress Pattern

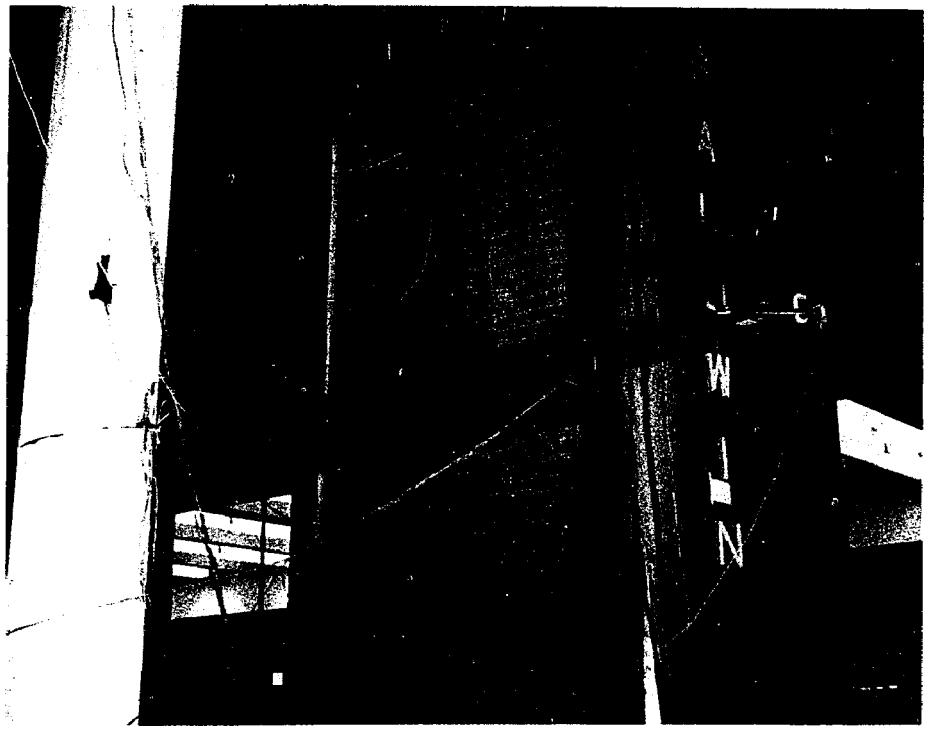

a) Distant View Showing Long Wires from Specimen to Gages

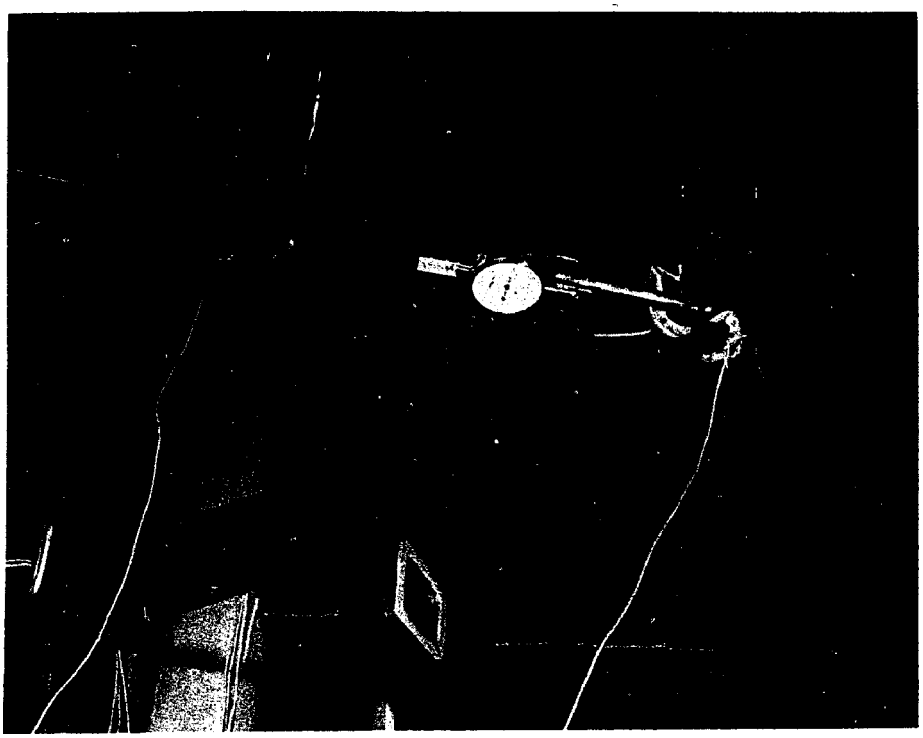

b) Close-up Shows Dial Gage (mid-height only) and Potentiometer

Fig. 3.13 Lateral Deflection Measuring Apparatus at Quarter Points

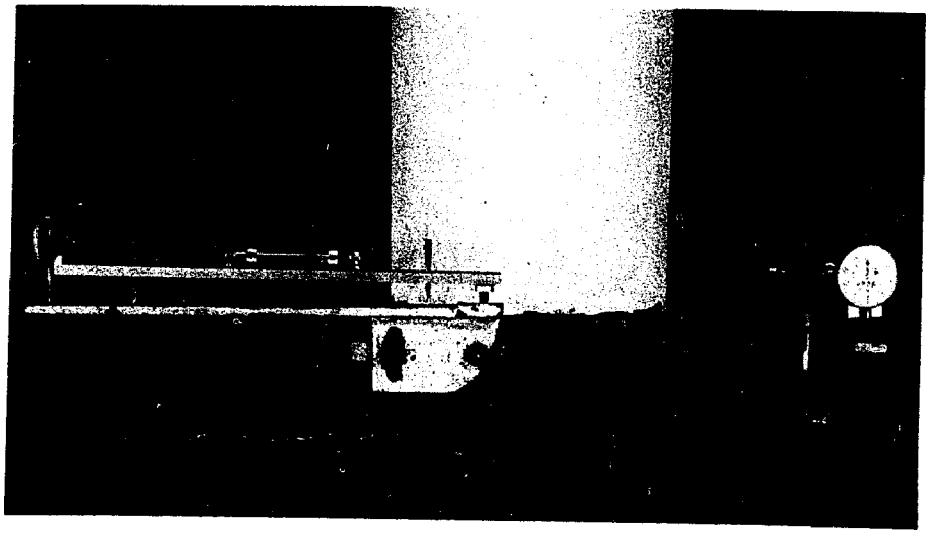

Fig. 3.14 Measurement of Bottom Head Rotation

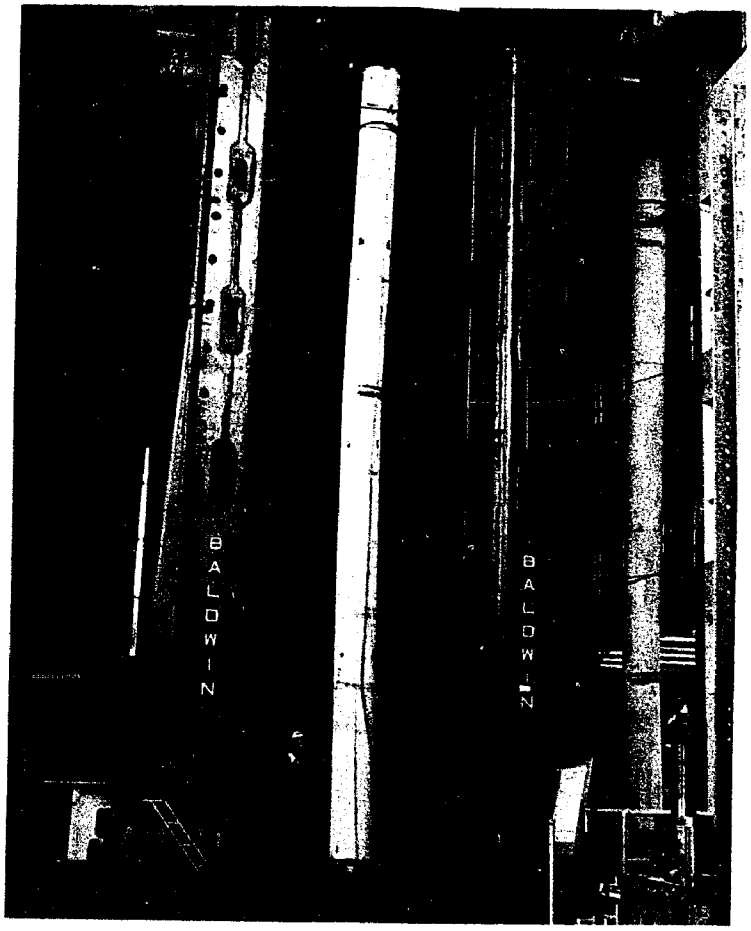

Fig. 3.15 Specimen 10 after Failure
(with Specimen 9 against wall)

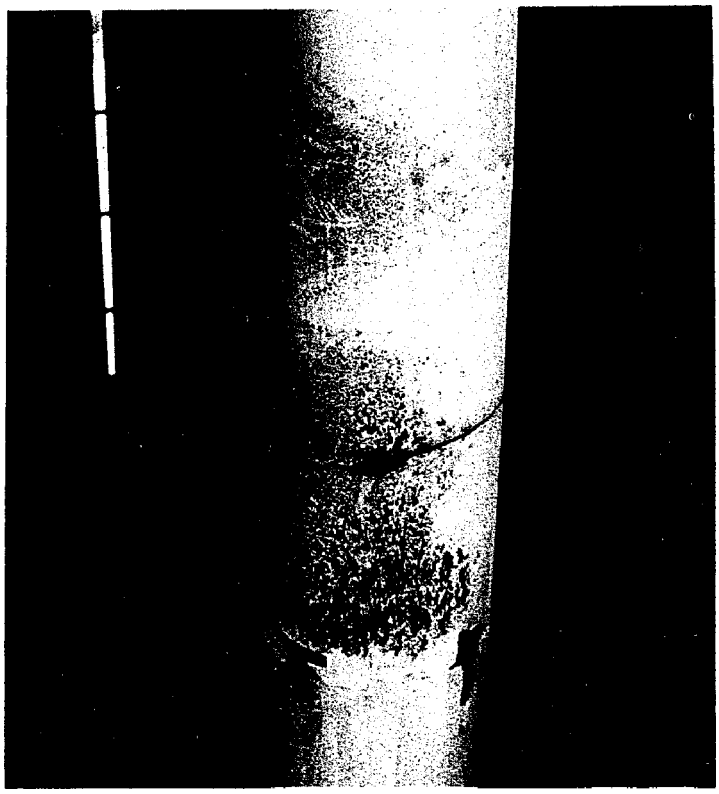

a) General Inelastic Instability (Specimen 2)

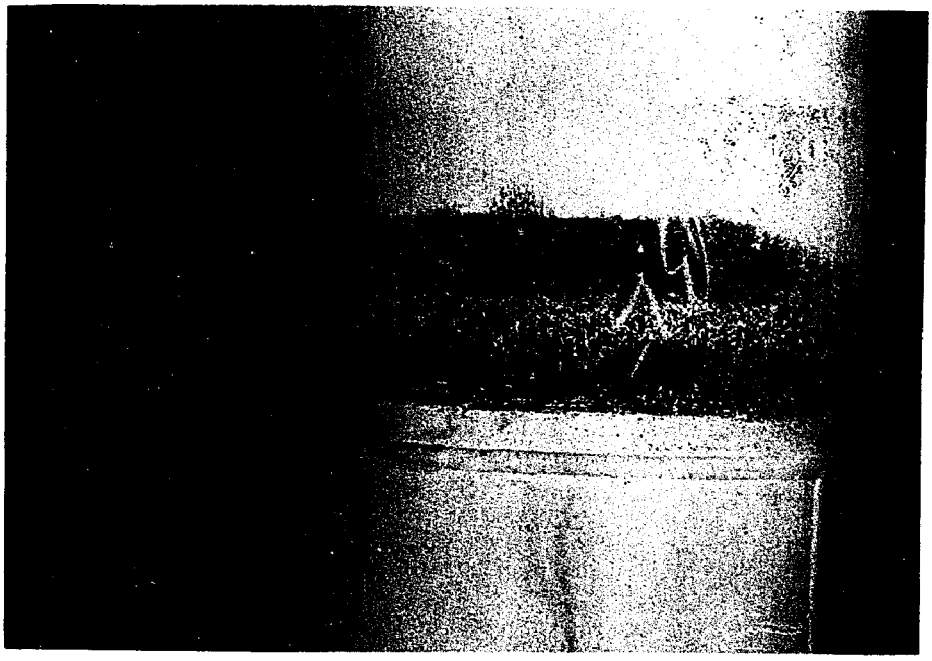

b) Interactive Instability (Specimen 10)

Fig. 3.16 Experimentally Observed Buckling Modes

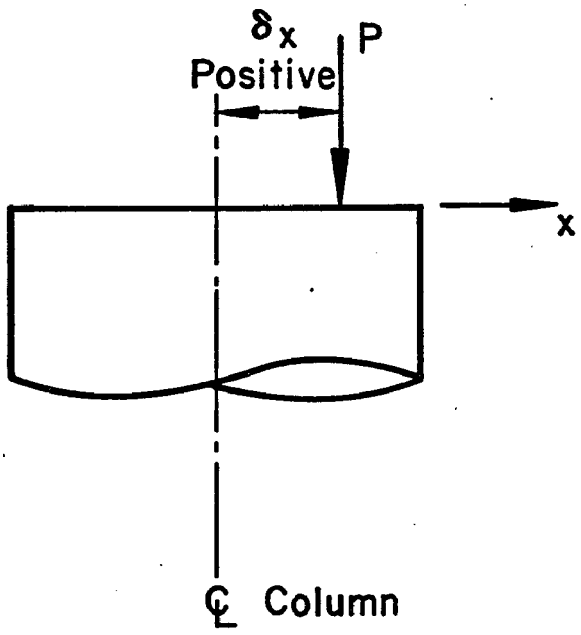

Fig. 3.17 Sign Convention for End Eccentricities

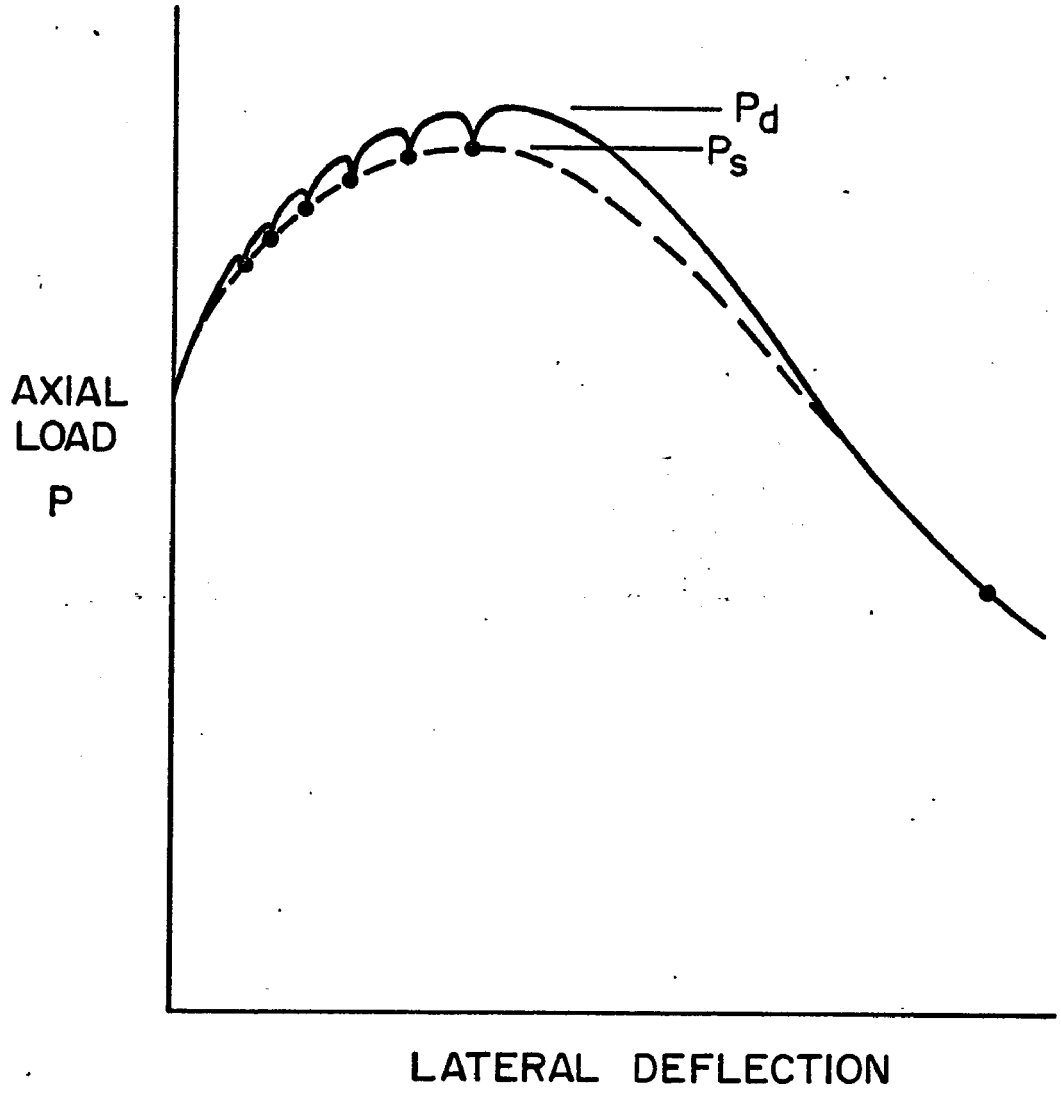

Fig. 3.18 Definition of "Static" and "Dynamic" Buckling Loads

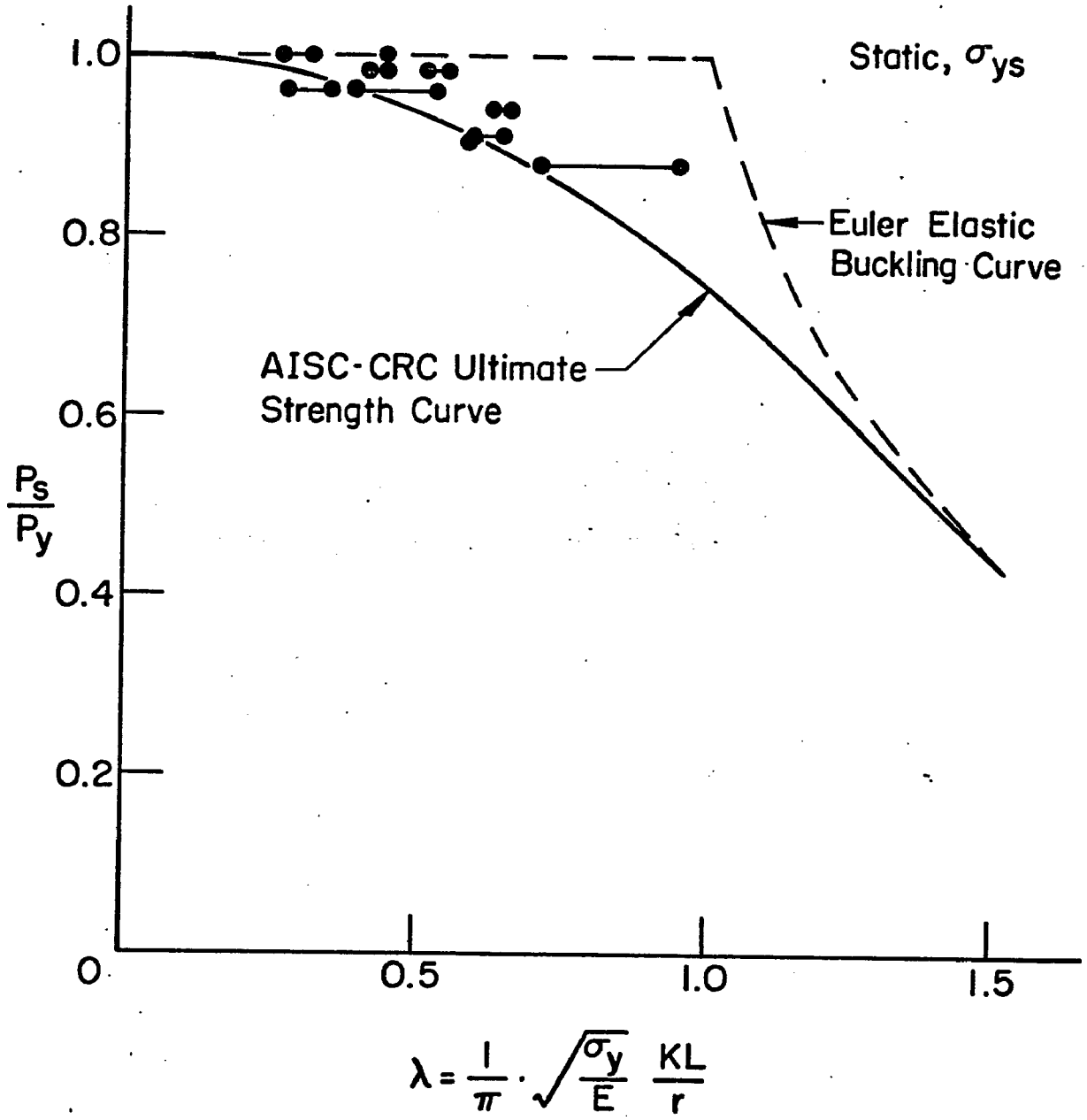

Fig. 3.19 Comparison of Test Results with AISC-CRC Column Strength Curve Based on Static Yield Strength

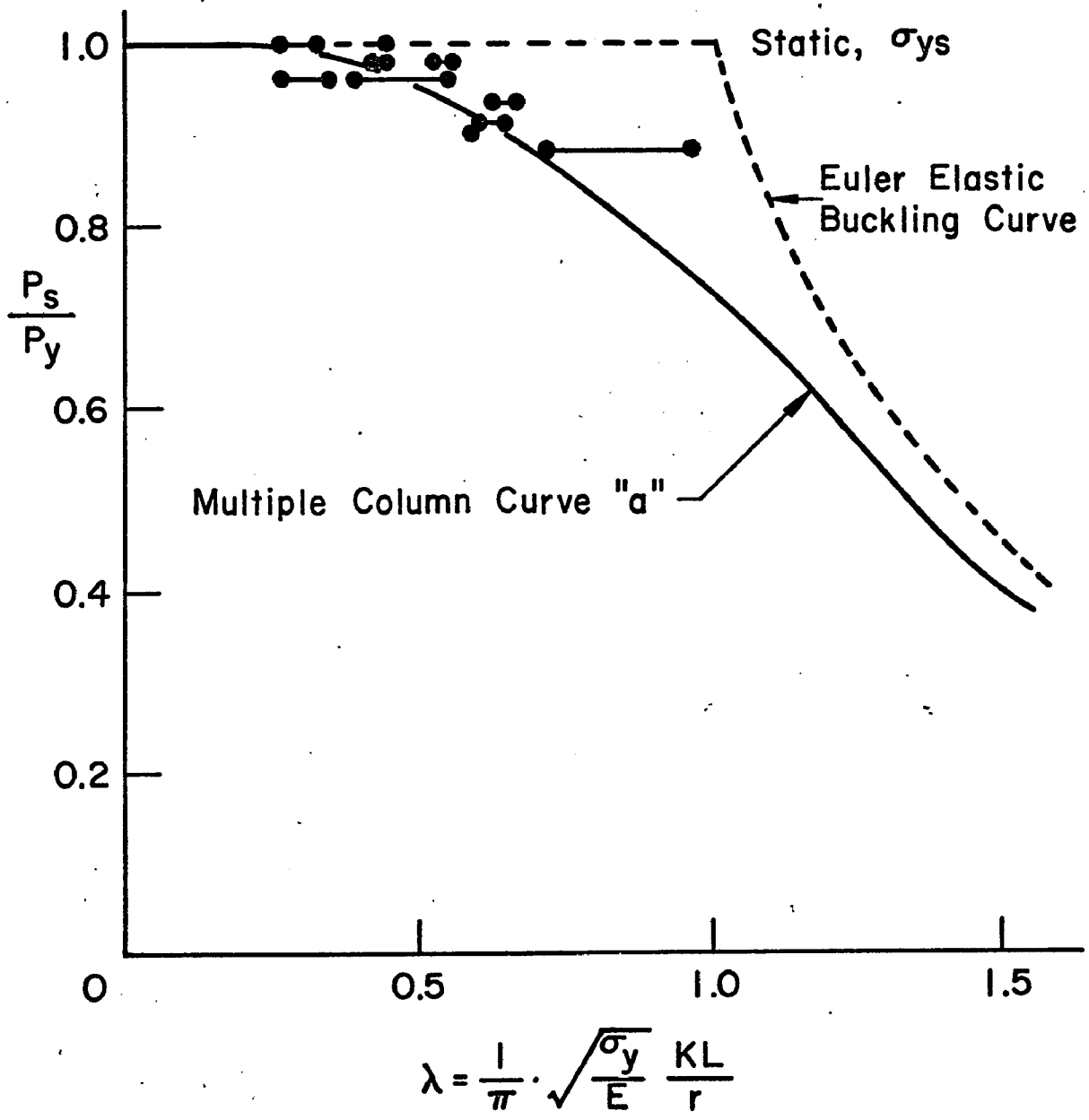

Fig. 3.20 Comparison of Test Results with Multiple Column Curve "a" Based on Static Yield Strengths

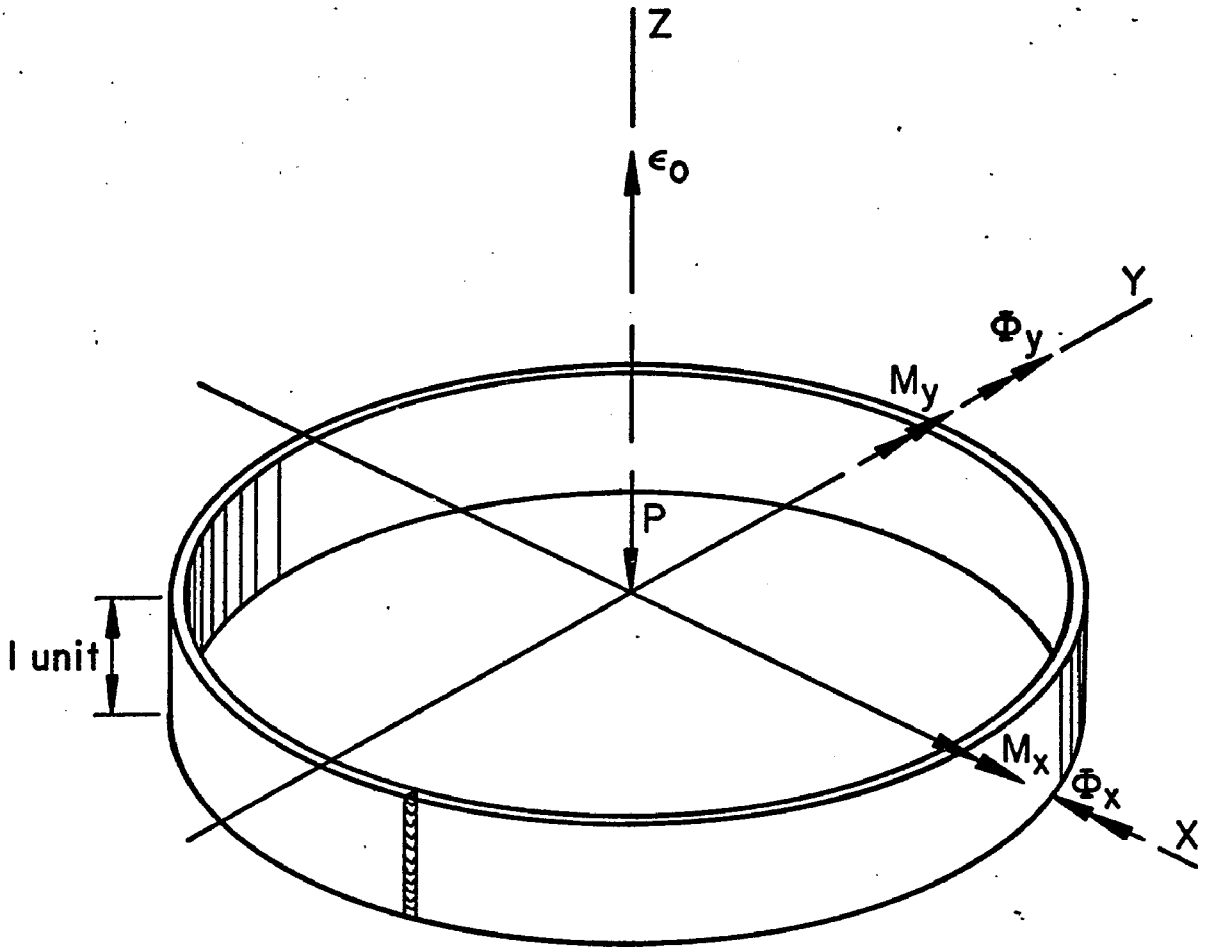

Fig. 4.1 Positive Direction of Forces and Deformations

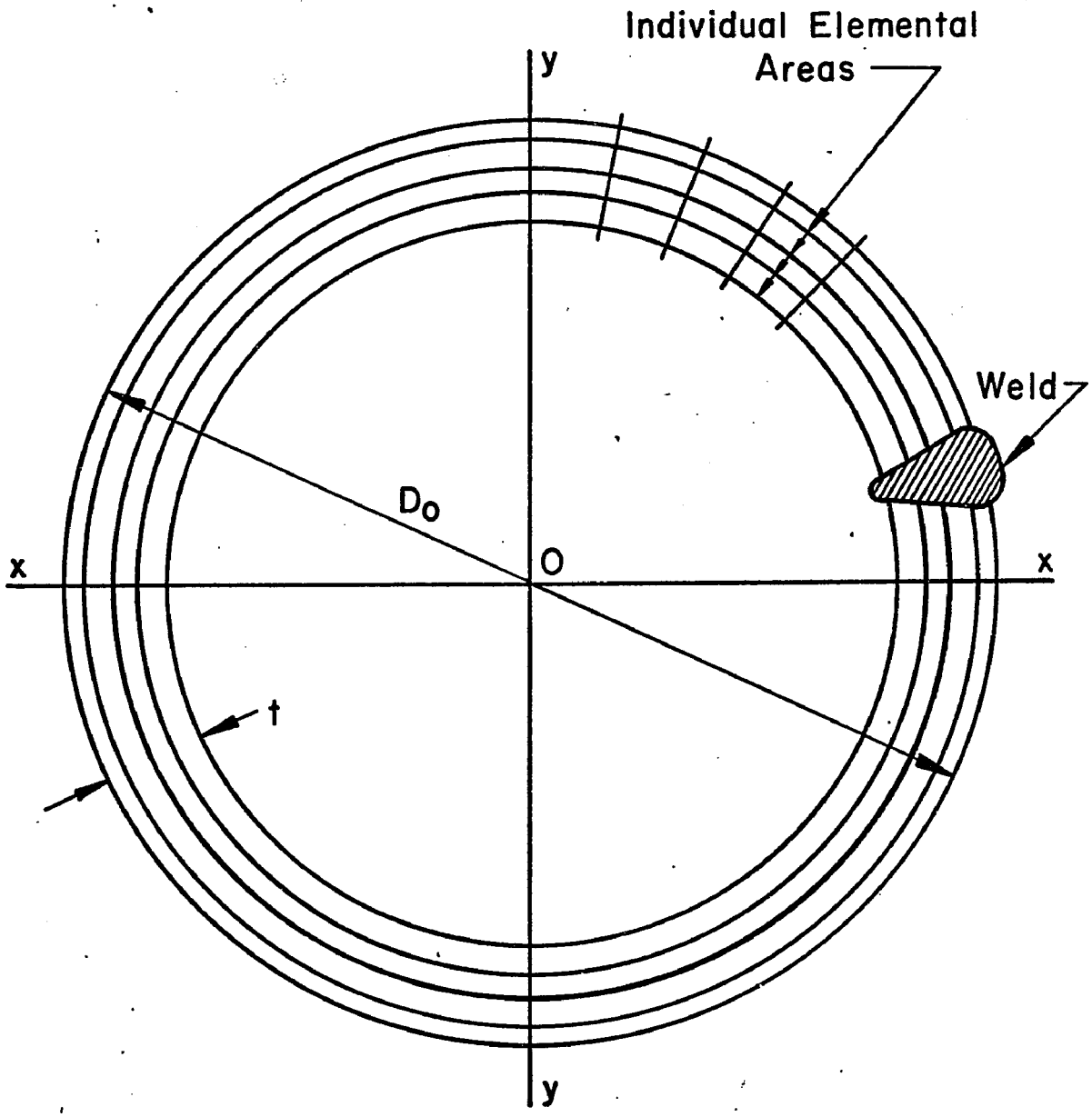

Fig. 4.2 Division of a Cross Section into Elemental Areas

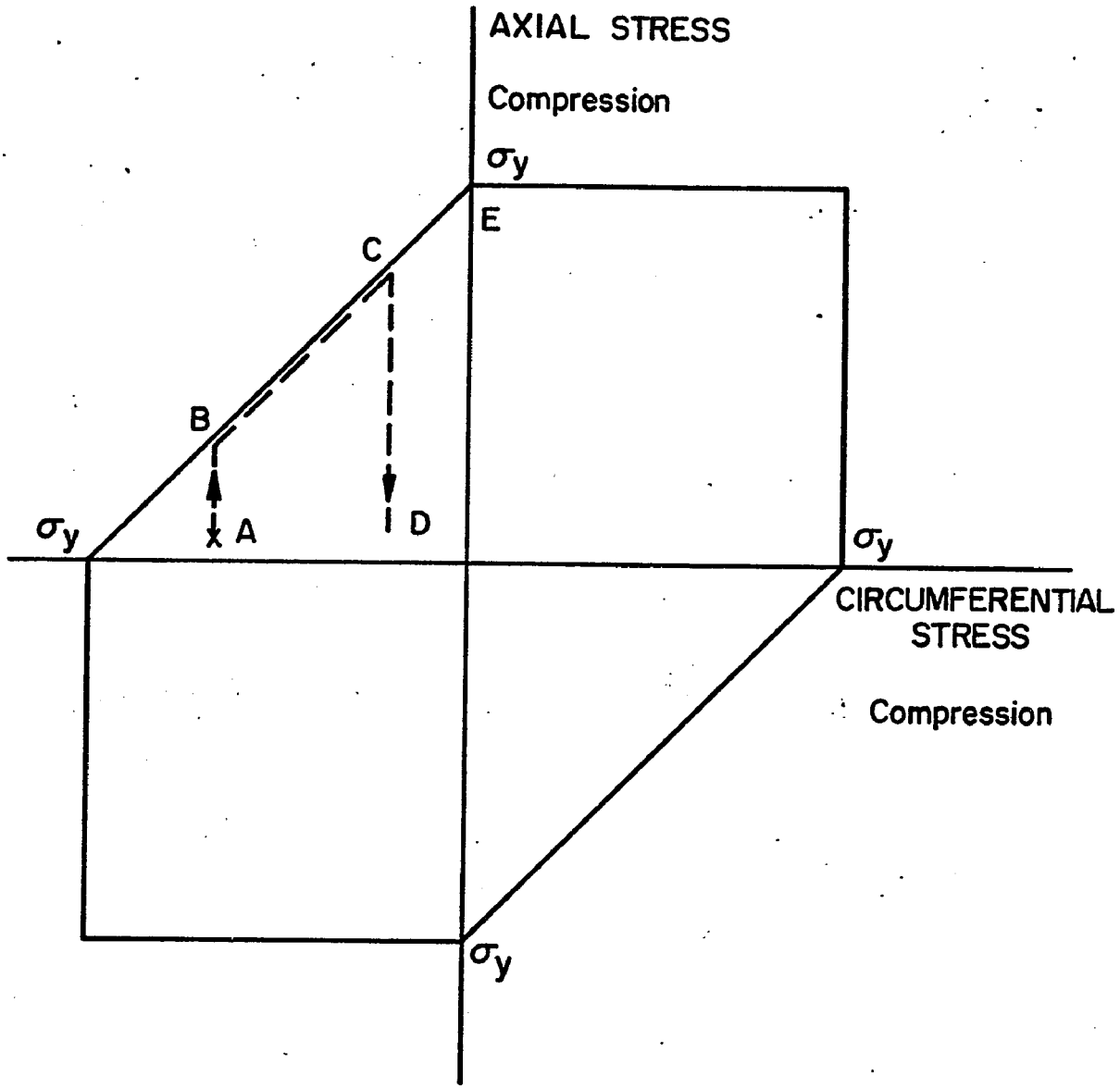

Fig. 4.3 Tresca Yield Criterion for Two-Dimensional Stress Situations

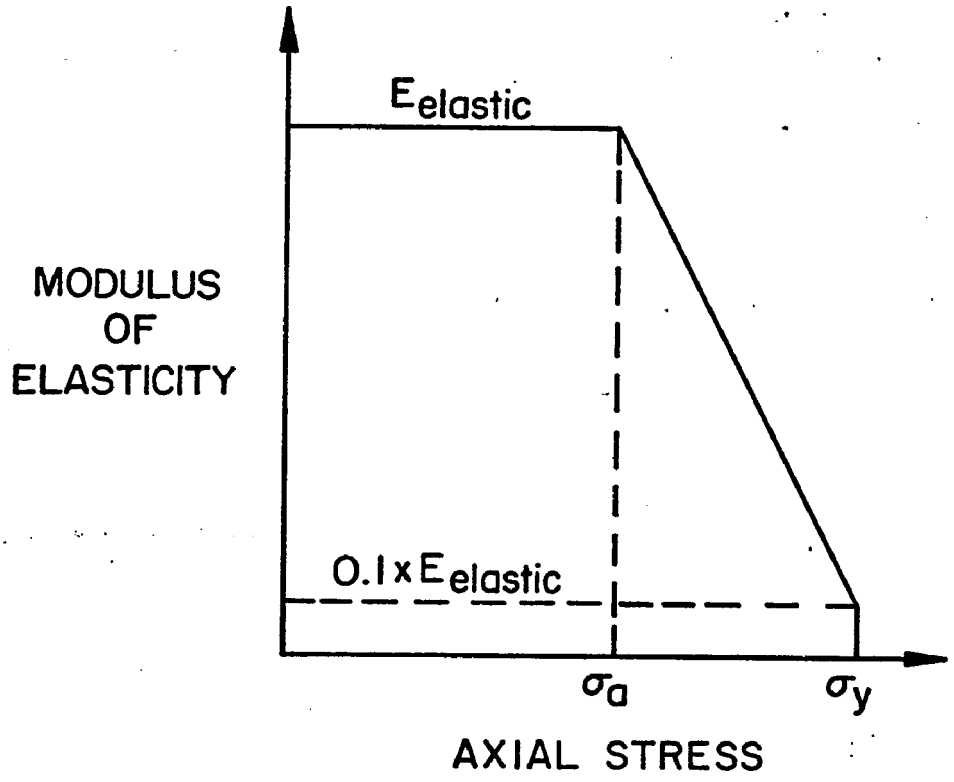

Fig. 4.4 Assumption for Effective Modulus of Elasticity

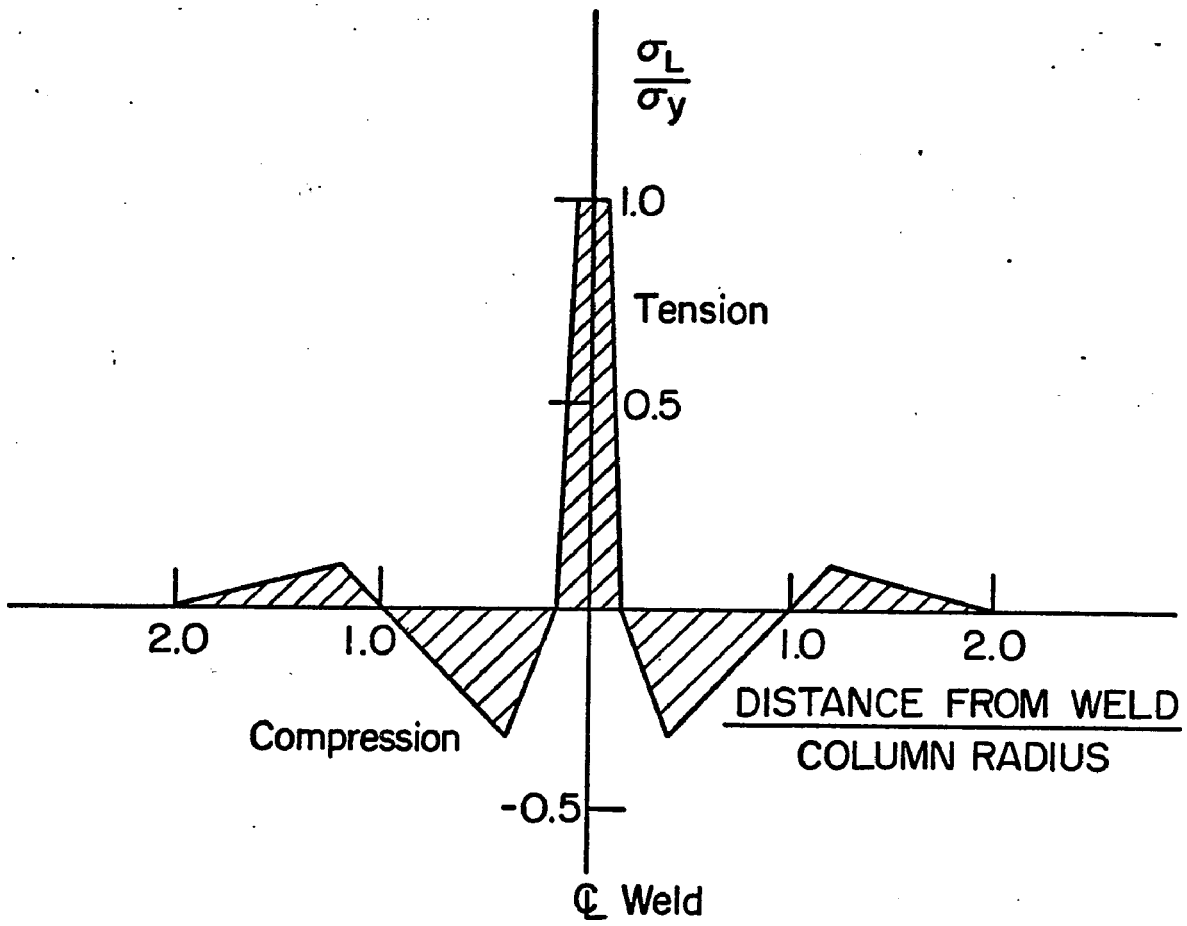

Fig. 4.5 Longitudinal Residual Stress Distribution (straight-line fit of measured values)

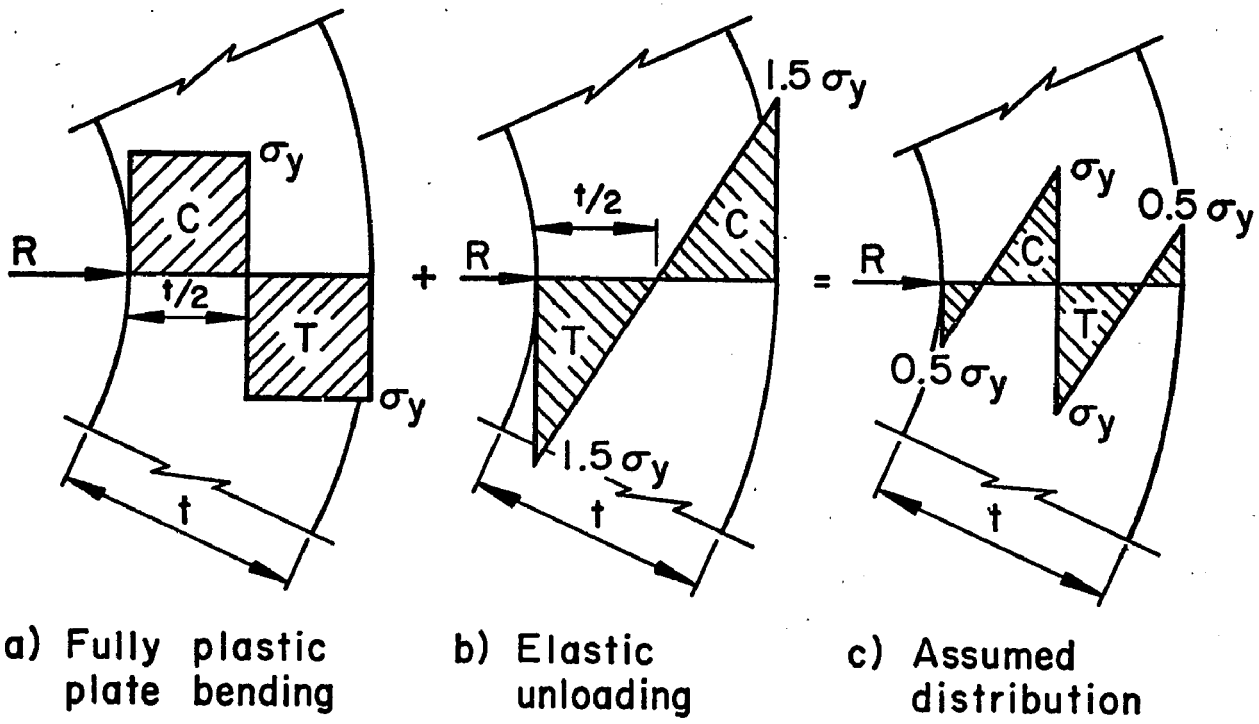

Fig. 4.6 Derivation of Assumed Circumferential Residual Stress Distribution

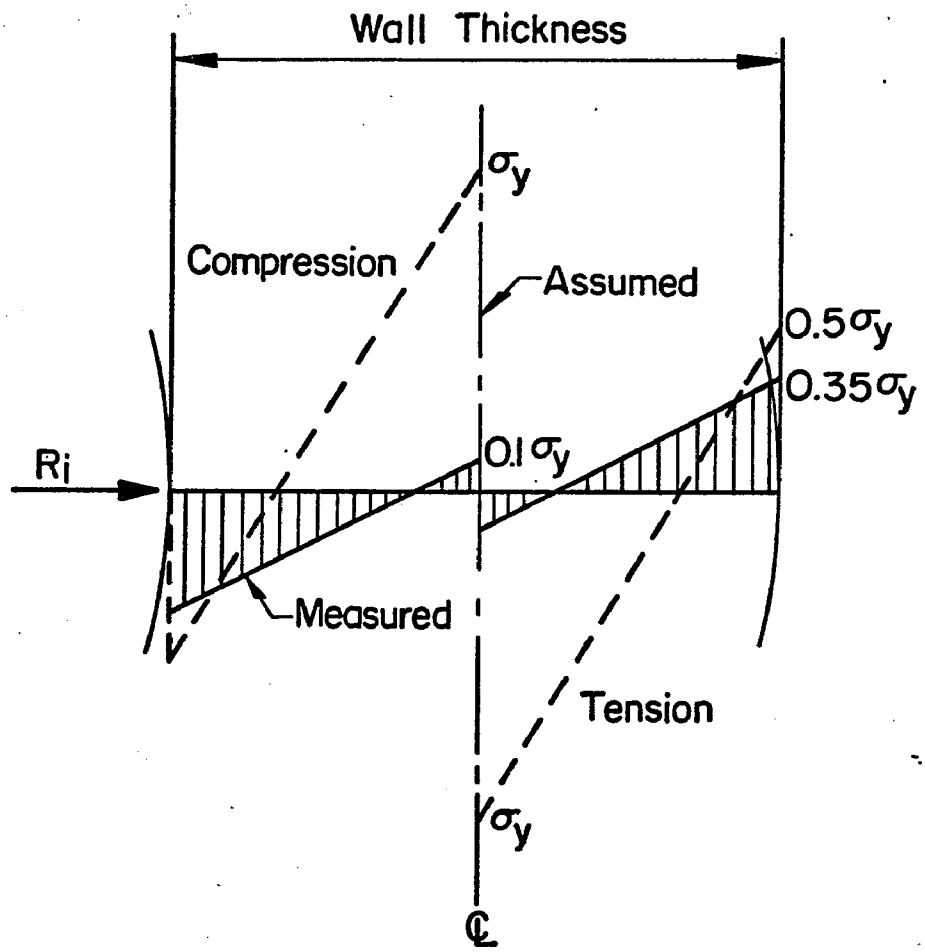

Fig. 4.7 Comparison of Measured and Assumed Circumferential Residual Stress Distributions

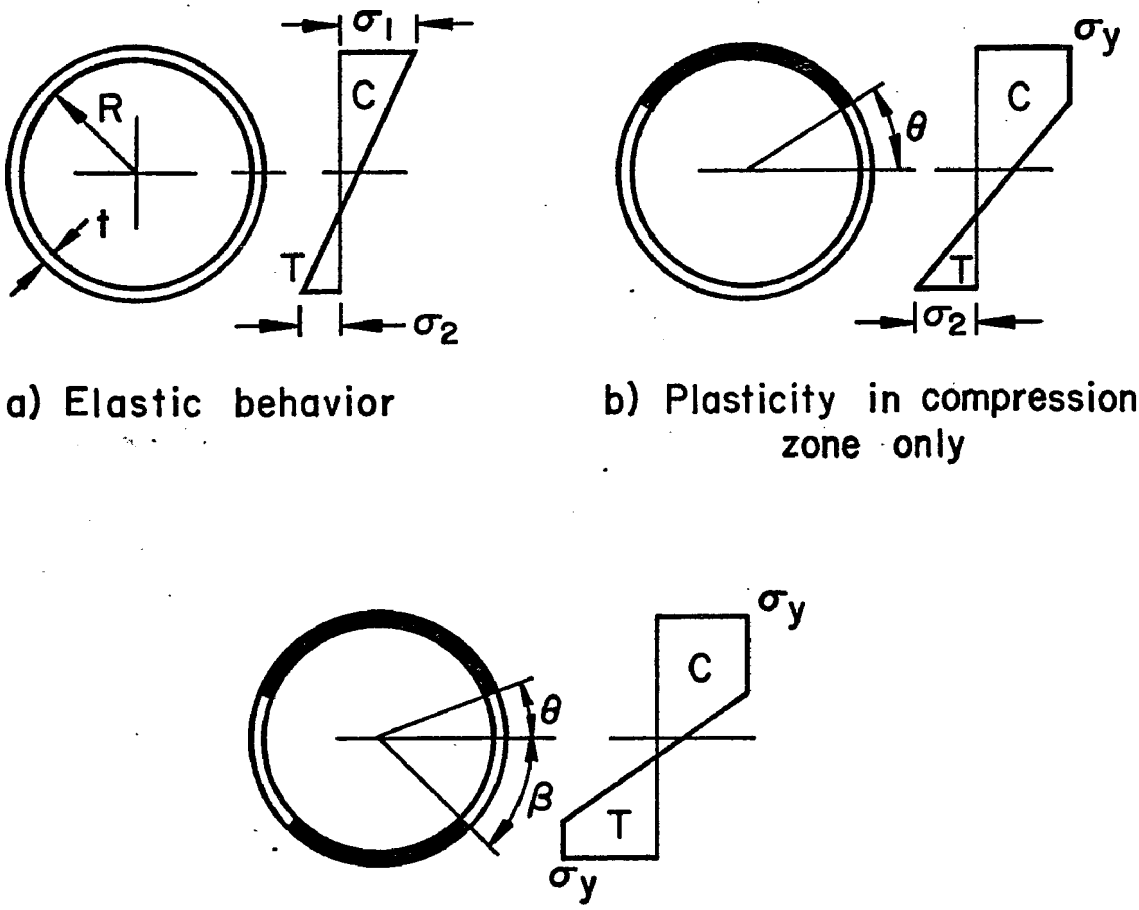

a) Elastic behavior

b) Plasticity in compression zone only

c) Plasticity in both zones

Fig. 4.8 States of Stress Considered by Ellis

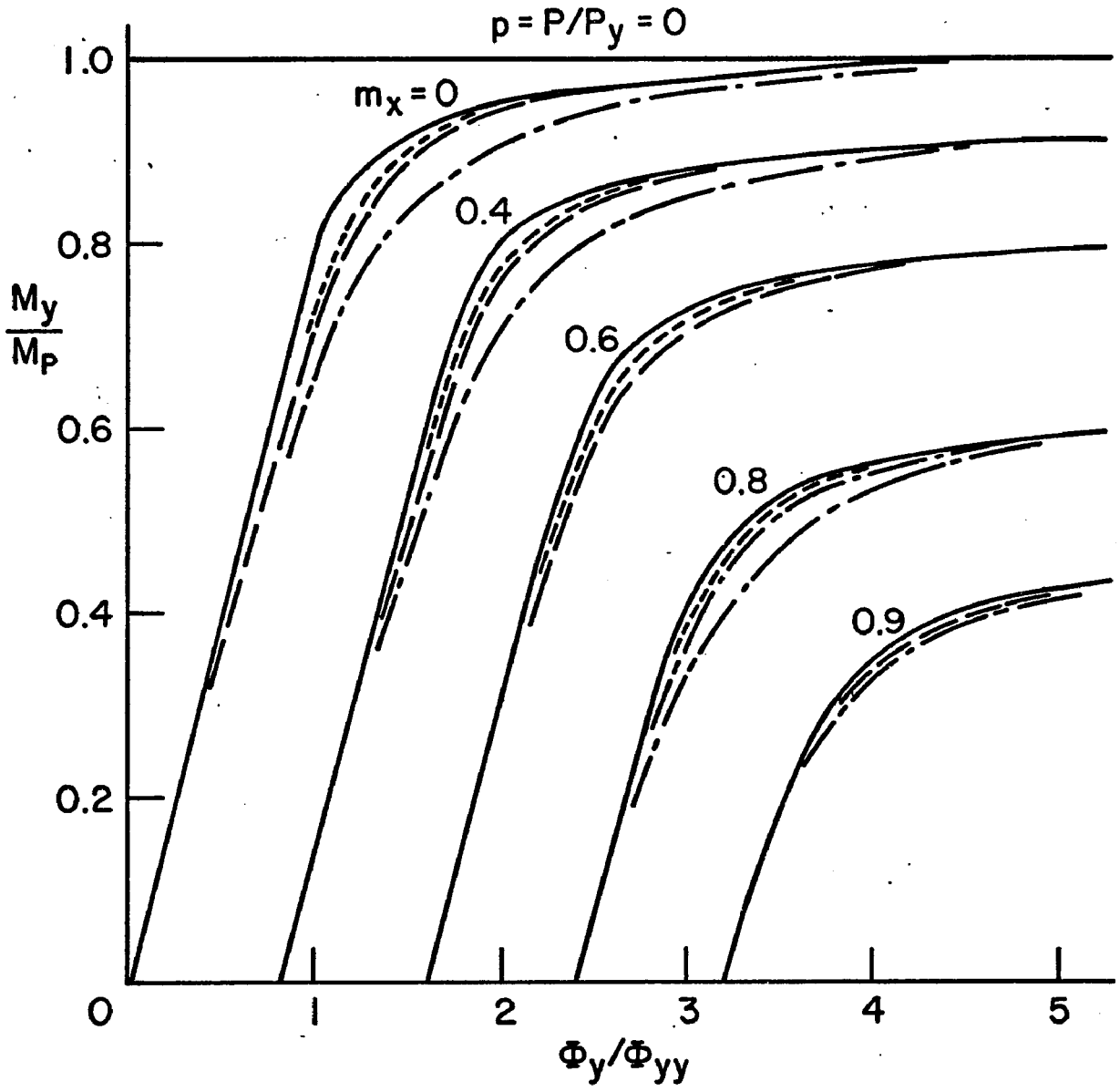

——— No Residual Stresses Included

- - - - Longitudinal Residual Stresses Only Included

— — Longitudinal + Measured Circumferential Residual Stresses

—·— Longitudinal + Assumed Circumferential Residual Stresses

Fig. 4.9 Moment-Axial Load-Curvature Curves for p = 0

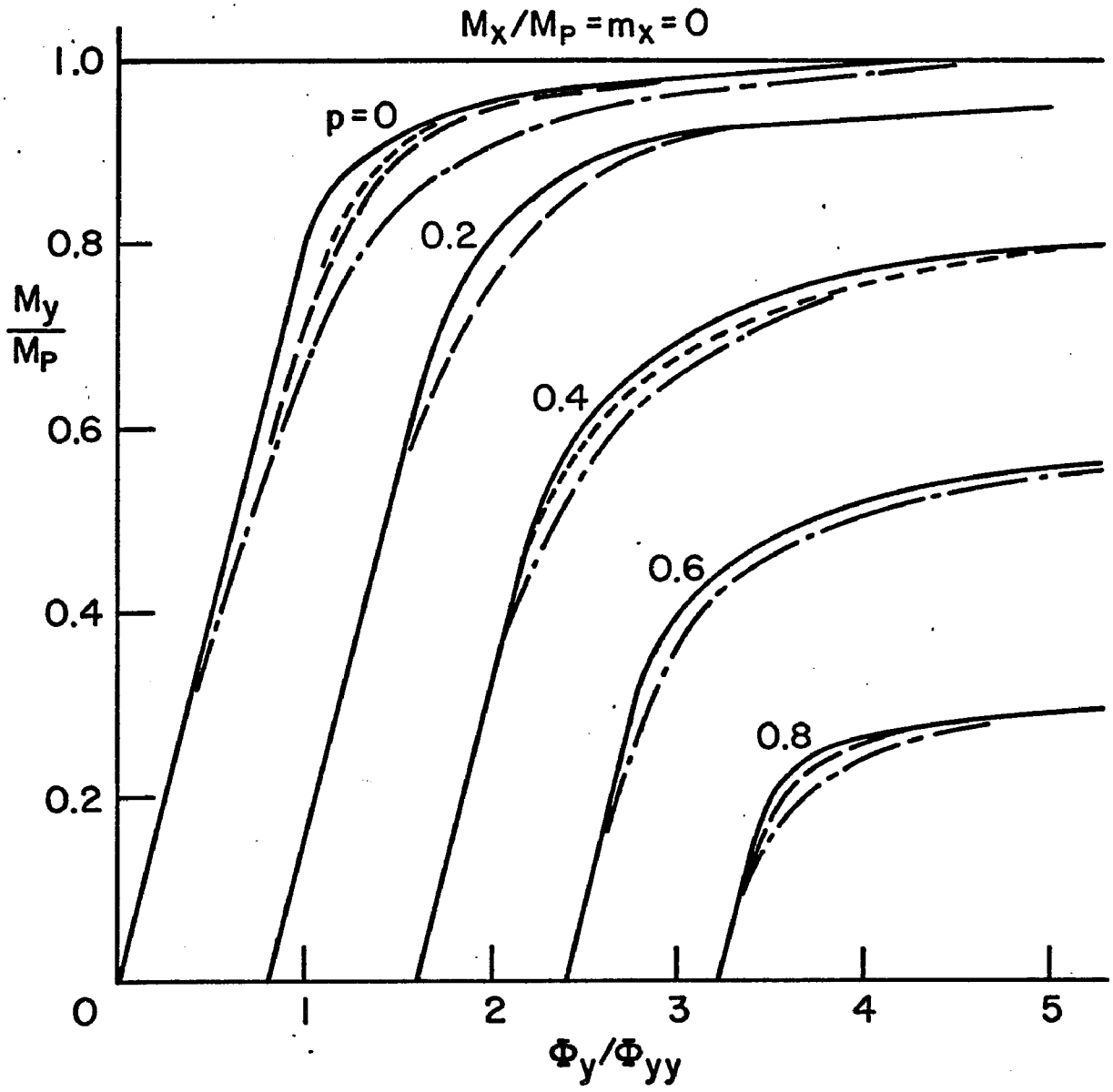

——— No Residual Stresses Included

- - - - Longitudinal Residual Stresses Only Included

— — Longitudinal + Measured Circumferential Residual Stresses

—·— Longitudinal + Assumed Circumferential Residual Stresses

Fig. 4.10 Moment-Axial Load-Curvature Curves for $m_x = 0$

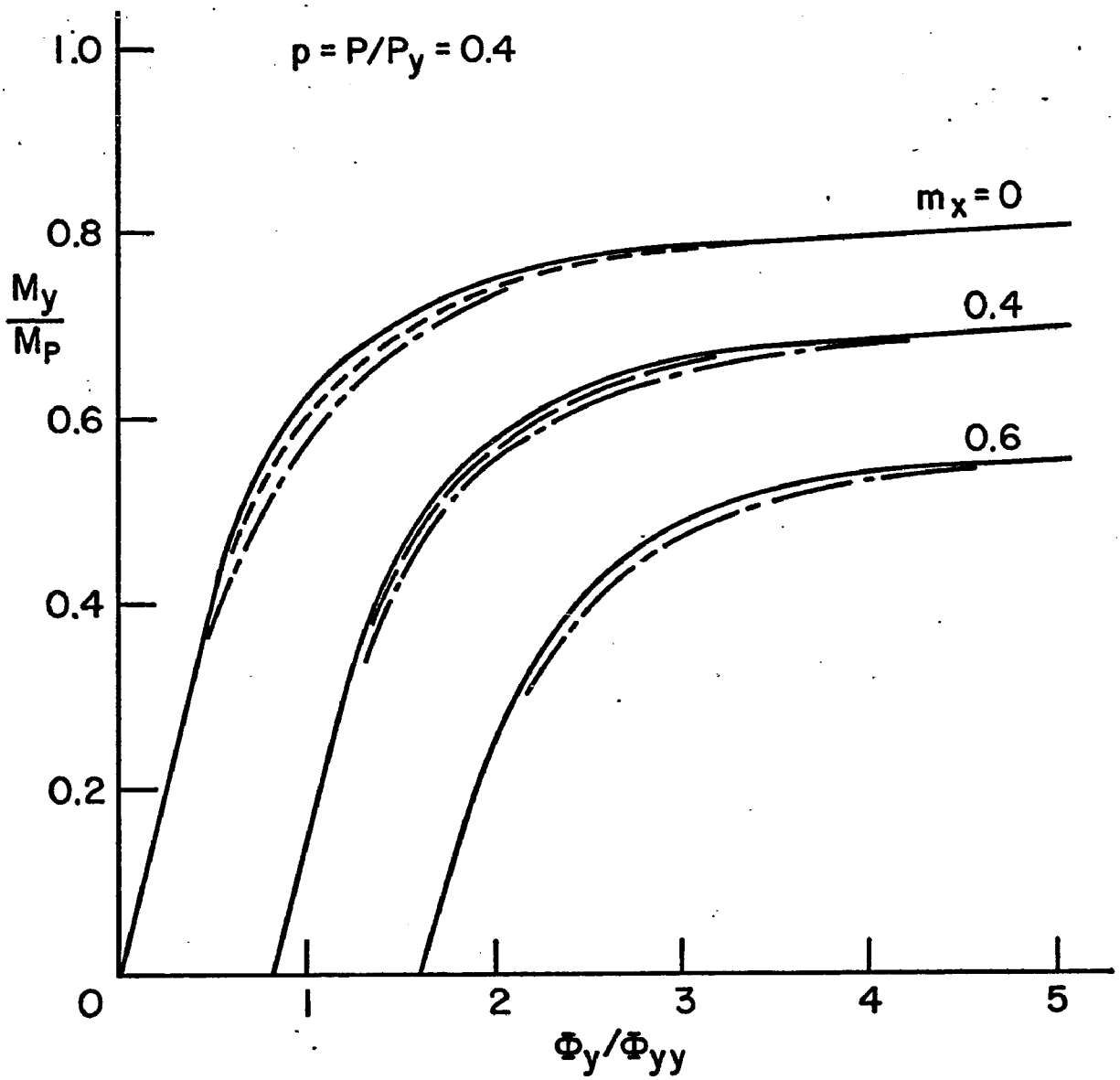

——— No Residual Stresses Included

- - - - Longitudinal Residual Stresses Only Included

— — Longitudinal + Measured Circumferential Residual Stresses

—·— Longitudinal + Assumed Circumferential Residual Stresses

Fig. 4.11 Moment-Axial Load-Curvature Curves for p = 0.4

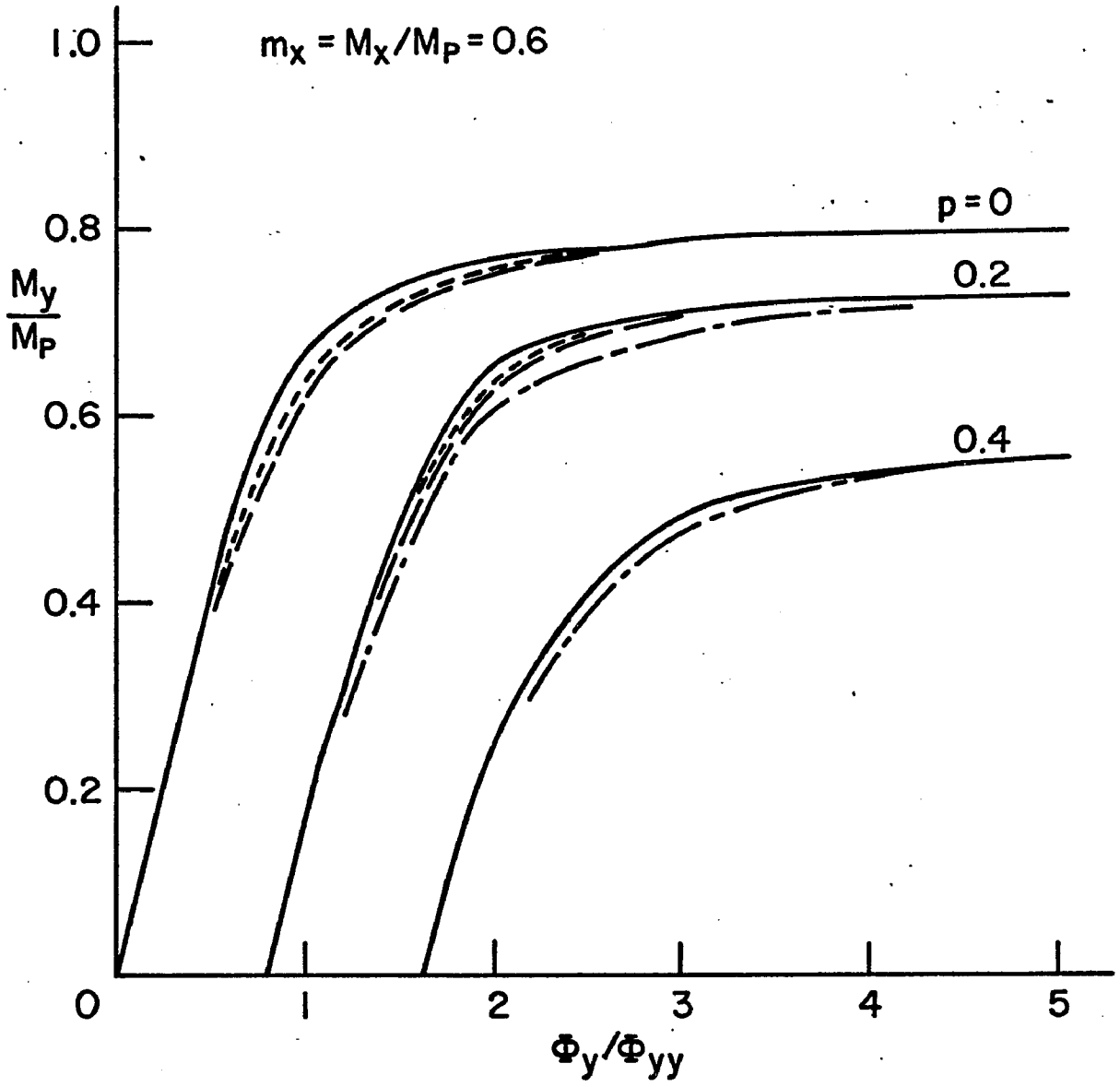

——— No Residual Stresses Included

- - - - Longitudinal Residual Stresses Only Included

— — Longitudinal + Measured Circumferential Residual Stresses

—·— Longitudinal + Assumed Circumferential Residual Stresses

Fig. 4.12 Moment-Axial Load-Curvature Curves for $m_x = 0.6$

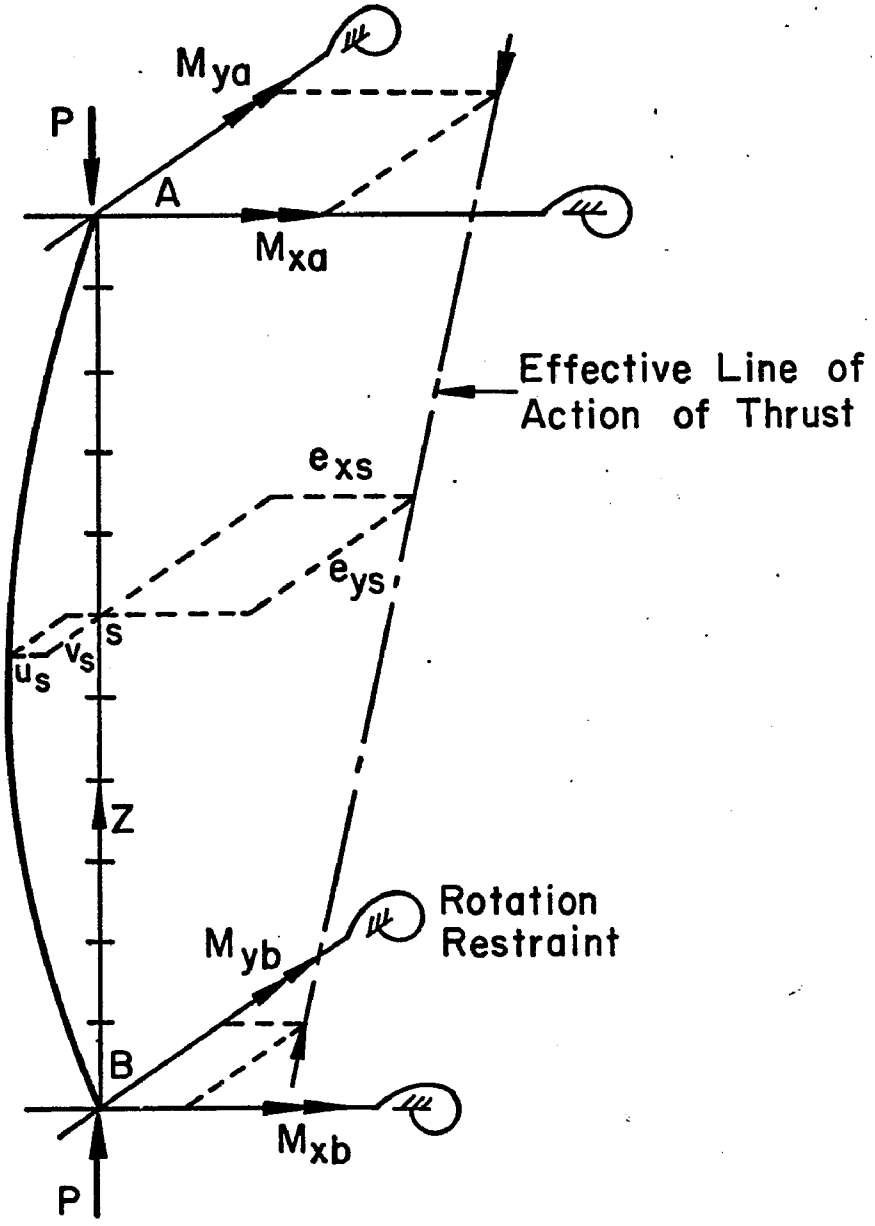

Fig. 5.1 Notation for Column Analysis

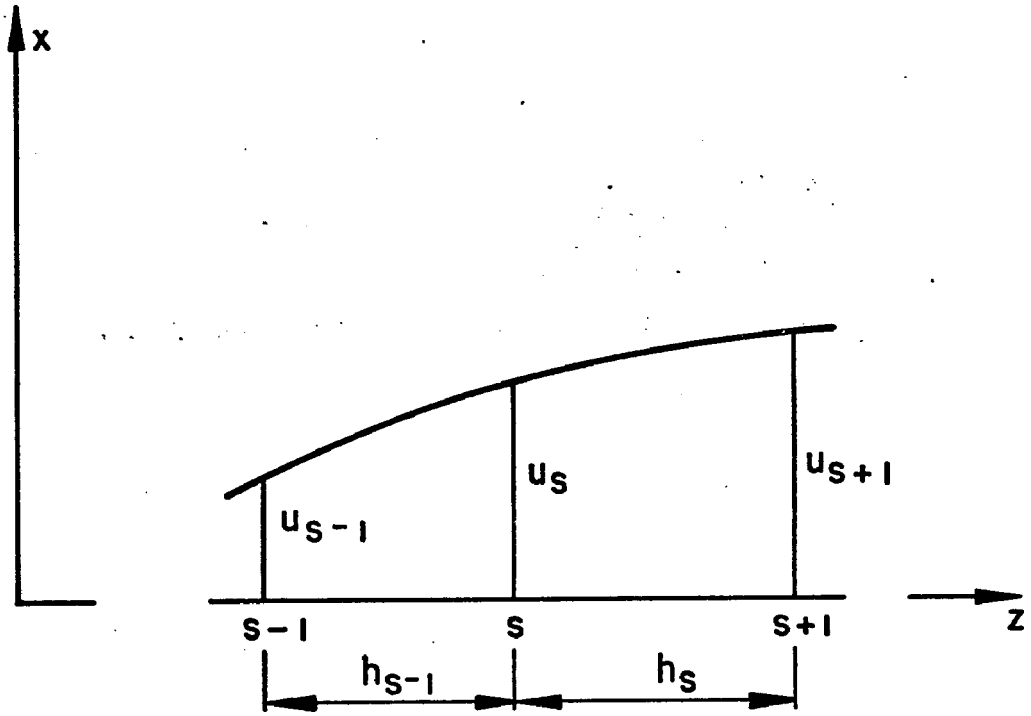

Fig. 5.2 Defining Terms in x-z Plane for Curvature Derivation

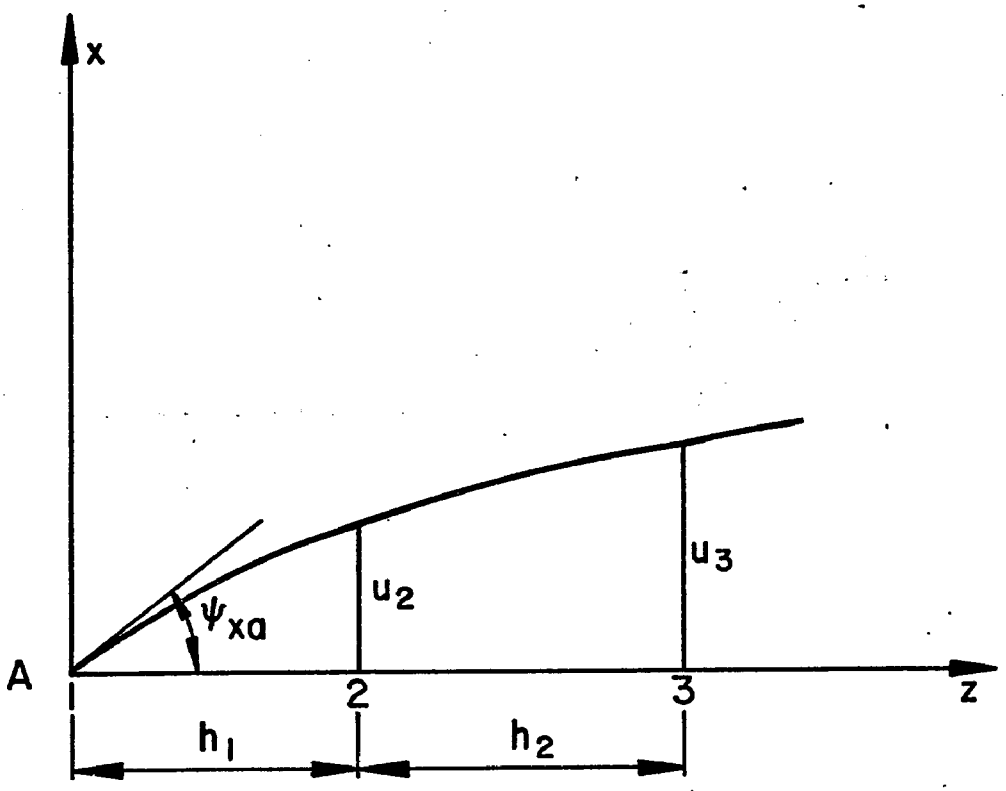

Fig. 5.3 Slope Conditions at End A in the x-z Plane

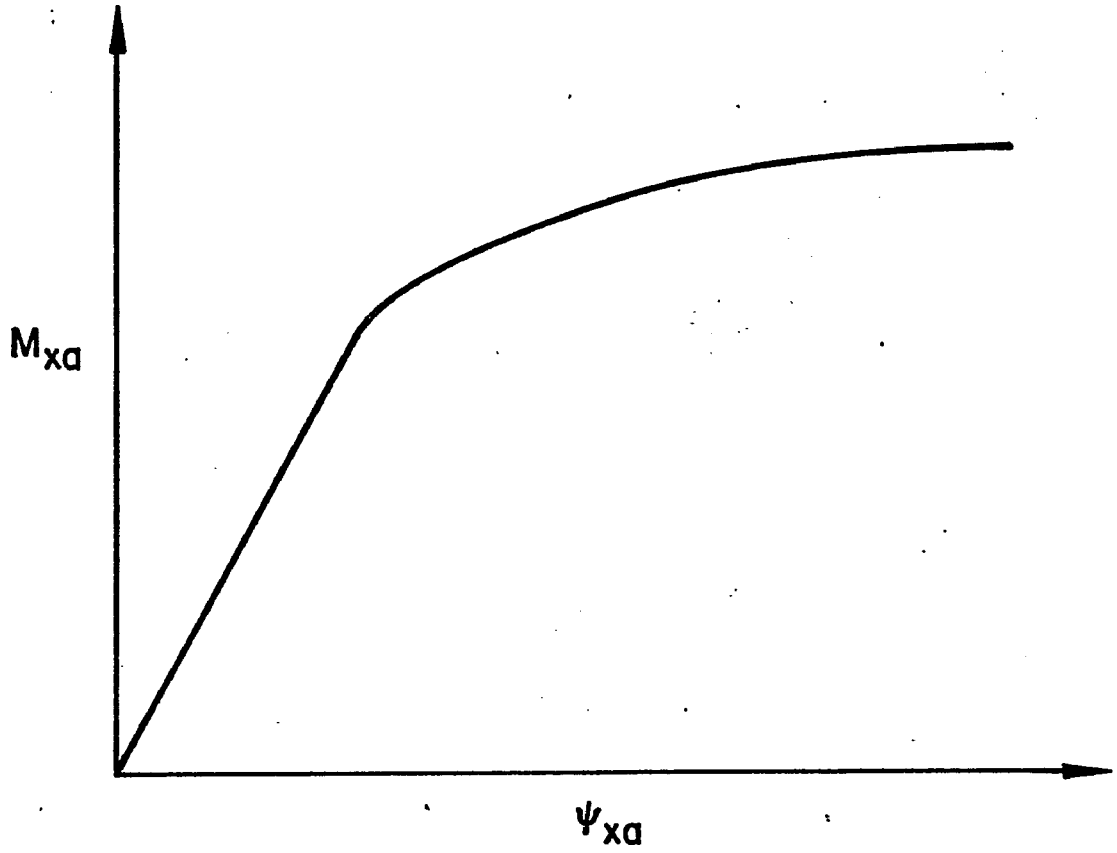

Fig. 5.4 Generalized Moment-Rotation Characteristic of the End Restraint on a Column

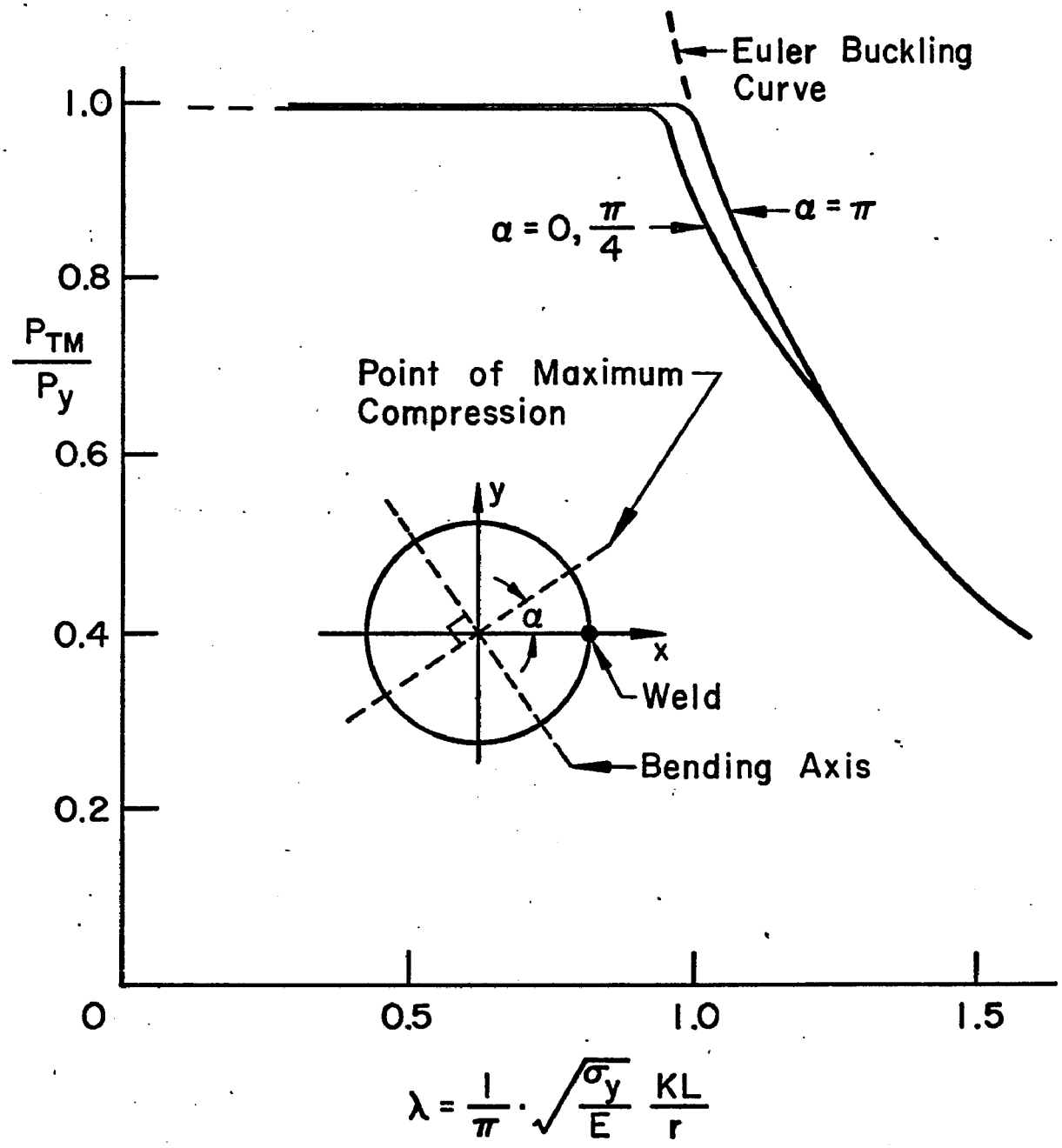

Fig. 5.5 Tangent Modulus Buckling Load Predictions

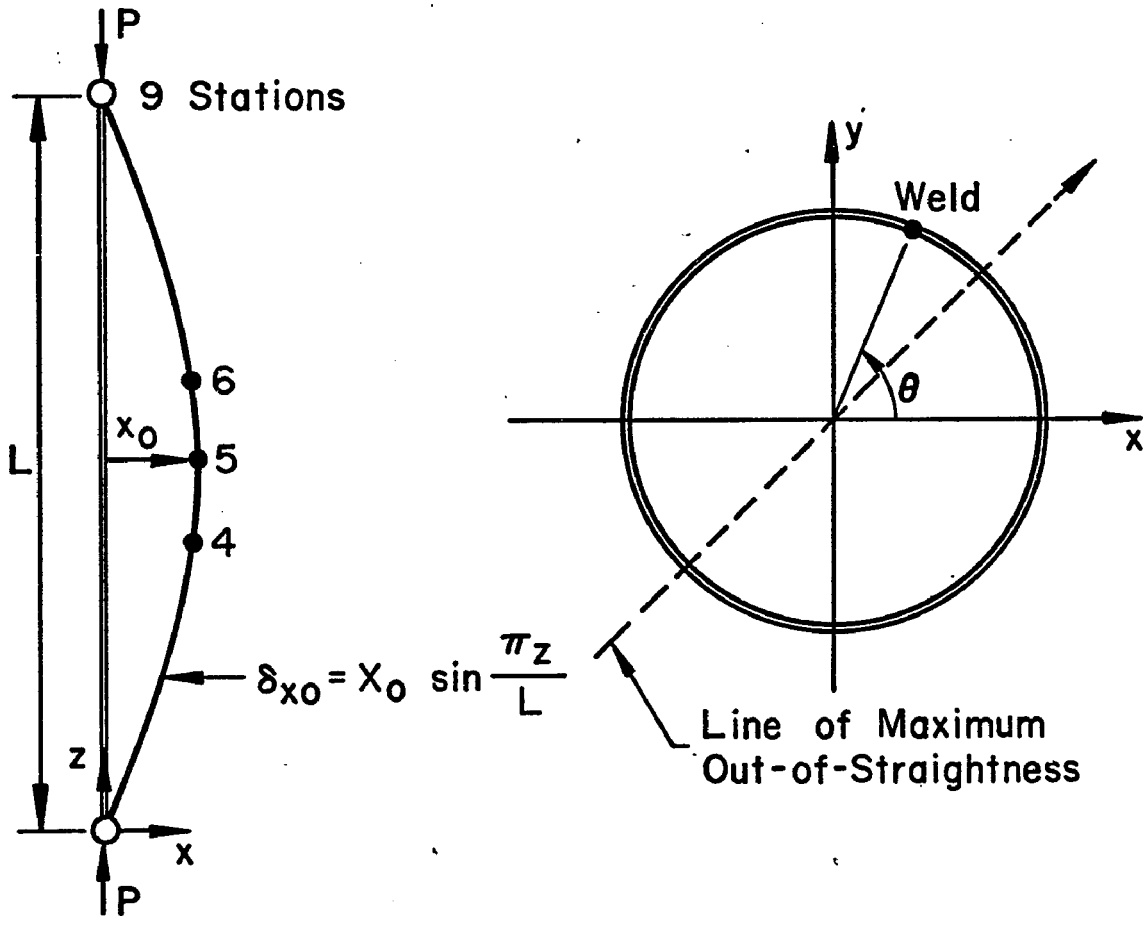

a) Typical x-z plane elevation

b) Typical section detail

Fig. 5.6 Elevation and Section Definitions

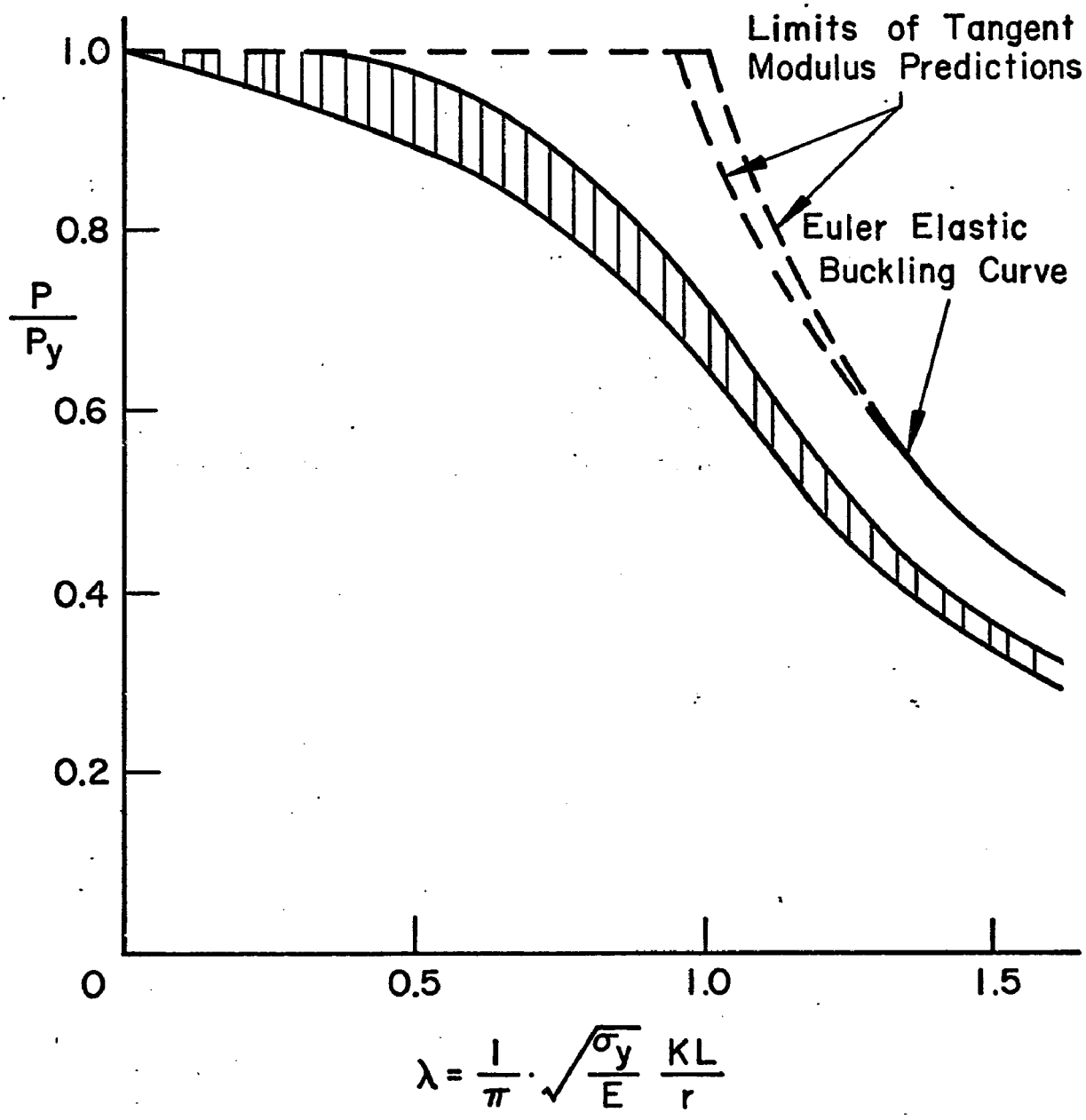

Fig. 5.7 Comparison of Tangent Modulus Column Buckling of a Straight Column and Maximum Axial Load of a Pinned-End Column with Out-of-Straightness Equal to (0.001) x (column length)

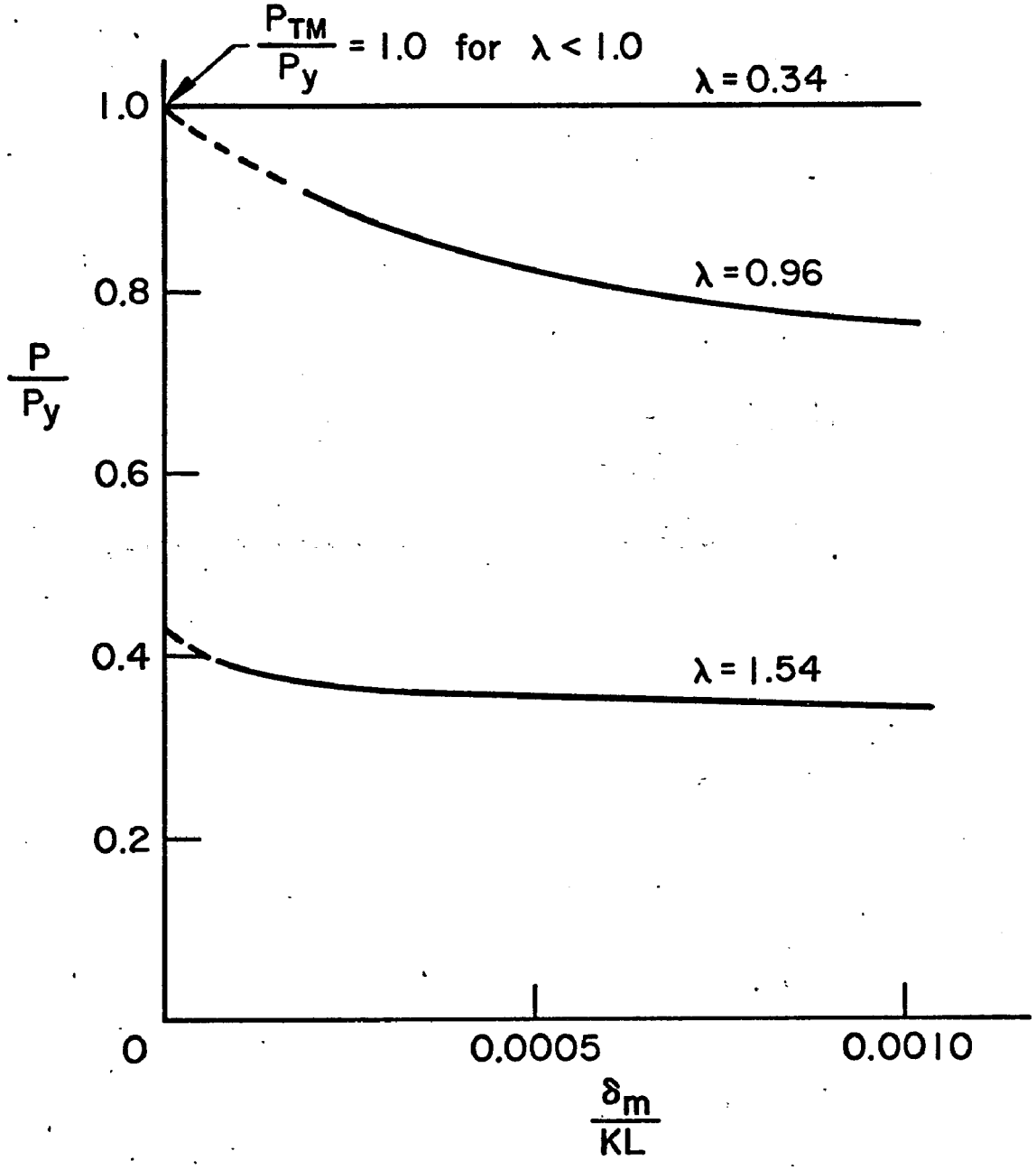

Fig. 5.8 Ultimate Load Capacity of a Stress-Free Tubular Column as a Function of Length and Initial Out-of-Straightness

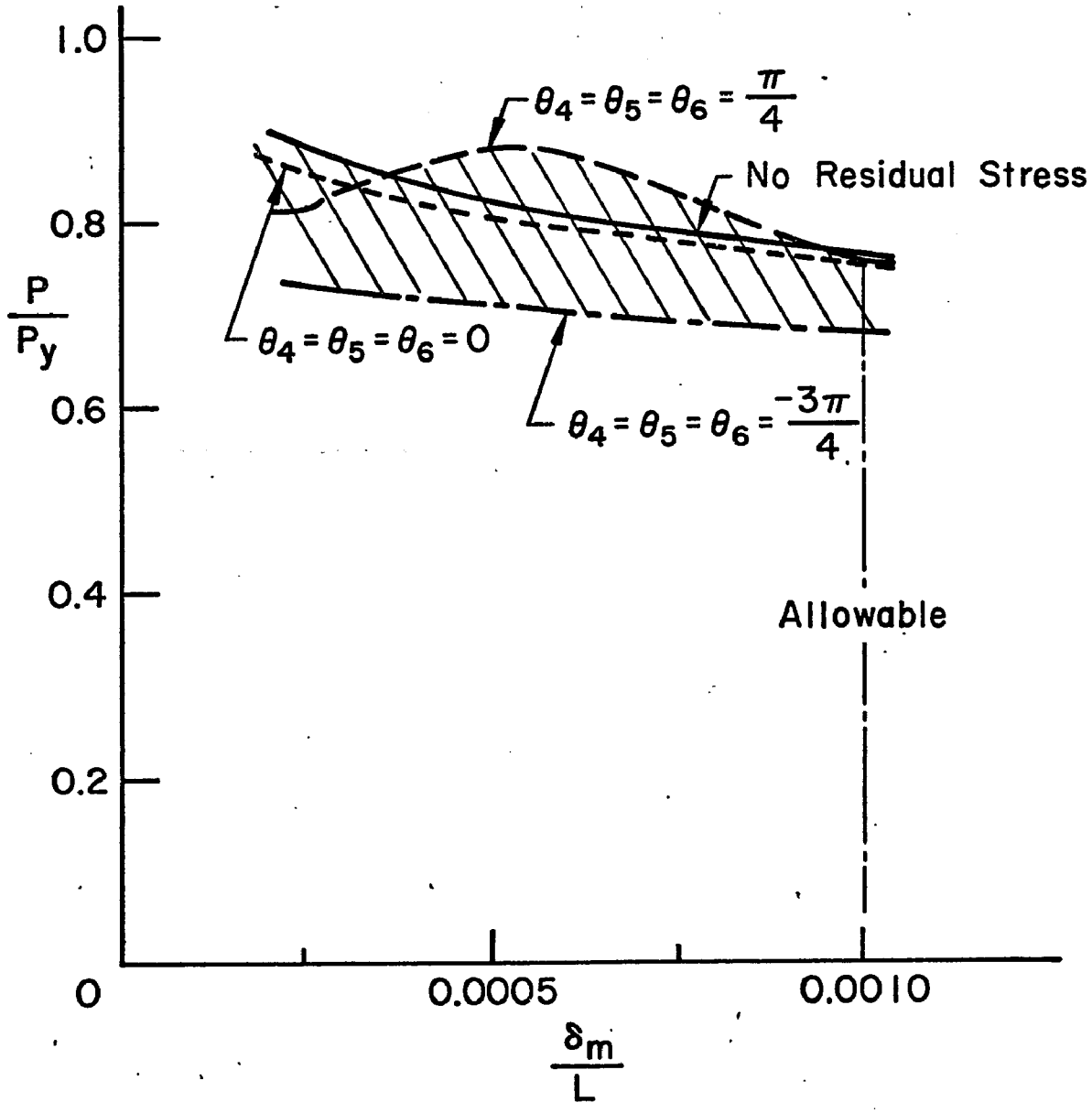

Fig. 5.9 Ultimate Load of a Tubular Column with $\lambda = 0.96$ as a Function of Weld Location and Initial Out-of-Straightness

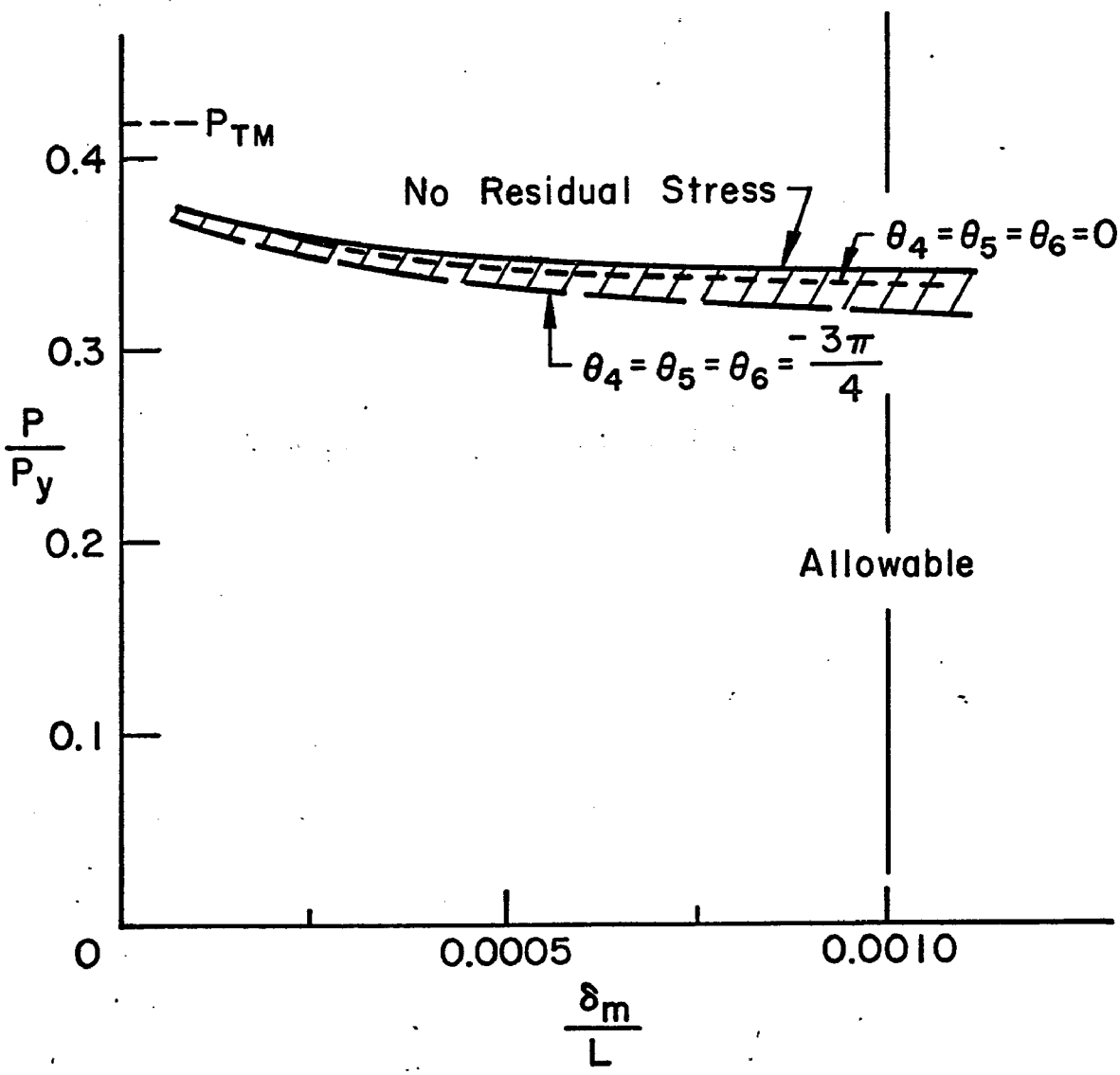

Fig. 5.10 Ultimate Load of a Tubular Column with $\lambda = 1.54$ as a Function of Weld Location and Initial Out-of-Straightness

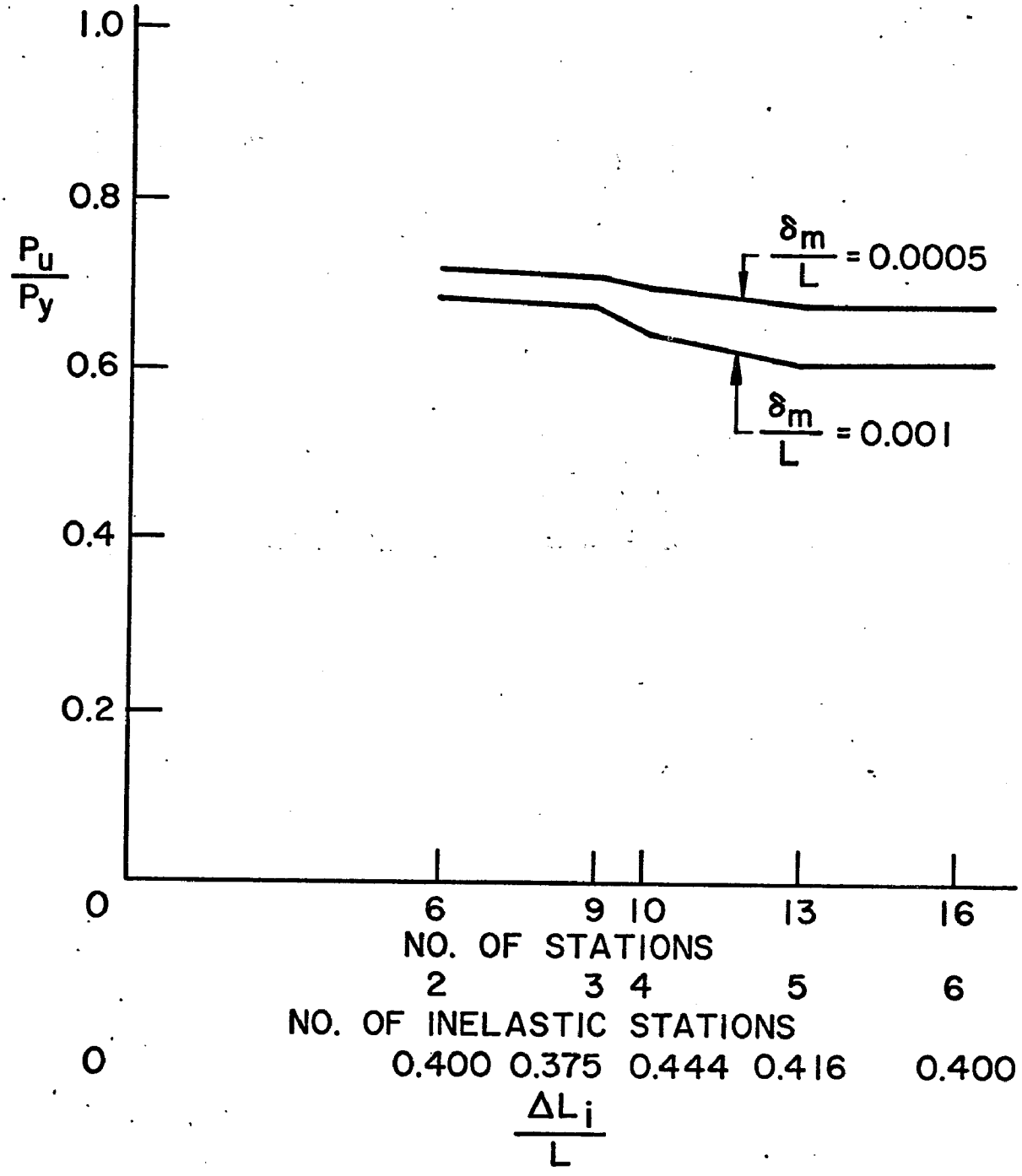

Fig. 5.11 Variation of Column Ultimate Load with Number of Stations along Column Length

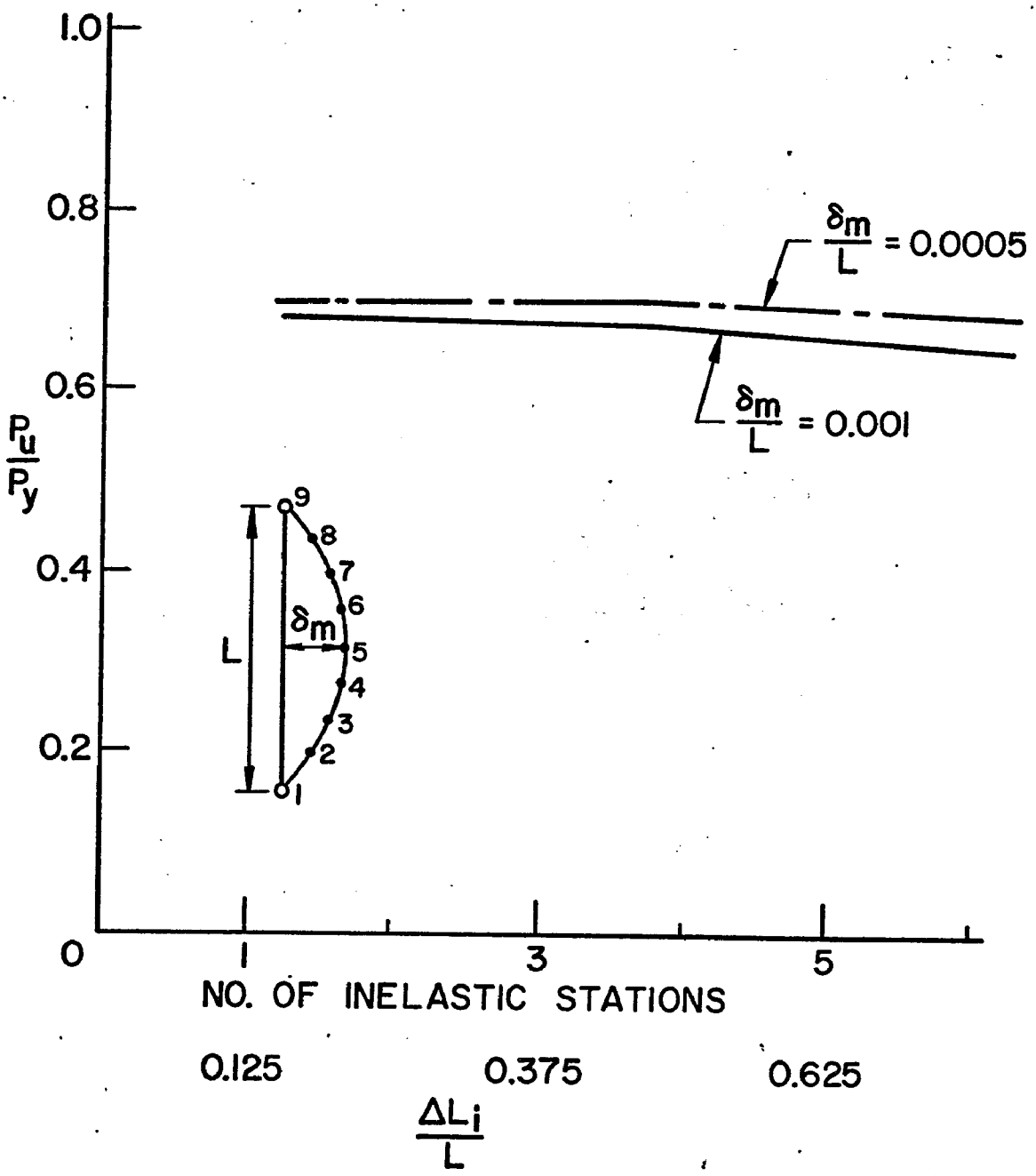

Fig. 5.12 Variation of Column Ultimate Load with Proportion of Column with Inelastic Behavior Capability

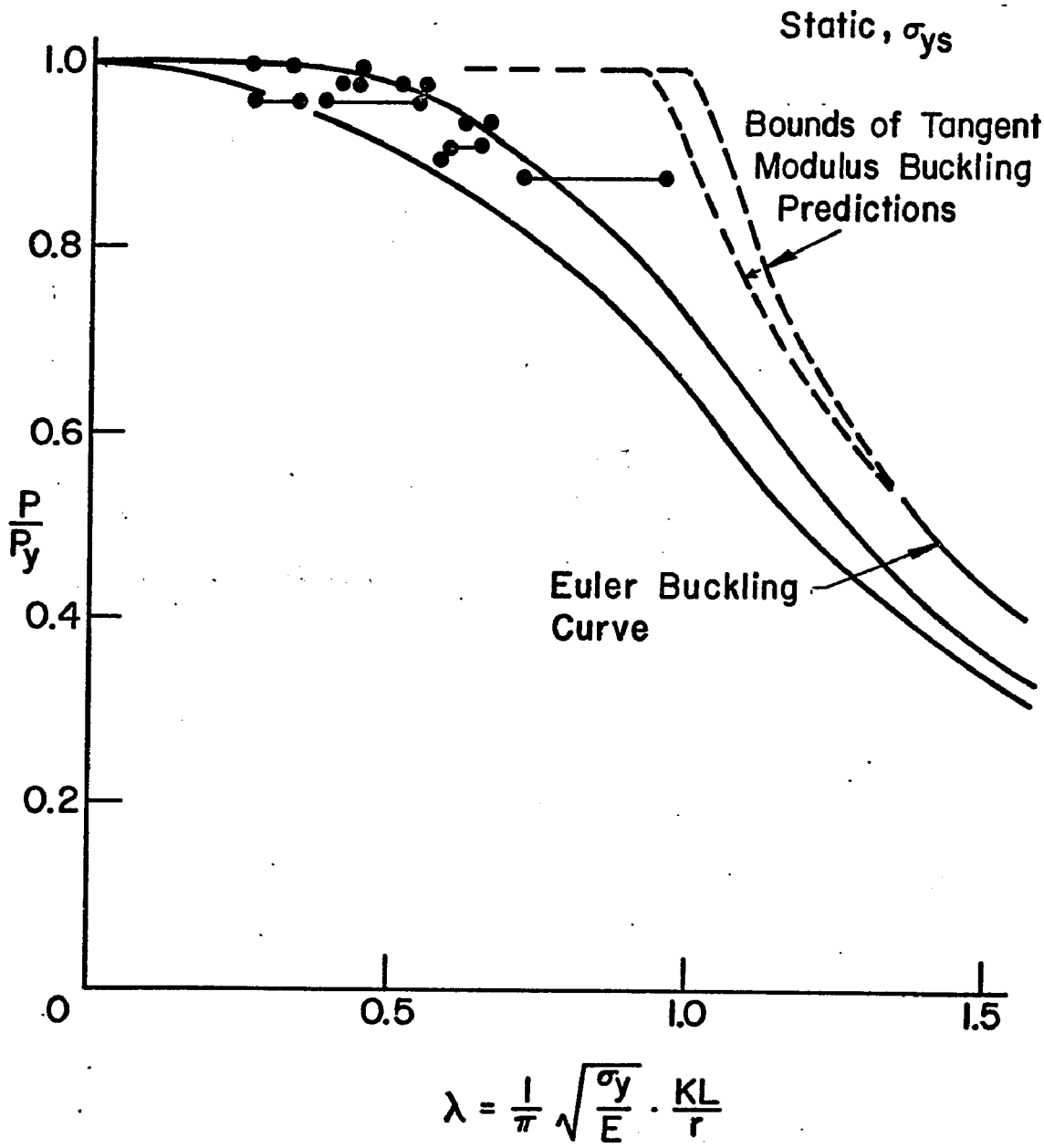

Fig. 6.1 Comparison of Predicted and Experimental Values of Ultimate Column Axial Load

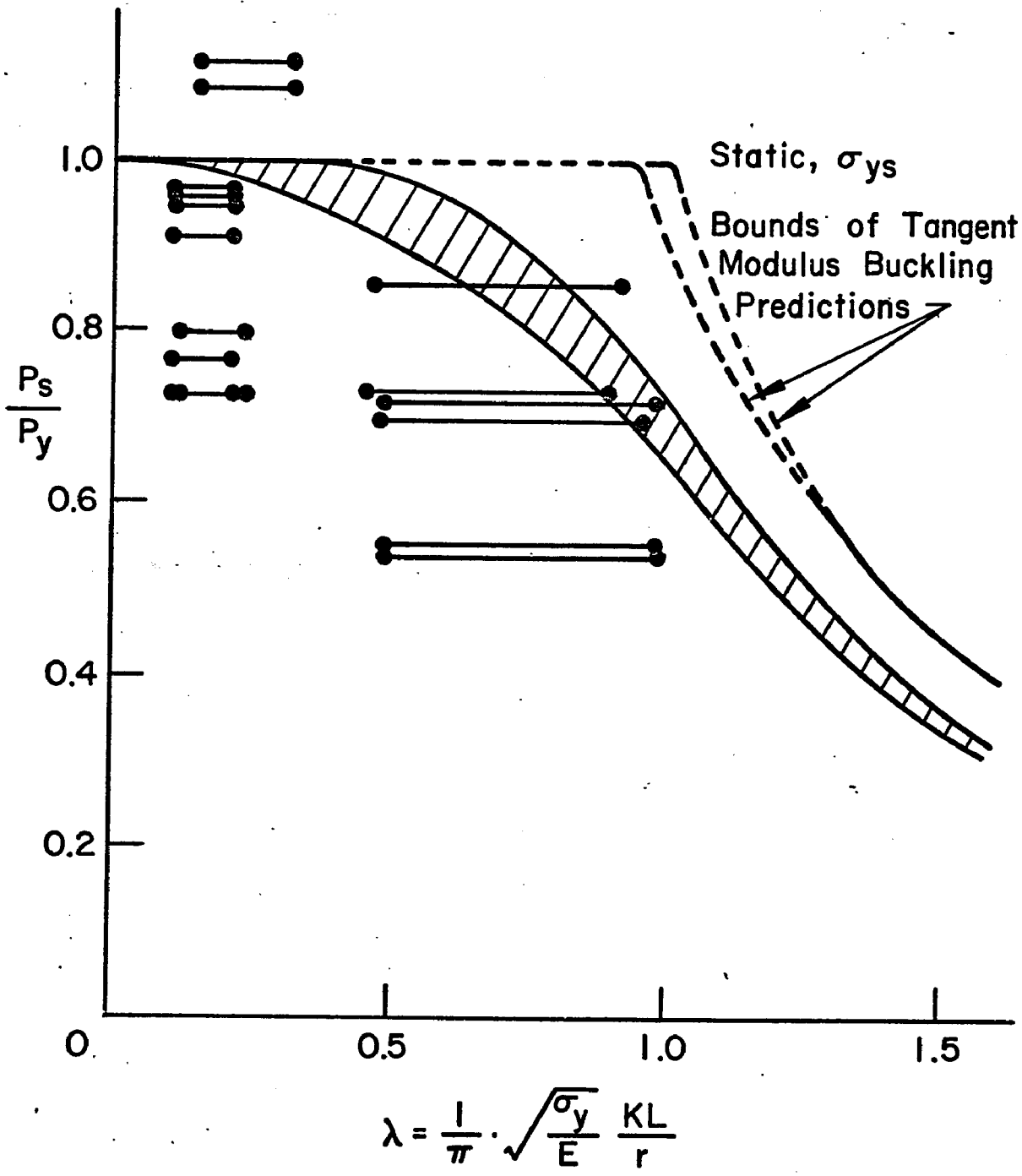

Fig. 6.2 Comparison of Wilson's Results with Theoretical Column Buckling Curve

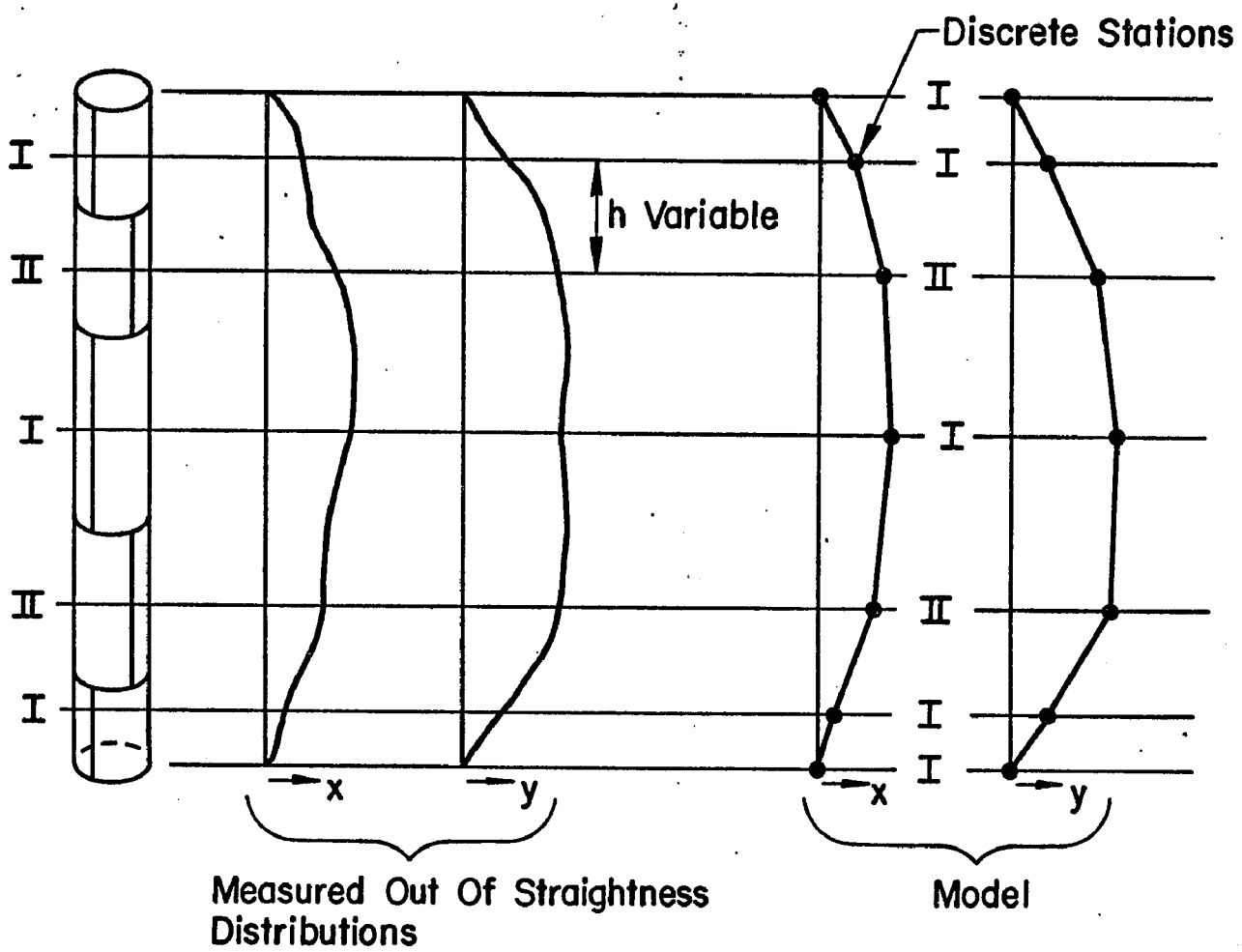

Fig. 6.3 Long Column Modelling and its Relationship to a Prototype Column

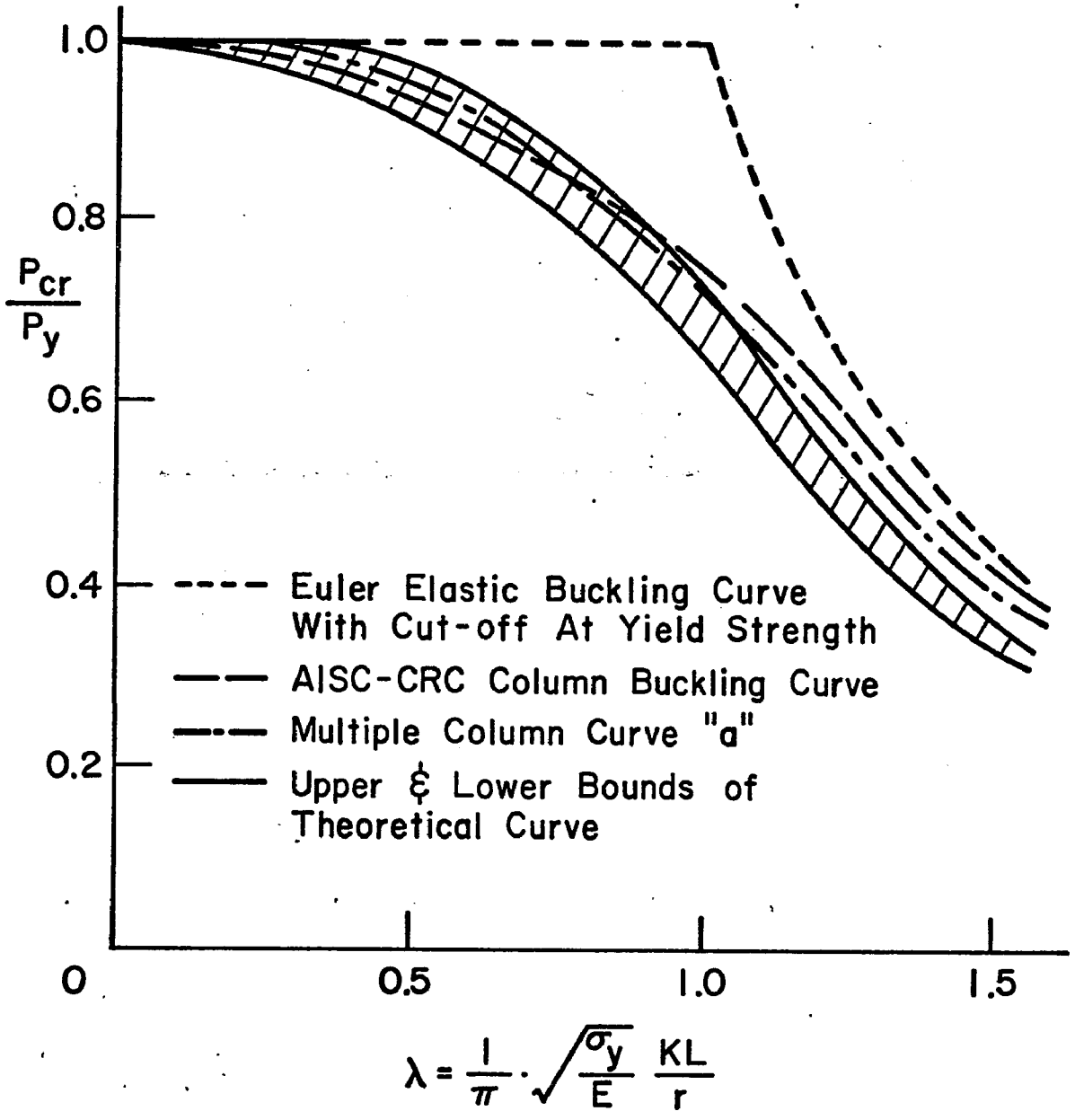

Fig. 6.4 Comparison of Theoretical Column Buckling Curve and Design Curves

11. LIST OF REFERENCES

1. Santathadaporn, S. and Chen, W. F., "Tangent Stiffness Method for Biaxial Bending," Journal of the Structural Division, ASCE, Vol. 98, No. ST1, Proc. Paper 8637, January 1972, pp. 153-163.

2. Gurfinkel, G., "Analysis of Footings Subjected to Biaxial Bending," Journal of the Structural Division, ASCE, Vol. 96, No. ST6, Proc. Paper 7329, June 1970, pp. 1049-1059.

3. Harstead, G. A., Birnstiel, C. and Leu, K. C., "Inelastic Behavior of H-Columns under Biaxial Bending," Journal of the Structural Division, ASCE, Vol. 94, No. ST10, Proc. Paper 6173, October 1968, pp. 2371-2398.

4. Wagner, A. L., Mueller, W. H. and Erzurumlu, H., "Design Interaction Curves for Tubular Steel Beam Columns," Offshore Technology Conference, Houston, Texas, Paper No. OTC 2684, May 1976.

5. Wagner, A. L., Mueller, W. H. and Erzurumlu, H., "Ultimate Strength of Tubular Beam-Columns," ASCE National Water Resources and Ocean Engineering Convention, San Diego, California, Preprint No. 2695, April 1976.

6. Ellis, J. S., "Plastic Behavior of Compression Members," Journal of the Mechanics and Physics of Solids, Vol. 6, pp. 282-300, Pergamon Press, 1958.

7. Chen, W. F. and Atsuta, T., "Interaction Equations for Biaxially Loaded Sections," Journal of the Structural Division, ASCE, Vol. 98, No. ST5, Proc. Paper 8902, May 1972, pp. 1035-1052.

8. Chen, W. F. and Atsuta, T., "Interaction Curves for Steel Sections under Axial Load and Biaxial Bending," The Engineering Journal, EIC, Vol. 17, No. A-3, March-April 1974.

9. Shanley, F. R., "Inelastic Column Theory," Journal of Aeronautical Science, 14 (5), May 1947.

10. Tall, L., "The Strength of Welded Built-Up Columns," Ph.D. Thesis, Lehigh University, May 1961, University Microfilms, Inc., Ann Arbor.

11. Beedle, L. S. and Tall, L., "Basic Column Strength," Journal of the Structural Division, ASCE, Vol. 86, No. ST7, July 1960, p. 139.

12. Johnston, B. G., editor, "Guide to Stability Design Criteria for Metal Structures," 3rd Edition, Wiley, 1976.

13. Bjorhovde, R., "Deterministic and Probabilistic Approaches to the Strength of Steel Columns," Ph.D. Thesis, Lehigh University, May 1972.

14. Sfintesco, D., "Experimental Basis of the European Column Curves," Construction Metallique, No. 3, 1970, p. 5.

15. Beer, H. and Schultz, G., "Theoretical Basis of the European Column Curves," Construction Metallique, No. 3, 1970, p. 58.

16. Marshall, P. W., "Stability Problems in Offshore Structures," presentation at the Annual Technical Meeting of the Column Research Council, St. Louis, Missouri, March 25, 1970.

17. "Rules for the Design, Construction and Inspection of Fixed Offshore Structures," Det Norske Veritas, Oslo, 1974.

18. "Planning, Design and Constructing Fixed Offshore Platforms," RP 2A, American Petroleum Institute, Revisions, 1974.

19. "API Specification for Fabricated Structural Steel Pipe," American Petroleum Institute, API Specification 2B, October 1972.

20. Fukumoto, Y. and Galambos, T. V., "Inelastic Lateral-Torsional Buckling of Beam Columns," Journal of the Structural Division, ASCE, Vol. 92, No. ST2, Proc. Paper 4770, April 1966, pp. 41-61.

21. Chen, W. F., "General Solution of the Inelastic Beam-Column Problem," Journal of the Engineering Mechanics Division, ASCE, Vol. 96, No. EM4, Proc. Paper 6382, February 1969, pp. 21-39.

22. Chen, W. F., "Further Studies of the Inelastic Beam-Column Problem," Journal of the Structural Division, ASCE, Vol. 97, No. ST2, Proc. Paper 7922, February 1971, pp. 529-544.

23. Chen, W. F. and Atsuta, T., "Column Curve Method for Analysis of Beam Columns," The Journal of the Institution of Structural Engineers, Vol. 50, No. 6, June 1972, pp. 233-240.

24. Galambos, T. V., "Structural Members and Frames," Englewood Cliffs, New Jersey, Prentice Hall, 1968.

25. Santathadaporn, S. and Chen, W. F., "Analysis of Biaxially Loaded Steel H-Columns," Journal of the Structural Division, ASCE, Vol. 99, No. ST3, Proc. Paper 9621, March 1973, pp. 491-509.

26. Tebedge, N., Chen, W. F. and Tall, L., "On the Behavior of a Heavy Steel Column," International Colloquium on Column Strength, IABSE, Paris, November 1972.

27. Tebedge, N. and Chen, W. F., "Design Criteria for H-Columns under Biaxial Loading," Journal of the Structural Division, ASCE, Vol. 100, No. ST3, Proc. Paper 10400, March 1974, pp. 579-598.

28. Ross, D. A. and Chen, W. F., "Design Criteria for Steel I-Columns under Axial Load and Biaxial Bending," Canadian Journal of Civil Engineering, Vol. 3, No. 3, 1976, pp. 466-473.

29. Canadian Standard S16.1-1974, "Steel Structures for Buildings - Limit States Design."

30. Tebedge, N. and Tall, L., "Linear Stability Analysis of Beam-Columns," Journal of the Structural Division, ASCE, Vol. 99, No. ST12, December 1973, pp. 2439-2457.

31. Tebedge, N., Marek, P. and Tall, L., "Comparison of Testing Methods for Heavy Columns," Fritz Engineering Laboratory Report No. 351.2, Lehigh University, October 1969.

32. Vinnakota, S. and Äysto, P., "Inelastic Spatial Stability of Restrained Beam-Columns," Journal of the Structural Division, ASCE, Vol. 100, No. ST11, Proc. Paper 10919, November 1974, pp. 2235-2254.

33. Vinnakota, S., "The Influence of Initial Deformations and Residual Stresses on the Maximum Strength of Biaxially Bent Columns," presentation to the Column Research Council Annual Technical Meeting, Toronto, Canada, May 1975.

34. Tebedge, N., discussion of "Elastic Stability of Tapered I-Beams," by S. Kitipornchai and N. S. Trahair, Journal of the Structural Division, ASCE, Vol. 99, No. ST1, Proc. Paper 9462, January 1973, pp. 211-214.

35. Virdi, K. S. and Dowling, P. J., "The Ultimate Strength of Biaxially Restrained Columns," Proceedings, Institution of Civil Engineers, Part 2, Vol. 61, March 1976, pp. 41-58.

36. Matlock, H. and Taylor, T. P., "A Computer Program to Analyze Beam-Columns under Movable Loads," Research Report No. 56-4, Center for Highway Research, The University of Texas at Austin, June 1968.

37. Mathar, J., "Determination of Initial Stresses by Measuring the Deformation around Drilled Holes," Transactions, ASME, Vol. 56, 1934, pp. 249-254.

38. Gadd, C. W., "Residual Stress Indications in Brittle Lacquer," Proceedings of the Society for Experimental Stress Analysis, Vol. IV, No. 1, 1946, pp. 74-77.

39. Soate, W. and Vancrombrugge, R., "An Industrial Method for the Determination of Residual Stresses," Proceedings of the Society for Experimental Stress Analysis, Vol. 8, No. 1, 1950, pp. 17-28.

40. Kelsey, R. A., "Measuring Nonuniform Residual Stresses by the Hole Drilling Method," Proceedings of the Society for Experimental Stress Analysis, Vol. 13, No. 1, 1956, pp. 181-194.

41. Davidson, T. E., Kendall, D. P. and Reiner, A. N., "Residual Stresses in Thick-Walled Cylinders Resulting from Mechanically Induced Overstrain," The Journal of Experimental Mechanics, November 1963, pp. 253-262.

42. Rendler, N. J. and Vigness, I., "Hole Drilling Strain-Gage Method of Measuring Residual Stresses," Journal of Experimental Mechanics, December 1966, pp. 577-586.

43. Lake, B. R., Appl, F. J. and Bert, C. W., "An Investigation of the Hole Drilling Technique for Measuring Planar Residual Stress in Rectangularly Orthotropic Materials," Journal of Experimental Mechanics, June 1970, pp. 233-240.

44. "Instruction Manual for Model RS-200-01 Milling Guide," Photoelastic, Inc., 1972.

45. Redner, S., "Measurement of Residual Stresses by Blind Hole Drilling Method," Bulletin TDG-5, Photoelastic Inc., May 1974.

46. "Residual Stress Investigation of a Porcupine Shaft," Fritz Engineering Laboratory Report No. 200.70.25.5, Lehigh University, August 1970.

47. Kalakoutsky, N., "The Study of Internal Stresses in Cast Iron and Steel," London, 1888, also; St. Petersburgh, 1889 (in Russian).

48. Tebedge, N., Alpsten, G. and Tall, L., "Residual Stress Measurement by the Sectioning Method," presented at the Spring Meeting of the Society for Experimental Stress Analysis, Cleveland, Ohio, May 23-26, 1972.

49. Sherman, D. R., "Residual Stress Measurement in Tubular Members," Journal of the Structural Division, ASCE, Vol. 95, No. ST4, Proc. Paper 6502, April 1969, pp. 635-647.

50. Tebedge, N., Alpsten, G. and Tall, L., "Residual Stress Measurements - A Study of Methods," Fritz Engineering Laboratory Report No. 337.8, Lehigh University, February 1970.

51. Ostapenko, A. and Gunzelman, S. X., "Local Buckling of Tubular Steel Columns," Proceedings of the National Structural Engineering Conference, ASCE, Madison, Wisconsin, August 22-25, 1976.

52. Wilson, W. M. and Newmark, N. M., "The Strength of Thin Cylindrical Shells as Columns," Engineering Experiment Station, University of Illinois, Urbana, Bulletin No. 255, February 1933.

53. Wilson, N. M., "Tests of Steel Columns - Thin Cylindrical Shells, Laced Channels, Angles," Engineering Experiment Station, University of Illinois, Urbana, Bulletin No. 292, April 1937.

54. Clark, J. W. and Rolf, R. L., "Design of Aluminum Tubular Members," ALCOA Research Laboratories, New Kensington, Pennsylvania, Report No. 12-64-2, January 1964.

55. Kato, B., "Column Buckling Curve of Welded Steel Tube," Proceedings, International Colloquium on Column Strength, IABSE, Paris, November 1972.

56. Bouwkamp, J. G., "Study of the Buckling and Post-Buckling Strength of Circular Tubular Sections," Berkeley, May 1974; report to Earl and Wright, Consulting Engineers, San Francisco.

57. Schilling, C. G., "Buckling Strength of Circular Tubes," Journal of the Structural Division, ASCE, Vol. 91, No. ST5, October 1965, pp. 325-348.

58. Graff, W. J., "Fabricated and Solid Section Column Test Data Compared with Various Formulas," Proceedings, Sixth Annual Offshore Technology Conference, Houston, Texas, Vol. 2, Paper No. OTC 2103, pp. 701-710, May 1974.

59. Troitsky, M. S., "On the Local and Overall Stability of Thin-Walled Large Diameter Tubular Columns," Canadian Structural Engineering Conference, 1976.

60. McGregor, W. P., "Spiral Welded Tubing," SAMPE, Twentieth National Symposium and Exhibition, San Diego, California, April 1975, pp. 387-401.

61. Sherman, D. R., "Tests of Circular Steel Tubes in Bending," Journal of the Structural Division, ASCE, Vol. 102, No. ST11, November 1976, pp. 2181-2195.

62. Gunzelman, S. X., "Experimental Local Buckling of Fabricated High-Strength Steel Tubular Columns," M.S. Thesis, Lehigh University, October 1976.

63. Marzullo, M. A. and Ostapenko, A., "Tests on Two High-Strength Short Tubular Columns," Tenth Annual Offshore Technology Conference, Houston, Texas, Paper No. OTC 3086, May 1978.

64. Ross, D. A. and Chen, W. F., "Residual Stress Measurements in Fabricated Tubular Steel Columns," Fritz Engineering Laboratory Report No. 393.4, Lehigh University, July 1975.

65. Ross, D. A. and Chen, W. F., "Preliminary Tests on Tubular Columns," Fritz Engineering Laboratory Report No. 393.5, Lehigh University, June 1976.

66. Ross, D. A. and Chen, W. F., "The Axial Strength and Behavior of Cylindrical Columns," Fritz Engineering Laboratory Report No. 393.6, Lehigh University, February 1976.

67. Ross, D. A. and Chen, W. F., "Tests of Fabricated Tubular Columns," Fritz Engineering Laboratory Report No. 393.7 (and Appendices), Lehigh University, January 1976.

68. Chen, W. F. and Ross, D. A., "The Axial Strength and Behavior of Cylindrical Columns," Eighth Annual Offshore Technology Conference, Paper No. OTC 2683, Houston, Texas, May 3-6, 1976, pp. 741-754.

69. Chen, W. F. and Ross, D. A., "Tests of Fabricated Tubular Columns," Journal of the Structural Division, ASCE, Vol. 103, No. ST3, Proc. Paper 12809, March 1977, pp. 619-634.

70. Tall, L., "Stub Column Test Procedure," Document C-282-16, Class C-281-61, Class C Document, International Institute of Welding, Oslo, June 1962; also, CRC Technical Memorandum No. 3, "Column Research Council Guide," Third Edition (B. G. Johnston, editor) John Wiley, 1976.

71. Yu, C. K. and Tall, L., "Significance and Application of Stub Column Test Results," Journal of the Structural Division, ASCE, Vol. 97, No. ST7, July 1971, pp. 1841-1861.

72. Desai, S., "Tension Testing Procedures," Fritz Engineering Laboratory Report No. 237.44, Lehigh University, February 1969.

73. Regec, J. E., Huang, J. S. and Chen, W. F., "Mechanical Properties of C-Series Connections," Fritz Engineering Laboratory Report No. 333.17, Lehigh University, April 1972.

74. Ostapenko, A. and Gunzelman, S. X., "Local Buckling Tests on Two High-Strength Steel Tubular Columns," Fritz Engineering Laboratory Report No. 406.2, Lehigh University, July 1975.

75. Estuar, F. R. and Tall, L., "Testing of Pinned-End Steel Columns," Test Methods for Compression Members, ASTM STP 419, American Society for Testing and Materials, 1967, pp. 80-96.

76. American Institute of Steel Construction, "Specification for the Design, Fabrication and Erection of Structural Steel for Building," AISC, New York, February 1969.

77. Tall, L. (editor), "Structural Steel Design," Second Edition, Ronald Press, New York, 1974.

78. Column Research Council, "The Basic Column Formula," CRC Technical Memorandum No. 1, May 1952.

79. Tall, L., "Welded Built-Up Columns," Fritz Engineering Laboratory Report No. 249.29, Lehigh University, April 1966.

12. VITA

The author was born in Auckland, New Zealand on February 25, 1951, the first child of Richard and Iris Ross.

He attended the Auckland Grammar School before entering the University of Auckland in 1969. There he was awarded the degrees of Bachelor of Engineering (Honours) (Engineering Science) in May 1972, and Master of Engineering (Civil) in May 1974. He was also employed as an assistant structural design engineer by a firm of architects, civil and structural engineers in Hamilton, New Zealand, for most of the year 1974. During this time he was part of a design team involved in the design and construction of multistory structures, including hospitals and dairy factories, as well as other industrial facilities.

The author came to Lehigh University in November 1974 as research assistant for Project 393, "The Strength and Behavior of Fabricated Tubular Columns". Since September 1976 he has been a teaching assistant.